MONTHLY NOTICES

OF THE

ROYAL ASTRONOMICAL SOCIETY

Vol. 110 No. 1 1950

Published and Sold by the
ROYAL ASTRONOMICAL SOCIETY
BURLINGTON HOUSE
LONDON, W. 1

Price Nine Shillings

NOTICE TO AUTHORS

1. *Communications.*—Papers must be communicated to the Society by a Fellow. They should be accompanied by a summary at the *beginning* of the paper conveying briefly the content of the paper, and drawing attention to important new information and to the main conclusions. The summary should be intelligible in itself, without reference to the paper, to a reader with some knowledge of the subject; it should not normally exceed 200 words in length. Authors are requested to submit MSS. in duplicate. These should be typed, using double spacing and leaving a margin at one side. Corrections to the MSS. should be made in the text and not in the margin. By Council decision, MSS. of accepted papers are retained by the Society for one year after publication; unless their return is then requested by the author, they are destroyed.

2. *Presentation.*—Authors are allowed considerable latitude, but they are requested to follow the general style and arrangement of *Monthly Notices*. References to literature should be given in the standard form, including a date, for printing either as footnotes or in a numbered list at the end of the paper. Each reference should give the name of the author cited, irrespectively of the occurrence of the name in the text (some latitude being permissible, however, in the case of an author referring to his own work).

3. *Notation.*—Authors should conform closely with the recommendations of Commission 3 of the International Astronomical Union (*Trans. I.A.U.*, Vol. VI, p. 345, 1938). Council has decided to adopt the I.A.U. 4-letter abbreviations for constellations where contraction is desirable (Vol. IV, p. 221, 1932).

4. *Diagrams.*—These should be drawn about twice the size required in print and prepared for direct photographic reproduction except for the lettering which should be inserted in pencil. Legends should be given in the manuscript indicating where in the text the figure should appear. Blocks are retained by the Society for 10 years; unless the author requires them before the end of this period they are then destroyed.

5. *Tables.*—These should be arranged so that they can be printed upright on the page.

6. *Proofs.*—Costs of alteration exceeding 5 per cent of composition must be borne by the author. Fellows are warned that such costs have risen sharply in recent years, and it is in their own and the Society's interests to seek the maximum conciseness and simplification of symbols and equations consistent with clarity.

7. *Revised Manuscripts.*—When papers are submitted in revised form it is especially requested that they be accompanied by the original MS.

Reading of Papers at Meetings

8. If a paper is to be read at a meeting it should be received by the Assistant Secretary not later than the previous Friday.

9. When submitting papers authors are requested to indicate whether they will be willing and able to read the paper at the next or some subsequent meeting, and approximately how long they would like to be allotted for speaking.

10. Postcards giving the programme of each meeting are issued some days before the meeting concerned. Fellows wishing to receive such cards whether for the Ordinary Meetings or for the Geophysical Discussions or both should notify the Assistant Secretary.

MONTHLY NOTICES

OF THE

ROYAL ASTRONOMICAL SOCIETY

Vol. 110 No. 1

MEETING OF 1950 JANUARY 13

Professor W. M. Smart, President, in the Chair

The election by the Council of the following Fellows was duly confirmed:—

Lt.-Col. William Arthur Garstin, C.B.E., 65 Campden Hill Court, London, W.8 (proposed by E. A. Milne);

*Franz Daniel Kahn, 41 St. Margaret's Road, Edgware, Middlesex (proposed by S. Chapman);

Thomas David Kinman, University Observatory, Oxford (proposed by H. H. Plaskett);

Joan Lilly, Waveney High School, Wortwell, Harleston, Norfolk (proposed by J. G. Read);

Michael Selwyn Longuet-Higgins, Trinity College, Cambridge (proposed by H. Jeffreys);

Hugh Ryan, B.Sc., 127 Princess Court, London, W.2 (proposed by F. M. Holborn);

William Court Parsons Tapper, O.B.E., M.I.E.E., Godrevy, Whitecliff Road, Parkstone, Poole, Dorset (proposed by A. Hunter);

Hugh Harold Lawrence Carmichael Vredenburgh, 10 Beauchamp Place, London, S.W.3 (proposed by W. H. Steavenson);

Gert Claes Johan Walén, Roslagsgatan 25, Stockholm, Sweden (proposed by S. Chapman); and

Kevin Charles Westfold, Queen's College, Oxford (proposed by S. Chapman).

The election by the Council of the following Junior Members was duly confirmed:—

John Andrew Bastin, 24 The Drive, London, E.17 (proposed by H. H. Plaskett);

Lewis Grenville Bentley, 13 Romeyn Road, Streatham, London, S.W.16 (proposed by F. M. Holborn);

Daphne May Fooks, H.M. Nautical Almanac Office, Herstmonceux Castle, Sussex (proposed by F. M. McBain);

* Transferred from Junior Membership.

Mavis McIntyre Smith Gibson, B.Sc., H.M. Nautical Almanac Office, Herstmonceux Castle, Sussex (proposed by F. M. McBain); and
Angela Margaret James, B.Sc., H.M. Nautical Almanac Office, Herstmonceux Castle, Sussex (proposed by F. M. McBain).

One hundred and eighty-one presents were announced as having been received since the last meeting.

The President announced that the Council had awarded the Gold Medal of the Society to Professor Joel Stebbins, late Director of the Washburn Observatory, Madison, Wisconsin, U.S.A., for his development of physical methods in astronomical photometry and for the results obtained by the use of those methods.

ON A PERIODIC FLUCTUATION IN THE LENGTH OF THE DAY

H. F. Finch

(Communicated by the Astronomer Royal)
(Received 1950 January 10)

Summary

From a study of the performance of a number of quartz-crystal clocks employed in the Greenwich Time Service an annual periodic fluctuation in the length of the day is deduced. The variation is of the order of $\pm 0^s{\cdot}001$ and has an accumulative effect in time of approximately $\pm 0^s{\cdot}060$. This is in very close agreement with results obtained from independent data by N. Stoyko and demonstrates the persistent character of the phenomenon.

1. With the development of the quartz-crystal oscillator as a frequency standard, a demand has arisen for time signals capable of providing frequency checks to a precision consistent with the standard of performance of the crystals themselves. In undertaking to furnish these signals the Royal Greenwich Observatory has at its disposal a number of quartz clocks which serve to bridge the gap between the time determinations, the observational errors of which they also serve to smooth out. But to control the emission of a system of daily time signals that will define intervals of 24 hours to an accuracy as good as or better than one millisecond has proved a very intractable task. Of the difficulties encountered, only that of establishing the length of the current day, or alternatively, of determining the rates of the observatory clocks with the desired accuracy, is discussed in this paper.

2. Beat-frequency measurements have shown that over short periods of time frequency stabilities of the order of one part in 10^{11} can be achieved with quartz crystals, while the frequency difference of two crystals whose characteristic performances are known, can be predicted, in certain circumstances, over a period of months to within several parts in 10^8. In justice to the crystal, therefore, if the frequency of a standard oscillator is to be quoted in cycles per second, the length of the second must be known to something better than one part in 10^8. In other words, the astronomical observations must be capable of establishing the current rates of the observatory clocks to within $0^s{\cdot}001$/day.

3. At the Greenwich Observatory the available accuracy tends to be limited by two factors: (*a*) The time determinations have, up to the present, been made visually and it has not proved possible to reduce the probable error of a single determination much below $\pm 0^s{\cdot}020$. If the clock rate, assumed to be constant, is determined from two such observations, they would need to be separated by an interval of months for the rate to be derived with certainty to the desired accuracy. The interval can be reduced by increasing the number of time determinations, but the gain is by no means proportional to the increased effort. (*b*) The rates of crystal clocks are not constant, though they may be very uniform. A quartz crystal, when first set into oscillation, shows a marked frequency (rate) drift. The drift gradually diminishes until, after some months, it settles down to

a fairly constant value. The clock correction (E) can then be represented very closely by the expression $E=a+bt+ct^2$, where a, b and c are constants and t is reckoned in time from some arbitrary epoch. When t is expressed in days and E in seconds, the value of c is found in general to be between the values of $\pm 0{\cdot}00005$. The daily rate (R) is given by $R=b+2ct$. Reliable prediction of the error of the clock requires c to be determined with great accuracy, because its effect increases with the square of the time. The existence of a frequency drift greatly increases the interval required to establish the current rate of the clock. Moreover, even the best clocks are liable to small erratic changes of b and c, and although sudden changes of rate are shown up in the daily intercomparisons, minor variations in the value of the frequency drift are not so readily detected. In order to obtain increased accuracy, and also to allow for the contingency of failures, a considerable number of clocks must be available for use in the service.

4. After quartz clocks had been introduced into the Time Department and experience with them had established their high standard of performance, the policy of predicting their errors on a long-term basis was introduced. The clock constants a, b and c were derived from a series of time determinations extending over many months. The extrapolated corrections were then heavily weighted against those indicated by current observations, which might appear discordant because of large observational errors. As observations accumulated, any persistent departure of the clock corrections from the ephemeris was allowed for graphically and the constants were subsequently adjusted to secure the best fit over the last few months. Using the adopted current corrections to the standard clocks and the daily intercomparisons it was possible to deduce the amount by which the clock controlling the time signal should be corrected prior to transmission.

5. The method appeared for a while to work fairly satisfactorily, but in the autumn of 1945 the observed clock corrections began rapidly to diverge from the predicted. The magnitude of this divergence varied somewhat from clock to clock, but all appeared to have undergone an acceleration of rate. A change in the period of rotation of the Earth was suspected. It was then noted that there had been a similar occurrence, though to a much less marked degree, during the previous autumn, which suggested the existence of a seasonal effect. There appeared to be little evidence, however, of a compensating retardation of the clocks during the spring. In subsequent years, as more clocks became available, the apparent autumnal acceleration was again observed. When, therefore, in the autumn of 1948 a discordance between the observed and predicted clock corrections again began to show, the weight given to the current observations was greatly increased. In the spring of 1949 there appeared a fairly definite indication of a retardation amongst a number of the clocks. The agreement was qualitative rather than quantitative, but it was felt that the differences between individual clocks might easily arise from erratics and the difficulty of establishing the true frequency drifts.

6. The strong suspicion of a seasonal fluctuation aroused by the spring changes led to an examination being made of the final corrections to the times of emission of the Rugby time signals, which are based on the subsequent assessment of the performance of the clocks. Since the time signals are under the control of the Greenwich Time Service, the corrections are a measure of the errors in the predicted clock corrections irrespective of which clocks are in use as

standards at the time of transmission. The four years 1944–47 agree in showing a pronounced seasonal fluctuation in the signal trend, i. e. the mean daily increase in the value of the signal corrections (signal slow). It does not appear before 1944 because the technique of long-term prediction had not then been fully developed; it disappears in 1948 because of the autumn change in technique. The mean seasonal trend of the signal for the four years 1944–47 is shown in Fig. 1. The form of this curve has necessarily been influenced to some extent by the discretion of the predictor in modifying his adopted clock corrections in the light of accumulating observations.

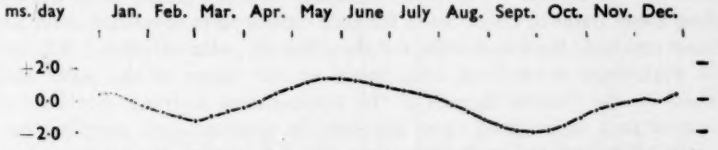

FIG. 1.—*Mean "trend" of GBR time signal at* 10.00 *U.T. for the years* 1944–1947.

7. The true form of the fluctuation must be derived from the observed corrections. The material suitable for this purpose is limited by various factors. It is possible to use only those clocks which have been free from disturbances occasioned by faults and have had undisturbed runs for many months. For the period 1943–47 the usable data were provided by four clocks, 4*A*, 4*B* and 4*C* in service at the Post Office, and *A*1 at the Royal Observatory, Edinburgh (where a time service was operated during the war). Considerable trouble was experienced during this period with the clocks at Abinger. From the beginning of 1948, following the replacement of the original defective beat counters of the Abinger clocks, the installation at Greenwich of six crystal clocks, and further additions at Dollis Hill, a greatly increased amount of material became available. From about the middle of 1947 the observational data were strengthened by a considerable increase in the number of time determinations and by an improvement in the accuracy consequent upon the installation at Abinger of a better transit instrument. The material falls naturally into two groups ; separate analyses have therefore been made for the two periods 1943–47 and 1948–49.

8. The analysis has been based on the assumption that the observed clock corrections can be fitted to an ephemeris of the form

$$E = a + bt + ct^2 + f,$$

where f is a periodic function of the time representing a hypothetical seasonal fluctuation, having therefore a yearly period and arising from some cause independent of the clocks. The second differences of a series of clock corrections determined at equal intervals are then of the form $2c + \Delta''f$ and will differ from clock to clock only through the different values of the frequency drift. The third differences, $\Delta'''f$, correspond with those that would be obtained from a clock having zero values for a, b and c. Random errors will be present, but their effect is reduced by taking means of the various values obtained for $\Delta'''f$ throughout set intervals of the calendar year. Nevertheless, owing to the possible small variations in rate and frequency drift and to residual random errors, it is unlikely that the sum of the mean values of $\Delta'''f$ for the whole twelve months will be zero. The form of their distribution is not affected, however, by reducing each term

by its mean value for the year. The adjusted values can be integrated to give a series of mean values for $\Delta''f$, the constant of integration being adjusted so that the mean yearly value is again zero. The integration can be continued to give first the values of $\Delta'f$ and then those of f itself.

9. The formation of the third differences was greatly eased by employing the residual clock corrections, which had been derived for the purpose of prediction, with reference to a parabolic ephemeris. These residuals had already been corrected for the effects of sudden discontinuities due to stoppages of the phonic motors and their subsequent restarting; such stoppages do not affect the rates of the clocks. The mean residual clock corrections with the corresponding mean dates of observation for each month were tabulated, after which the mean residuals were corrected for the effect of polar variation. Up to the end of 1948 these corrections were based on the values of the polar motion published by the Central Bureau of the International Latitude Service. The 1949 corrections were based upon the latitude variation data supplied by the U.S. Naval Observatory at Washington. The data were then adjusted to an adopted date for each month by correcting for the residual rate. As the correction was always small, the effect of departures of the mean from the standard date was never critical. The standard dates were selected to be separated as nearly as possible by alternate intervals of 30 and 31 days in order to make the data suitable for differencing. The weights of the final monthly values necessarily differ considerably.

10. In order to reduce the effect of observational error in relation to the fluctuation, the months were divided into two groups, odd and even, to give a uniform working interval of 61 days. The two sets of figures were separately differenced and independently reintegrated as described above. Two sets of values for f were thus obtained, which were finally dovetailed together. This treatment of the figures required a minimum undisturbed run of seven months for any clock to furnish a single third difference.

11. The values of the third differences for the two periods 1943–47 and 1948–49 are given in Table I. The clock and the year are indicated in the first two columns and at the head of each succeeding column is listed the calendar month corresponding to the centre of each seven-month period involved in the derivation of the figures below. At the foot of the table are given the mean values for each column and the weight as defined by the number of entries above. Table II shows the number of time determinations obtained in each month during the whole period 1943–49.

12. The reintegration of $\Delta'''f$ through the stages $\Delta''f$, $\Delta'f$ to f is contained in Table III; the left- and right-hand sides are devoted respectively to the odd and even months. The mean value printed at the bottom of each column is subtracted from each of the values given above it to obtain $\Delta''f$, $\Delta'f$ and f as explained above. Fig. 2 contains plots of $\Delta'''f$, $1/61 \cdot \Delta'f$ and f for each of the two periods. It will be noted how closely the results from the odd and even months separately are in agreement. The analysis of the f curves give:

$$\text{for 1943–47} \qquad f = +55{\cdot}7 \sin n(T+141)^\circ - 16{\cdot}8 \sin 2n(T+67)^\circ,$$

$$\text{and for 1948–49} \qquad f = +58{\cdot}3 \sin n(T+158)^\circ - 7{\cdot}1 \sin 2n(T+48)^\circ,$$

where T is the day of the year, f is expressed in milliseconds and n is the diurnal motion of the mean Sun in degrees of arc, i.e. 0·986.

Table I

Collected Third Differences

[unit = $0^{s}\cdot001$]

		Jan.	Feb.	Mar.	Apr.	May	June	July	Aug.	Sept.	Oct.	Nov.	Dec.
4*A*	1944	...	...	...	...	...	...	...	...	+ 49	+153	+175	+ 55
	1945	+ 15	−47	− 5	+ 73	+ 38	− 38	− 99	−106	− 30	+110	+115	− 37
	1946	−128	+47	+163	+ 12	+ 90	+ 30	−254	−113	+103	+ 50	− 18	+ 21
	1947	+ 13	+35	+ 97	+127	+ 3	− 53	− 2	−150	−144	+ 61	+ 51	− 38
	1948	−105	...	...	...	...	...	...	...	...	...	...	...
4*B*	1944	...	...	...	...	+ 11	+ 58	− 81	−214	− 30	+149	+ 85	+ 58
	1945	+ 72	−33	− 8	+ 83	+ 63	− 2	− 97	−166	−131	+ 37	+144	+ 10
	1946	−174	−43	+126	+ 83	+197	+ 60	−308	−204	+ 25	+ 14	− 53	+ 3
	1947	+ 34	−25	+145	...	...	...	...	...	...	...	...	...
4*C*	1943	− 17	+71	+ 63	− 27	...	...	...	...	...	...	+ 13	...
	1944	...	...	...	...	...	+ 18	−106	−166	+ 26	+157	+ 67	− 4
	1945	− 11	...	...	...	...	...	...	− 83	−134	− 85	− 20	+ 4
	1946	−121	+73	+160	...	...	...	...	...	...	...	...	...
*A*1	1944	...	...	...	...	...	...	...	...	...	...	+199	+ 96
	1945	+ 74	−10	− 15	+ 88	...	...	...	...	...	...	...	...
Means		− 32	0	+ 81	+ 63	+ 67	+ 10	−135	−150	− 29	+ 72	+ 69	+ 17
Wt.		11	9	9	7	6	7	7	8	9	9	11	10
*C*3	1948	...	...	...	+ 16	+ 58	+118	+ 14	− 58	+ 18	+ 13	+ 1	+107
	1949	+105	+70	+ 90	+ 54	+ 38	− 8	...	...	...	...	...	...
*D*3	1948	...	...	...	+134	+ 63	+ 7	− 85	−155	− 51	+57	+ 94	+158
	1949	+100	+22	+ 57	...	...	...	...	...	...	...	...	...
*A*1	1948	...	...	...	− 3	+ 28	+ 57	− 96	−189	− 54	+ 54	+ 47	+ 62
	1949	+ 14	+19	+ 94	+ 44	+ 25	...	...	...	...	...	...	...
*F*1	1948	...	...	...	− 54	− 72	+ 13	− 35	−142	− 83	+ 15	+ 75	+ 95
	1949	− 16	−45	+ 42	+ 48	+ 51	− 14	...	...	...	...	...	...
*F*3	1948	...	...	...	+ 2	− 9	+ 37	− 32	−109	...	...	...	...
	1949	...	...	...	+ 53	+ 66	− 36	...	...	...	...	...	...
5*B*	1948	...	...	...	+ 74	− 19	− 63	− 98	−101	+ 18	+ 74	+ 11	+ 38
	1949	+ 71	+26	− 24	...	...	...	...	...	...	...	...	...
9*A*	1948	...	...	...	...	+108	+ 67	− 44	− 89	+ 28	+ 91	+ 31	+ 63
	1949	+103	+88	− 24	+ 43	+ 48	− 19	...	...	...	...	...	...
Means		+ 63	+30	+ 39	+ 32	+ 32	+ 15	− 54	−120	− 21	+ 51	+ 43	+ 87
Wt.		6	6	6	11	12	11	7	7	6	6	6	6

The expressions represent that part of the clock correction caused by the seasonal variation, which is now clearly apparent. The effect upon the observed clock rates is obtained by differentiating these expressions with respect to T, when we obtain:

$$\text{for 1943–47} \qquad f' = -0{\cdot}958 \sin n(T+49)^\circ + 0{\cdot}578 \sin 2n(T+22)^\circ,$$

$$\text{and for 1948–49} \qquad f' = -1{\cdot}003 \sin n(T+67)^\circ + 0{\cdot}245 \sin 2n(T+2)^\circ,$$

the unit here being ms./day.

13. The similarity of the curves for the two periods is very marked, the deep trough occurring in August being the most striking feature of the $\Delta'''f$ curves. The second trough appearing in the $\Delta''f$ curve for 1943–47 is the enhanced effect of the second harmonic which is very apparent in f during this period, but much less so during the period 1948–49. It is the enhancement of this harmonic which causes the f' curves to differ more markedly than the f curves. In both periods, however, the clocks appear to go fast in the spring and slow in the autumn, the minima and maxima of the f, or correction curves, occurring in May and October respectively. The date on which f passes through zero on its upward trend occurs early in August during both periods, at the time when the apparent rate, as seen in f', is a maximum. The amplitudes of the two f curves are in close accordance and are about $\pm 0^s{\cdot}060$, while those of the f' curves indicate an annual fluctuation in the apparent rates of $\pm 0^s{\cdot}001$/day.

TABLE II

Number of Observations Secured

	Jan.	Feb.	Mar.	Apr.	May	June	July	Aug.	Sept.	Oct.	Nov.	Dec.
1942	...	...	...	...	...	...	...	...	...	27	33	26
1943	20	24	31	25	29	19	26	25	35	26	34	27
1944	23	17	29	24	20	15	14	23	24	20	19	24
1945	12	19	25	22	17	15	18	16	8	30	15	16
1946	16	10	10	15	16	10	14	24	16	24	20	21
1947	28	7	7	25	21	32	37	62	63	51	47	22
1948	29	48	65	50	38	22	28	25	22	47	34	25
1949	32	48	47	43	63	47	31	36	40	...	...	...

14. Having determined the seasonal fluctuation, the observed clock corrections can be corrected for its effects, and a new set of values for a, b and c for the various clocks determined. This has been done for the Post Office ring-crystal clock 5*B*, which from the daily intercomparisons was known to be amongst those whose performance was the most uniform. The full line in Fig. 3 represents the performance of the clock referred to the finally adopted G.M.T., after removal of a parabolic ephemeris and the polar effect; the dotted line represents its performance further corrected by the f term. The deviations from the ephemeris over the eighteen months ending 1949 June 15, when a failure of temperature control occurred, do not exceed $\pm 0^s{\cdot}020$. Some of the irregularities may be due to observational uncertainties, though at least one is apparent in the intercomparisons with other clocks. Nevertheless, the performance is truly remarkable and illustrates the difficulties with which the astronomer is faced when asked to check the frequencies of crystal oscillators by using the Earth as a standard.

15. The seasonal fluctuation f is one which clearly cannot be ascribed to the clocks, nor can it readily be associated with systematic errors in the observations due to faulty star places, instrumental defects or to local peculiarities.

Table III
Re-integration of Differences

	$\Delta'''f$	$\Delta''f$	$\Delta'f$	f	$\Delta'''f$	$\Delta''f$	$\Delta'f$	f
				Period 1943–47				
Jan.	− 32 − 35	...	...	...	...	...	...	...
Feb.	...	− 35 − 38	...	...	0 − 2	...	...	...
Mar.	+ 81 + 77	...	− 38 − 61	...	...	− 2 − 6	...	...
Apr.	...	+ 42 + 40	...	−61 −48	+ 63 + 61	...	− 6 −36	...
May	+ 67 + 64	...	+ 2 −22	...	...	+ 59 +55	...	− 36 −52
June	...	+106 +103	...	−83 −70	+ 10 + 8	...	+ 49 +19	...
July	−135 −139	...	+105 +82	...	...	+ 67 +63	...	− 17 −34
Aug.	...	− 33 − 35	...	− 1 +11	−150 −152	...	+112 +81	...
Sept.	− 29 − 32	...	+ 70 +46	...	...	− 85 −89	...	+ 64 +48
Oct.	...	− 65 − 68	...	+45 +58	+ 72 + 70	...	+ 23 − 7	...
Nov.	+ 69 + 65	...	+ 2 −21	...	...	− 15 −19	...	+ 57 +40
Dec.	...	0 − 2	...	+24 +37	+ 17 + 15	...	+ 4 −26	...
Jan.	...	...	0 −24	...	...	0 − 4	...	+ 31 +15
Feb.	...	...	...	0 +12	...	...	0 −31	...
Mar.	...	...	...	...	...	...	...	0 −17
Mean	+ 3·5	+ 2·5	+ 23·5	−12·7	+ 2·0	+ 4·0	+ 30·3	+ 16·5
				Period 1948–49				
Jan.	+ 63 + 46	...	...	...	...	...	...	...
Feb.	...	+ 46 + 16	...	...	+ 30 + 14	...	...	...
Mar.	+ 39 + 22	...	+ 16 −33	...	...	+ 14 +32	...	...
Apr.	...	+ 68 + 37	...	−33 −46	+ 32 + 16	...	+ 32 −12	...
May	+ 32 + 15	...	+ 53 + 4	...	...	+ 30 +48	...	− 12 −56
June	...	+ 83 + 53	...	−29 −42	+ 15 − 1	...	+ 80 +36	...
July	− 54 − 71	...	+106 +57	...	...	+ 29 +47	...	+ 24 −20
Aug.	...	+ 12 − 19	...	+28 +15	−120 −136	...	+127 +84	...
Sept.	− 21 − 38	...	+ 87 +38	...	...	−107 −89	...	+108 +64
Oct.	...	− 26 − 56	...	+66 +53	+ 51 + 35	...	+ 38 − 6	...
Nov.	+ 43 + 26	...	+ 31 −18	...	...	− 72 −54	...	+102 +58
Dec.	...	0 − 31	...	+48 +35	+ 87 + 71	...	− 16 −60	...
Jan.	...	...	0 −49	...	...	− 1 +17	...	+ 42 − 2
Feb.	...	...	...	− 1 −14	...	...	+ 1 −42	...
Mar.	...	...	...	...	...	...	...	0 −44
Mean	+ 17·0	+ 30·5	+ 48·8	+13·2	+ 15·8	− 17·8	+ 43·7	+ 44·0

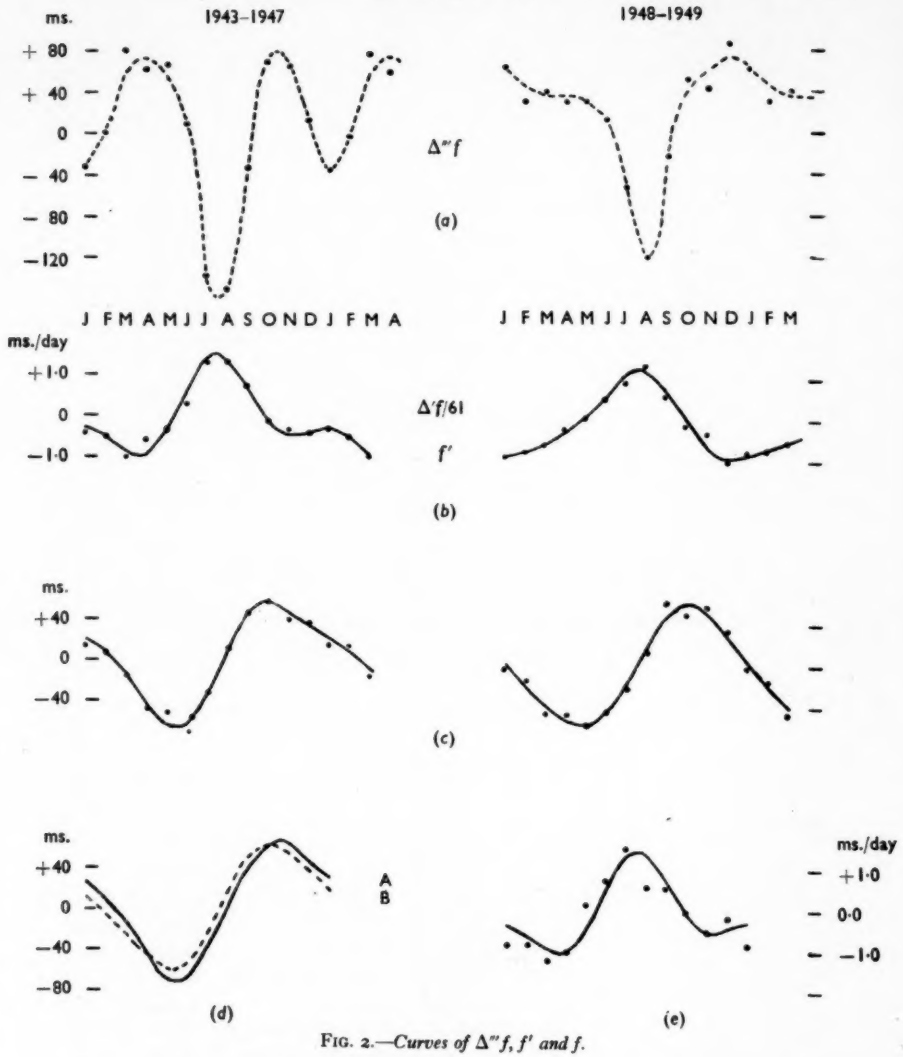

FIG. 2.—*Curves of* $\Delta''f$, f' *and* f.

It is present irrespective of which clocks are employed, and persists in the face of changes of observers, instruments and observing sites. If there were any doubt about this it would be dispelled by the fact that the fluctuations are revealed also by the Washington time observations. Reception at Abinger of the WWV radio signals renders it possible to obtain a close comparison between U.T. as determined at the Naval Observatory, Washington, and the Royal Observatory. After removal of a systematic difference of $+0^{s}\cdot016$ * and the

* Travel time of the signal, if allowed for, would make this about $+0^{s}\cdot036$.

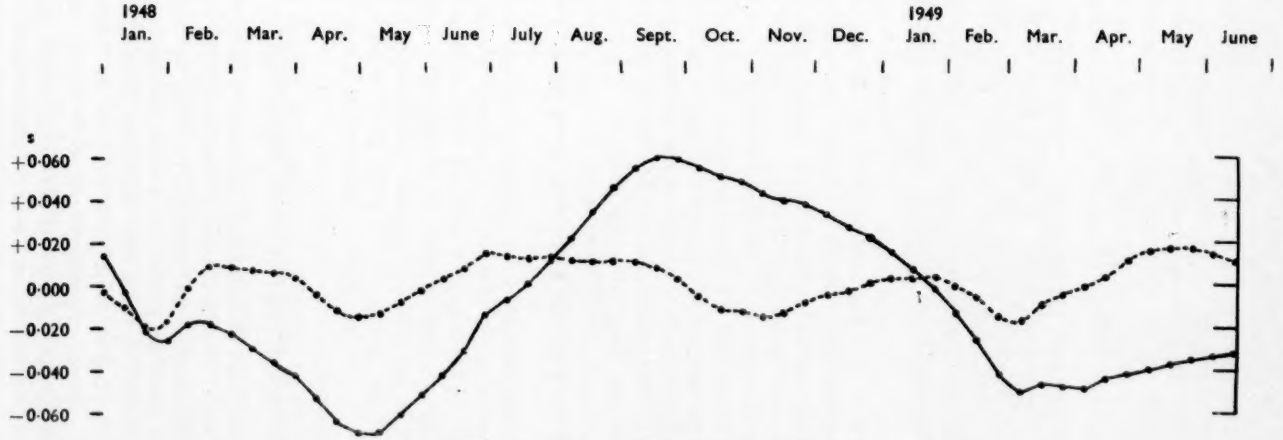

FIG. 3.—*Residual clock corrections of clock 5B, corrected for effect of polar variation.*

Full line : uncorrected for f term.
Dotted line : corrected for f term.
Ephemeris : $a = -0^{s}\cdot009$;
$b = -233\cdot648$ *ms/d* ;
$c = -0\cdot02792$ *ms/d*^{2} ;
Epoch : 1948 *January* 30, 10.00 *hrs.*

effect of polar variation, the monthly mean differences over the four years are, in milliseconds, as follows:—

Jan.	+14	May	−10	Sept.	−10
Feb.	+14	June	−13	Oct.	− 1
Mar.	+11	July	−11	Nov.	+ 9
Apr.	+ 2	Aug.	−12	Dec.	+ 8

These are given as corrections to be applied to the "Greenwich" f curve to obtain the corresponding Washington curve. There appears to be a slight annual variation between the two observatories, but this is small compared with the main fluctuation. Fig. 2 (d) contains a plot of the mean f curve for the two periods referred, A to the American observations and B to the British observations. The difference shows itself as a small phase shift and a slightly increased amplitude in the American curve.

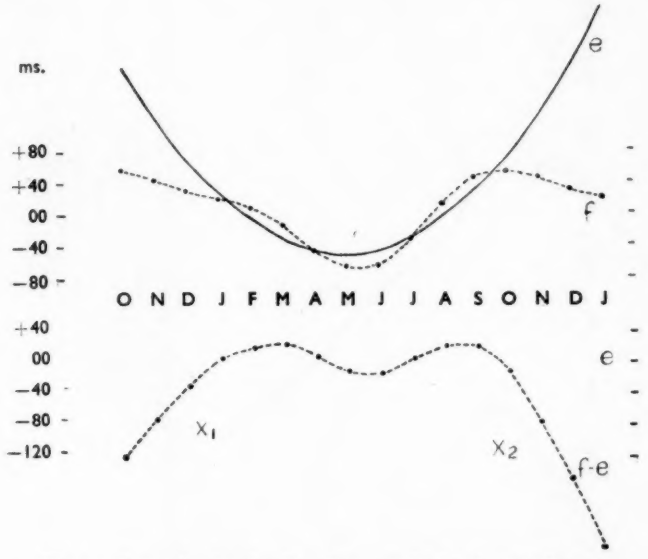

FIG 4.—*Curves showing the effect of an error in the adopted value of c.*

16. It may seem surprising that the sinusoidal character of the phenomenon had not been earlier recognized. During the period that the group 4 clocks were in operation, 4C was for good reasons acknowledged as being the most reliable. The value of c for this clock had been determined and the corresponding values for the others were readily derived by using their frequency drifts relative to 4C. It would now appear that the adopted value (+0·00005) for the frequency drift of 4C was slightly in error, though it provided a good fit over a considerable portion of the f curve. The resulting qualitative effect can be seen on reference to Fig. 4 in which the curve f represents the seasonal fluctuation and e that part of the parabolic ephemeris resulting from the error in the adopted value of c.

Beneath is given the residual curve (f–e). Over the interval X_1–X_2 the deviations from linearity are too small to be revealed by observations subject to a comparatively large scatter in the presence of minor variations in the clock rate. At X_2 the curve rapidly dips. Since no relative change has occurred in the various values of c all the clock curves will behave in the same way and the natural interpretation would be that a *sudden* change in the rotation period of the Earth had occurred. Following the initial run-off, the original value of c will again appear to hold, but at the end of twelve months the Earth will once more appear to slow up.

17. The claim to have established for the first time an annual fluctuation in the Earth's rotation was made by Pavel and Uhink *, based on an investigation of the performance of two quartz-crystal clocks at the Geodetic Institute, Potsdam, during the period 1934 May–1935 June. Referred to the Potsdam time determinations, both clocks showed similar fluctuations in the residuals from a parabolic ephemeris. As the time determinations did not show similar fluctuations relative to the mean of the times determined at nine observatories, it was concluded that the fluctuations were not due to errors of observation but to a variable rate of rotation of the Earth. The material employed did not justify this conclusion, neither clock had an unbroken run during the period discussed, and each was used to smooth over the disturbance of the other when a stoppage occurred. The deduced variations in the rotation, with a range from the mean of from $+0{\cdot}005$ to $-0{\cdot}004$ secs./day, are too large to be real.

On the other hand, N. Stoyko, by comparing the departures of mean monthly rates from a linear rate for the clocks at Paris, Washington and Berlin during the three years 1934–37 (which cover the period of investigations by Pavel and Uhink), obtained a result † in close agreement with that found in the present paper. This paper seems to have attracted little attention, probably because further confirmation of the reality of an annual fluctuation in the Earth's rotation appeared to be required.

The present investigation had been completed when Stoyko published, without details, the results of a study of the rates of the clocks at Paris and Washington from 1946 January to 1947 April ‡, which confirmed his previous conclusions. This period is covered by the Greenwich observations; in Fig. 2 (e) Stoyko's results for the variations in the rate of rotation are plotted in dots upon the Greenwich f' curve for the period 1943–47. Stoyko's representation of his results can be expressed in the form:

$$f' = -1{\cdot}18 \sin n(T+59)^\circ + 0{\cdot}43 \sin 2n(T+42)^\circ,$$

which is in very close agreement with the results obtained by the Greenwich clocks. Stoyko's conclusions about the existence of an annual fluctuation in the period of rotation of the Earth are completely confirmed by the present investigation; moreover, the similarity in amplitude and phase found during the different periods show the effect to be a persistent one.

18. In a recent paper §, van den Dungen, Cox and van Miegham, using observed barometric pressure over the surface of the Earth at opposite seasons, have shown that the effect can be accounted for, at least in part, by changes in

* F. Pavel and W. Uhink, *Ast. Nach.*, **257**, 365, 1935.

† N. Stoyko, *Comptes Rendus*, **203**, 39, 1936; and **205**, 79, 1937.

‡ N. Stoyko, *Bulletin de la Classe de Science, Académie royale de Belgique*, 5e Serie, **XXXV**, 1949.

§ F. H. van den Dungen, J. F. Cox and J. van Miegham, *Bulletin de la Classe de Science, Académie royale de Belgique*, 5e Serie, **XXXV**, 1949.

the Earth's moment of inertia caused by seasonal changes in the distribution of air masses. The data are incomplete and further investigation is required, but the paper constitutes a first attempt to account quantitatively for the phenomena.

19. Since the fluctuation occurs in the unit of time it will introduce a corresponding fluctuation into the observed longitude of the Moon. The observations of occultations have shown for many years a fluctuation of approximately annual period in the Moon's mean longitude. Brouwer and Watts have analysed the results of the occultation observations and of the Washington meridian observations of the Moon*, deriving corrections to the elements of the orbits of the Moon and the Earth. They suggested that one term, not otherwise accounted for, might be attributed to an annual variation in the rate of rotation of the Earth. The variations shown by Stoyko's and by the present investigation are, however, much too small to account for this term in the Moon's longitude for which, therefore, some other explanation must be sought.

20. In conclusion, the practical importance of the fluctuation and its effect upon the estimated frequency of standard oscillators must be emphasized, together with the need for a precise definition of the Mean Solar Second which takes into account both this and the effect of the polar variation upon time.

The author wishes to acknowledge the assistance received from his colleagues in the present investigation and the close cooperation of the Post Office Engineers, without which the data available would have been greatly restricted.

Royal Greenwich Observatory,
Abinger :
1949 *December* 15.

* D. Brouwer and C. B. Watts, *Astron. J.*, **52**, 169, 1947.

ADDENDUM

Since going to press a further paper by W. Uhink (*Ast. Nach.*, **278**, No. 3, 1950) dealing with the above subject has now become available. This paper contains an account of results obtained during recent years in Germany.

RELATIVE GRADIENTS FOR 166 SOUTHERN STARS

S. C. B. Gascoigne

(Communicated by the Commonwealth Astronomer)

(Received 1950 February 10) *

Summary

Relative gradients for 166 southern stars were determined by photographic spectrophotometry with a slitless spectrograph attached to the 30-inch Reynolds reflector. The system is believed to be uniform with that of Greenwich. The relations between the Mount Stromlo gradients and the colours of other observers are examined, and the colours of a group of very blue B stars discussed with regard to their bearing on the spectrum-colour relation and on the stellar temperature scale.

---

1. *Introduction.*—This paper describes observations of the relative spectrophotometric gradients of a number of the brighter southern stars. The programme was designed as a southward extension of the Greenwich relative gradient programme (**1, 2**), and follows Greenwich closely, both in instrumental equipment and in general observing procedure. Observations were commenced in 1948 May with a slitless spectrograph attached to the 30-inch Reynolds reflector. By 1949 June about 2500 spectra of 170 odd stars had been taken, yielding gradients with standard errors of 0·02 or 0·03, a satisfactorily small figure and a comparable one to that attained at Greenwich. At this stage it was decided to suspend the programme, with the intention of resuming it with lower dispersion and so reaching fainter stars. The present is therefore a convenient time for describing the results so far obtained. This is especially so, as the programme includes a number of interesting stars for which no other spectrophotometric data exist at all.

The first part of the paper describes the observing procedure and concludes with the catalogue of gradients. In the second the Mount Stromlo gradients are compared in detail with those of a number of other observers; an apparent anomaly in the colours of α C Maj and α Cari is examined; and the colours of a group of very blue stars are discussed with regard to their bearing on the spectrum-colour relation and on the stellar temperature scale.

2. *The Spectrograph.*—The spectra were taken on the 30-inch Reynolds reflector, on a slitless spectrograph similar to that described by Davidson (**3**), and built in the Observatory shops to a design by Dr Allen and Mr Gottlieb. The optical arrangement is shown in Fig. 1. The dispersion at $H\gamma$ was 45 A./mm. The diagonal mirror D immediately before the plate was mounted on a spindle about which it could be given a small to-and-fro rotation by the usual heart-shaped cam-and-lever arrangement, to widen the spectra to $\frac{1}{2}$ mm. Irregularities in the telescope drive presented difficulties for a while, by introducing streaks into the spectra. A careful remachining of the main worm, carried out at the Marybyrnong Defence Research Laboratories, substantially reduced the trouble, which was finally almost eliminated by the adoption of a simple guiding device.

* Received in original form 1949 November 28.

The third (plane) mirror A was mounted so that it could be rotated about an axis coincident with the axis of the primary mirror, the amount of rotation being controlled by an arm and screw at B. The star under observation was centred on the guiding eyepiece cross-wire, and during exposure was maintained there, an appropriate rotation of the screw B counteracting any tendency to wander, induced by faulty driving. The scheme worked well, and only a few spectra had finally to be rejected because of streaks.

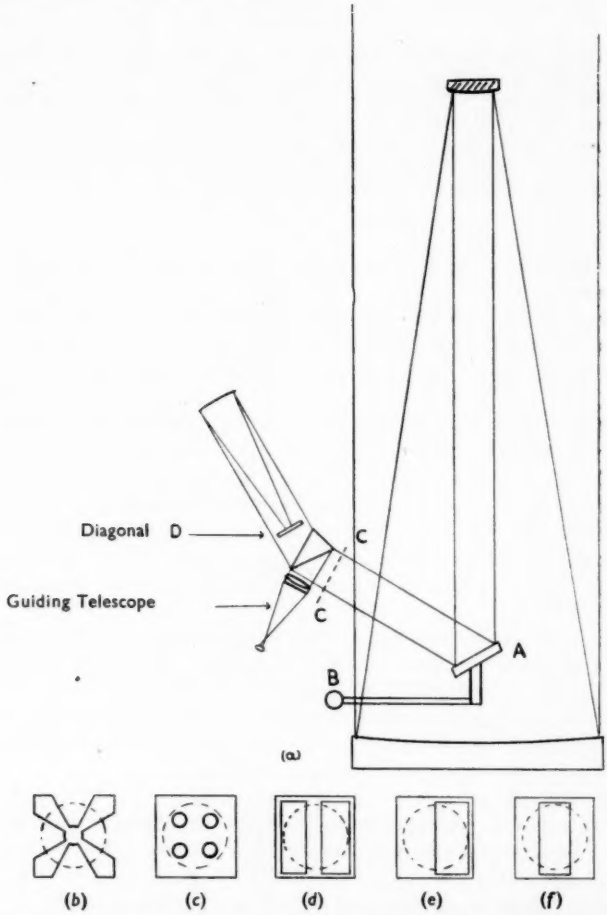

FIG. 1.—*(a) The optical train. (b)–(f): Diaphragms inserted into the collimated beam at CC. B is a screw and arm which rotates A about an axis coincident with the axis of the primary mirror. The diagonal D is rocked to widen the image.*

3. *Plate Calibration.*—Plates were calibrated at the telescope, by taking a number of equal-interval exposures of the same star, with a series of diaphragms inserted in turn into the collimated beam (in the plane CC) to give varying reduction factors. Two sets of diaphragms were constructed. The first, which

consisted of six half-magnitude steps, took the form of Maltese crosses for the ½ and 1 magnitude steps, and of plates with four equal symmetrical holes for the 1½, 2, 2½ and 3 magnitude steps. (See Fig. 1 (*b*) and (*c*).) The calculation of the fraction of incident light transmitted by a diaphragm involved a calculation of the cross-sectional area of the beam, and this was made difficult by the complicated nature of the obstructions introduced by the secondary and diagonal mirrors and their supports. However, Mr Hogg and Miss Mason, who were working on the same spectrograph on a programme of monochromatic photoelectric photometry, kindly undertook a direct calibration of the diaphragms with their photocell. They repeated this twice, with results which agreed to about 0·01 mag. in the mean, and were of ample accuracy for photographic work.

The constancy of the transmission factors of diaphragms of this sort depends on the constancy of cross-section of the collimated beam, and would have been upset by any such variations as, say, those introduced by changes in the setting of the Cassegrain paraboloid. Variations of this sort were apt to occur on the replacing and realigning of the spectrograph after it had been removed to make way for other programmes, and did on one occasion lead to a change (of 0·03 mag.) in the constants of diaphragms (Fig. 1). However, it was found possible to check the beam cross-sections, and indeed to get a good idea of the area of most of the obstructions, by setting on a bright star and exposing a half-plate at CC. With Canopus ($-0{\cdot}8$ mag.) an image of the beam cross-section was recorded in about a minute.

Moreover, as reference to Fig. 1 will show, the transmission factors for the Maltese crosses (*b*), and especially the *relative* transmissions for the plates (*c*), should have been independent of the beam cross-section. Our limited evidence on this point was certainly not opposed to this conclusion. (It was also found that the relative transmissions for plates (*c*) as measured by the photocell agreed to within 0·01 mag. with those computed from the hole diameters.) Whenever possible the step 1–1½ mag. was avoided in deriving the actual calibration curves, and, this precaution having been adopted, the writer feels that errors arising from possible variations in the beam cross-section have been effectively eliminated.

Although no trouble was expected from this source, it seemed desirable to carry out a completely independent basic calibration, and a second set of diaphragms was accordingly constructed. These are illustrated in Fig. 1 (*d*, *e* and *f*) and worked on the half-aperture principle. In calibrating a plate, diaphragm (*d*) was first inserted, and three successive exposures made, the first with (*d*) only, and the remaining two with (*e*) added in such a way as to cut out the east and west halves of the mirror in turn. The order of these exposures was varied from star to star. The three diaphragms (*f*) were used to reduce the light of brighter stars. These three proceeded at approximately ¾ magnitude steps and gave, with (*e*), a total range of three magnitudes. This method of calibration was independent of the beam cross-sections.

To verify the equivalence of these two methods of calibration there were available 42 programme stars for which, with a few exceptions, at least two determinations of gradient had been made by each method. For the 42 stars the unweighted mean difference (diaphragm gradient)–(half-aperture gradient) was $-0{\cdot}011 \pm 0{\cdot}008$ (s.e.). For the 16 bluest stars of the group it was $-0{\cdot}015 \pm 0{\cdot}012$, and for the 10 reddest stars it was $+0{\cdot}005 \pm 0{\cdot}013$. These figures are considered satisfactorily small. Not much significance is attached to

the slight systematic trend from blue to red, especially as one would have expected the effects of faulty calibration to be most marked for the red stars, for which, on our plates, the red end was much more heavily exposed than the blue.

4. *Plate Measurement.*—We had intended to use Eastman 103-F plates but as they could not be obtained in time Kodak Panatomic-X were used instead. Apart from the drawback that their red sensitivity did not extend beyond about λ6400, these Pan-X plates were very satisfactory, with fine grain, low contrast (an advantage in this work) and speed enough to record a fifth magnitude early-type star in three minutes. 22 spectra were normally secured on one quarter-plate, usually, although by no means invariably, all with the same exposure time, which was 20, 60 or 180 seconds. Each star was taken twice, if possible with different diaphragms, so that its spectra could be obtained at different density levels. If the calibration was performed with the first set of diaphragms four exposures of the calibrating star were usually made, to give four calibrating spectra (sometimes three or five). With the second set of diaphragms only three exposures were necessary, and two stars were then used to calibrate a plate.

Plates were developed four at a time, in a tank with a plunger for agitating the developer. Kodak D-19 was used throughout. In the wave-length range used, λ6209 to λ4050, three calibration curves usually represented well enough the variation of contrast with wave-length, and these curves were assumed common to all four plates of any one batch.

We measured the plates in the projection photometer described previously (**4**), at the following eleven wave-lengths: $\lambda\lambda$6209, 6035, 5825, 5550, 5259, 4945, 4660, 4510, 4250, 4170, 4050. The harmonic mean is λ4938. These wave-lengths were chosen with some care, to ensure that they were as free as possible from absorption lines, and so that they would avoid regions where the plate sensitivity was changing rapidly. Stars of spectral type later than about F6 were measured only at the first eight wave-lengths, as over the last three they showed the deficiency of radiation noted by Plaskett (**5**) and others. For the same reason it was decided not to measure farther into the violet than λ4050, as beyond that point early A stars on our plates are weakened, presumably because of confluence of the wings of the hydrogen lines.

The usual assumption was made, that the relative monochromatic magnitude difference Δm_λ between two stars varies with wave-length according to the law $a+b/\lambda$. The relative gradient is then $0{\cdot}921\,b$ (λ in microns), and was found from a least squares solution for a and b, the Δm_λ having been measured as above.

One small but important addition to the photometer was that of a rheostat in the plate circuit for varying the amplification. This provided a means for holding the clear glass deflection at 100, and so enabled transmissions to be read directly as percentages, a considerable saving in time and clerical work. Plates were measured once only, previous experience, and a number of trials with the present series, having shown that there is little to be gained from a second measurement.

It has been pointed out that spectra were not always taken with the same exposure times, and we had to find whether this necessitated a correction. For this purpose we had available about thirty pairs of spectra, taken with exposure times either of 20 and 60 sec., or of 60 and 180 sec., and hence always in the ratio of three to one. We measured and reduced these on the lines suggested by Greaves (**6**) but in spite of the appreciable reciprocity failure shown by

Panatomic-X (corresponding to a Schwarzschild exponent of about 0·8), it was found that with our small exposure time ratio the correction could be neglected, even for the reddest stars on the programme.

5. *The Standard System.*—We selected as standards eighteen stars of early type, well distributed about the sky, which were intercompared frequently, and relative to which the gradients of all other stars were determined. The selection is set out in Table I. It will be noted that seven of the eighteen are also Greenwich standards. All comparisons of standard stars were made at equal altitude. It was often possible to compare a run of three, four or sometimes more stars which would pass through a common altitude at closely succeeding times. Such groups were picked from a most convenient graph on which sec z for each standard star was plotted against sidereal time. Fig. 2 summarizes the scheme, each line representing a series of comparisons between the two stars it joins. A number of comparisons of low weight were omitted from this diagram.

TABLE I

The Standard Stars

Star	m_p	H.D. type	*S*	Wt.	*G*	*S–G*	*H*	*S–H*	*BC*	*S–BC*
γ Pegs	3·0	B2	−25·4	4	−29·7	4·3	−32	7	−27	2
α Erid	0·6	B5	−23·6	12	...	...	...	...	...	...
β Aris	2·7	A5	29·8	4	29·1	0·7	27	3	+33	−3
β Orio	0·3	B8p	− 0·9	8	...	...	8	−9	− 1	0
γ Orio	1·7	B2	−28·5	4	−23·7	−4·8	−33	5	−30	2
ε C Maj	1·6	B1	−27·8	8	...	...	...	...	−26	−2
δ Velr	1·9	Ao	6·0	8	...	...	...	...	...	...
β Cari	1·7	Ao	1·7	8	...	...	...	...	...	...
α Leon	1·3	B8	−11·8	4	− 8·5	−3·3	−12	0	−17	5
γ Cent	2·3	Ao	− 1·6	8	...	...	...	...	...	...
α Virg	1·2	B2	−33·7	8	...	...	−32	−2	−31	−3
β Cent	0·9	B1	−33·2	16	...	...	...	...	...	...
α Ophi	2·1	A5	30·5	12	30·1	0·4	30	0	+32	−2
ε Sgtr	1·9	Ao	3·6	12	...	...	...	...	...	...
α Aqil	0·9	A5	41·6	8	42·1	−0·5	45	−3	+43	−1
α Pavo	2·1	B3	−24·9	12	...	...	...	...	...	...
α Psc A	1·3	A3	10·7	12	...	...	...	...	+16	−5
α Pegs	2·6	Ao	0·1	4	− 3·0	3·1	− 8	8	− 8	8

S indicates the gradient as determined at Mount Stromlo; *G* at Greenwich; *H* by Hall; *BC* by Barbier and Chalonge. The unit is 0·01.

A least squares solution of all these data was made and the results entered in column 4 of Table I, with approximate weights in column 5, unit weight corresponding to a standard error of ±0·04. The zero, which of course is arbitrary, was adjusted to make the weighted mean difference Mount Stromlo minus Greenwich vanish. This adjustment fixes the zero of all the gradients in this paper. The Greenwich values in column 6 are from page 20 of reference (1). The figures after the decimal point in columns 4 and 6 have no real significance.

From the residuals of the least squares solution the standard error of one comparison was found to be ±0·04, appreciably lower than the Greenwich figure of ±0·07 or 0·08. The difference may well be attributed to the clearer atmosphere over the New South Wales table-lands. The unweighted r.m.s. difference Mount Stromlo minus Greenwich (col. 7) comes out as ±0·032 (allowance being

made for the zero adjustment), a very satisfactory figure in view of the s.e. of $\pm 0{\cdot}02$ quoted for the Greenwich standard stars. The unweighted mean absolute difference is $\pm 0{\cdot}025$.

The gradients in column 8 are taken from Hall's photoelectric work (**7**), the values in the table being the mean of the Sproul values with 0·01 subtracted, and of the Amherst values with 0·02 added. Hall made these adjustments to bring his gradients into systematic agreement with those of Greenwich. The mean absolute difference Mount Stromlo minus Hall is $\pm 0{\cdot}041$; the mean absolute difference Greenwich minus Hall was $\pm 0{\cdot}044$. According to Hall 0·01 should be added to our gradients.

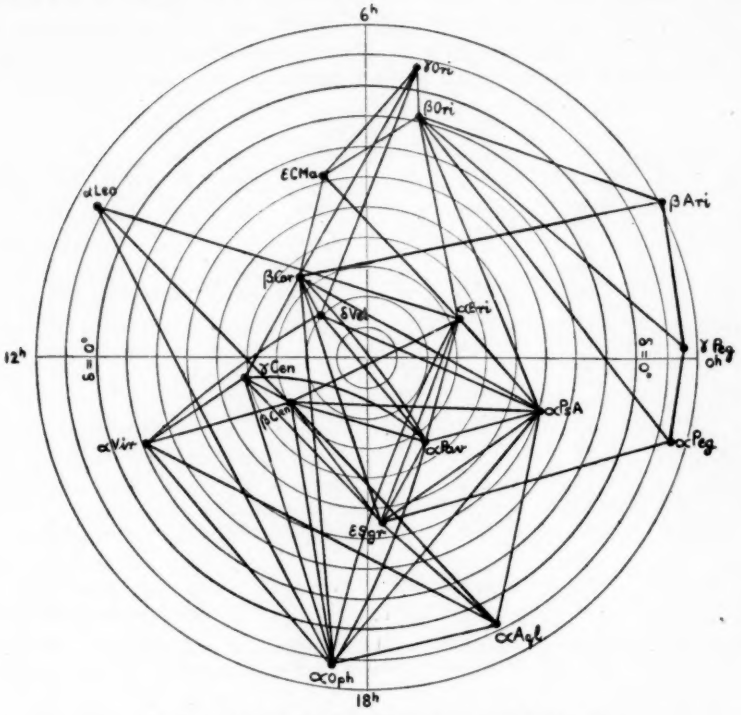

FIG. 2.—*Equialtitude comparisons between standard stars.*

Finally Barbier and Chalonge's gradients (**8**), measured photographically in the region $\lambda 3700$–4600, appear in column 10. We have tabulated $\phi_{1G} - 1{\cdot}06$, ϕ_{1G} being Barbier and Chalonge's ϕ_1 corrected by their Table VII, i.e. referred from a mean wave-length of $\lambda 4250$ to a mean of $\lambda 5000$, and the 1·06 a constant which brings the French gradients into systematic agreement with both Greenwich and ourselves. The mean absolute difference Mount Stromlo minus Barbier and Chalonge is then $\pm 0{\cdot}03$.

More complete comparisons with other observers are made later in the paper. As far as the standard stars are concerned, the general agreement must be considered good.

6. *Programme Stars.*—The programme was made up of most of the brighter southern stars of early type, enough northern stars to ensure a good overlap with northern observers, a number of later-type stars, and some fainter stars (down to 5·1 mag.) of interest. We planned to measure each programme star on at least three nights, against at least two standard stars. Actually only five stars received less than three full-weight determinations, and over half received four or more. As it was impracticable to make all programme star comparisons at equal altitudes we had to correct for atmospheric reddening. The usual assumption was made, that the lower of two stars being compared appears redder by $A(\sec z_1 - \sec z_2)$, where z_1 and z_2 are the zenith distances of the two stars and A is a coefficient which has to be determined. A was found as at Greenwich, by comparing standard stars at different altitudes, groups of standards, well distributed in azimuth, being compared where possible. The values for A ranged from 0·25 to 0·40; on the best nights A was very near 0·30, and only on two out of 42 nights did it exceed 0·40.

In Table II are assembled all the relative gradients determined. The columns show in order the number of the star in the Yale Bright Star Catalogue (i.e. the H.R. number), its name, its R.A. and Dec. for 1950, its galactic latitude and longitude and its visual magnitude. Column 8 is the H.D. spectral type, and column 9 the type either as given in the Yerkes "Atlas" (**9**) or as determined by Miss M. L. Woods at this Observatory from a classification on the Yerkes system of a large number of objective prism spectra taken by the late Mr W. B. Rimmer (**10**). "Atlas" types are italicized. Finally in column 10 is the mean gradient as determined at Mount Stromlo.

TABLE II

B.S. No.	Star	R.A. 1950	Dec. 1950	Galactic coords. l	b	m_v	Spectral type H.D.	MKK	Gradient G
39	γ Pegs	0 10·7	+14 54	79	−46	3·0	B2	*(B2 V)*	−0·25
98	β Hydi	0 23·2	−77 32	271	−40	2·8	Go	G1 IV	1·27
338	ζ Phoe	1 06·3	−55 31	263	−62	4·1	B8	B8 V	−0·08
472	κ Erid	1 35·9	−57 29	256	−59	0·6	B5	B5 IV	−0·24
509	τ Ceti	1 41·7	−16 12	142	−73	3·5	Ko	*(G8 V)*	1·43
553	β Aris	1 51·9	+20 34	111	−39	2·7	A5	*(A5 V)*	0·30
591	α Hydi	1 57·2	−61 49	255	−54	3·0	Fo	Fo V	0·59
674	ϕ Erid	2 14·7	−51 45	241	−60	3·7	B8	B8 V	−0·06
779	δ Ceti	2 36·9	+00 07	140	−51	4·0	B2	B2 V	−0·16
897*	θ Erid	2 56·4	−40 30	213	−60	3·4	A2	A3 III	0·40
1347	41 Eri d	4 16·0	−33 55	200	−47	3·6	B9	B8·5 V	−0·04
1443	δ Cael	4 29·3	−45 04	218	−42	5·1	B3	...	−0·17
1465	α Dora	4 32·9	−55 09	231	−41	3·4	Aop	Ao III (Si)	−0·08
1543	π^3 Orio	4 47·1	+06 53	159	−22	3·2	F8	*(F6 V)*	1·05
1552	π^4 Orio	4 48·5	+05 31	161	−22	3·7	B3	B2 IV	−0·10
1567	π^5 Orio	4 51·6	+02 22	164	−23	3·8v	B3	B2 IV	−0·13
1666	β Erid	5 05·4	−05 09	173	−24	2·9	A3	A3 V	0·34
1702	μ Leps	5 10·7	−16 16	184	−28	3·2	Aop	B9 III (Mn)	−0·08
1713	β Orio	5 12·1	−08 15	177	−24	0·3	B8p	*(B8 Ia)*	−0·01
1735	τ Orio	5 15·2	−06 54	176	−22	3·6	B5	B8 III	−0·10
1788	η Orio	5 22·0	−02 26	172	−19	3·3	B1	*(B1 V)*	−0·13
1790	γ Orio	5 22·4	+06 18	165	−14	1·7	B2	*(B2 IV)*	−0·28
1852	δ Orio	5 29·5	−00 20	171	−16	2·5	Bo	*(O9·5 III)*	−0·23
1865	α Leps	5 30·5	−17 51	188	−24	2·6	Fo	*(F0 Ib)*	0·56
1879	λ Orio	5 32·4	+09 54	163	−10	3·5	Oe5	*(O8)*	−0·13

TABLE II—*Continued*

B.S. No.	Star	R.A. 1950	Dec. 1950	Galactic coords. l	b	m_v	Spectral type H.D.	MKK	Gradient G
1899	ι Orio	5 33·0	−05 56	177	−18	2·9	Oe5	(*O9 V*)	−0·26
1903	ε Orio	5 33·7	−01 14	173	−16	1·7	Bo	(*B0 I*)	−0·13
1931	σ Orio	5 36·2	−02 38	175	−16	3·8	Bo	(*O9·5 V*)	−0·28
1948	ζ Orio	5 38·2	−01 58	174	−15	2·0	Bo	(*O9·5 III*)	−0·20
1956	α Colm	5 37·8	−34 06	206	−28	2·6	B5p	B8 Ve	−0·12
1983	γ Leps	5 42·4	−22 28	194	−23	3·7	F8	F6 V	1·03
1998	ζ Leps	5 44·7	−14 50	187	−19	3·6	A2	A3 V	0·22
2004	κ Orio	5 45·4	−09 41	182	−17	2·2	Bo	(*B0 II*)	−0·09
2282	ζ C Maj	6 18·4	−30 02	205	−18	3·1	B3	B3 V	−0·26
2294	β C Maj	6 20·5	−17 56	193	−13	2·0	B1	(*B1 II–III*)	−0·27
2326	α Cari	6 22·8	−52 40	228	−25	−0·8	Fo	Fo Ia	0·25
2421	γ Gemi	6 34·8	+16 27	164	+ 6	1·9	Ao	(*A1 V*)	0·06
2451	ν Pupp	6 36·2	−43 09	220	−20	3·1	B8	B8 III	−0·09
2456	15 Mono	6 38·2	+09 56	171	+ 4	4·7	Oe5	...	−0·26
2491	α C Maj	6 42·9	−16 39	195	− 8	−1·4	Ao	A1 V	−0·16
2550	α Pict	6 47·7	−61 53	239	−24	3·2	A5	A5 III	0·47
2618	ε C Maj	6 56·7	−28 54	208	−10	1·6	B1	(*B1 II*)	−0·28
2653	o^2 C Maj	7 00·9	−23 46	203	− 7	3·1	B5p	(*B3 I*)	0·03
2693	δ C Maj	7 06·4	−26 19	206	− 7	1·9	F8p	(*F8 Ia*)	1·17
2749	ω C Maj	7 12·8	−26 41	207	− 6	3·8	B3p	B3 IV(e)	−0·12
2781	29 C Maj	7 16·6	−24 29	205	− 4	4·5v	Oe	...	−0·09
2782	τ C Maj	7 16·6	−24 52	206	− 4	4·4	Oe5	...	−0·08
2827	η C Maj	7 22·1	−29 12	210	− 6	2·4	B5p	(*B5 I*)	0·04
2845	β C Min	7 24·4	+08 23	177	+13	3·0	B8	(*B8 V*)	−0·07
2943	α C Min	7 36·7	+05 21	181	+14	0·4	F5	(*F5 IV*)	0·88
3129	υ Pupp	7 56·8	−49 06	231	− 9	4·1v	B1p	...	−0·13
3165	ζ Pupp	8 01·8	−39 52	224	− 4	2·3	Od	(*O5*)	−0·28
3206	γ^1 Velr	8 07·9	−47 12	230	− 7	4·8	B3	...	−0·24
3207*	γ^2 Velr	8 08·0	−47 11	230	− 7	2·1	Oap	WC7	−0·28
3447	*o* Velr	8 38·9	−52 45	238	− 6	3·6	B3	B3 V	−0·33
3454	η Hyda	8 40·6	+ 3 55	192	+28	4·3	B3	B3 V	−0·23
3468	α Pyxi	8 41·6	−33 00	223	+ 6	3·7	B2	B2 II	−0·17
3485	δ Velr	8 43·3	−54 31	240	− 7	1·9	Ao	Ao V	0·06
3482	ε Hyda	8 44·1	+ 6 36	189	+30	3·5	F8	(*G0 III*)	1·35
3571	106 G Cari	8 53·9	−60 27	245	−10	3·9	B8	B8·5 III	−0·08
3659	α Cari	9 09·7	−58 45	245	− 7	3·4	B3	B3 IV	−0·27
3665	θ Hyda	9 11·8	+ 2 32	197	+34	3·8	Ao	Ao Vp	−0·06
3685	β Cari	9 12·7	−69 31	253	−15	1·7	Ao	Ao III	0·02
3734	κ Velr	9 20·6	−54 48	244	− 3	2·5	B3	B2 IV	−0·27
3786	ψ Velr	9 28·7	−40 15	234	+ 8	3·5	F5	F2 III	0·78
3940	φ Velr	9 55·1	−54 20	246	0	3·6	B5	B5 I–II	−0·05
3982	α Leon	10 05·7	+12 13	195	+50	1·3	B8	(*B8 V*)	−0·12
4037	ω Cari	10 12·6	−69 47	257	−12	3·4	B8	B8·5 IV	−0·08
4133*	ρ Leon	10 30·2	+09 34	204	+54	3·8	Bop	B1 I	−0·10
4140	205 G Cari	10 30·2	−61 26	253	− 4	3·4	B5p	B5 IVpe	−0·08
4199	θ Cari	10 41·2	−64 08	257	− 5	2·9	Bo	Bo Vp	−0·32
4467	λ Cent	11 33·5	−62 45	262	− 2	3·2	B9	B9 III	−0·04
4520	λ Musc	11 43·2	−66 27	264	− 6	3·7	A5	A5 V	0·36
4534	β Leon	11 46·5	+14 51	222	+72	2·4	A2	(*A3 V*)	0·22
4621	δ Cent	12 05·8	−50 27	264	+12	2·9	B3p	B2 Ve	−0·11
4656	δ Crux	12 12·5	−58 28	266	+ 4	2·9	B3	B2 IV	−0·32
4662	γ Corv	12 13·2	−17 01	261	+44	2·6	B8	B8·5 III	−0·12
4730/31*	α Crux	12 23·8	−62 49	268	− 2	0·9	B1	B1 IV	−0·41
4757	δ Corv	12 27·3	−16 14	264	+45	2·9	Ao	(*B9 V*)	−0·05
4773	γ Musc	12 29·5	−71 51	269	−10	3·9	B5	B5 IV	−0·21

TABLE II—*Continued*

B.S. No.	Star	R.A. 1950	Dec. 1950	Galactic coords. l	b	m_v	Spectral type H.D.	MKK	Gradient G
4798	α Musc	12 34·2	−68 52	269	− 6	2·8	B3	B3 IV	−0·28
4819	γ Cent	12 38·7	−48 41	269	+13	2·3	Ao	Ao III	−0·02
4825	γ Virg	12 39·1	−01 11	268	+61	2·8	Fo	*(F0 V)*	0·80
4844	β Musc	12 43·2	−67 50	270	− 6	3·1	B3	B3 V	−0·24
4853	β Crux	12 44·8	−59 25	270	+ 3	1·4	B1	Bo III	−0·36
4898*	μ Crux	12 51·7	−56 54	271	+ 5	4·3/5·5	B3/B3p	B3 V	−0·18
5020	γ Hyda	13 16·2	−22 54	281	+38	3·1	G5	*(G5 III)*	1·72
5028	ι Cent	13 17·8	−36 27	278	+25	2·9	A2	A2 V	0·08
5056	α Virg	13 22·6	−10 54	286	+50	1·2	B2	*(B1 III–IV)*	−0·34
5132	ε Cent	13 36·7	−53 13	278	+ 8	2·4	B1	B1 IV	−0·30
5190	ν Cent	13 46·5	−41 26	283	+19	3·5	B2	B2 V	−0·29
5193	μ Cent	13 46·6	−42 14	282	+19	3·2	B2p	B2 Ve	−0·10
5231	ζ Cent	13 52·4	−47 03	282	+14	3·0	B2p	B2 IV	−0·31
5235	η Boot	13 52·3	+18 39	332	+72	2·7	Go	*(G0 IV)*	1·05
5248	φ Cent	13 55·2	−41 52	284	+18	4·0	B3	B2 V	−0·26
5267	β Cent	14 00·3	−60 08	280	+ 1	0·7	B1	B1 II	−0·33
5354	ι Lupi	14 16·2	−45 50	286	+14	4·1	B3	B3 V	−0·22
5440	η Cent	14 32·3	−41 56	291	+16	2·5	B3p/A2p	...	−0·23
5459/60*	α Cent	14 36·2	−60 38	284	− 2	0·1	Go/K5	G2 V	1·27
5463	α Circ	14 38·4	−64 46	283	− 6	3·3	Fo	Fo VSr	0·49
5469	α Lupi	14 38·6	−47 10	290	+11	2·8	B2	B2 II	−0·25
5531	α^2 Libr	14 48·1	−15 50	310	+37	2·8	A3	A3 (met)	0·39
5571	β Lupi	14 55·2	−42 56	294	+13	2·7	B2p	B2 IV–V	−0·25
5576	κ Cent	14 55·9	−41 54	295	+14	3·3	B3	B2 V	−0·29
5671	γ Tri A	15 14·2	−68 30	283	−10	3·0	Ao	Ao VEu	0·03
5685	β Libr	15 14·3	−09 12	320	+38	2·7	B8	*(B8 V)*	−0·09
5695	δ Lupi	15 18·1	−40 28	299	+13	3·3	B2	B2 IV	−0·31
5708	ε Lupi	15 19·3	−44 31	297	+ 9	3·6	B3	B3 V	−0·22
5776	γ Lupi	15 31·8	−41 00	301	+11	2·9	B3	B3 V	−0·24
5812	τ Libr	15 35·6	−29 37	309	+19	3·7	B3	B3 V	−0·18
5897	β Tri A	15 50·7	−63 17	290	− 9	3·0	Fo	F2 V	0·68
5928	ρ Scor	15 53·7	−29 04	313	+17	4·0	B3	B2 V	−0·26
5944	π Scor	15 55·8	−25 58	315	+19	2·9	B2	*(B2 IV)*	−0·23
5948	η Lupi	15 56·8	−38 16	307	+10	3·6	B3	B2 IV–V	−0·29
5953	δ Scor	15 57·4	−22 29	318	+21	2·5	Bo	*(B0 IV)*	−0·11
5984	β Scor	16 02·5	−19 40	321	+22	2·8	B1	*(B0·5 IV)*	0·01
6084	σ Scor	16 18·1	−25 28	319	+16	3·0	B1	*(B1 III)*	0·48
6165	τ Scor	16 32·8	−28 07	319	+12	2·9	Bo	*(B0 V)*	−0·27
6175	ζ Ophi	16 34·4	−10 28	334	+22	2·6	Bo	*(O9·5 V)*	0·22
6241	ε Scor	16 46·9	−34 12	317	+ 5	2·2	Ko	K2 III–IV	2·00
6247*	μ^1 Scor	16 48·5	−37 58	314	+ 3	3·1v	B3p	...	−0·26
6252	μ^2 Scor	16 49·0	−37 56	314	+ 3	3·7	B2	B2 IV	−0·30
6262*	ζ^1 Scor	16 50·4	−42 17	311	0	4·9	B1p	...	1·45
6378	η Ophi	17 7·5	−15 40	335	+12	2·5	A2	*(A2 V)*	0·13
6380	η Scor	17 8·6	−43 11	312	− 4	3·4	F2	F2 III	0·86
6453	θ Ophi	17 18·9	−24 57	328	+ 5	3·3	B3	*(B2 IV)*	−0·21
6462	γ Arae	17 21·2	−56 19	302	−13	3·4	B1	B1 V	−0·11
6500	δ Arae	17 26·6	−60 39	299	−16	3·6	B8	B8 V	−0·14
6508	υ Scor	17 27·4	−37 15	319	− 3	2·7	B3	B2 IV	−0·33
6510	α Arae	17 28·0	−49 50	308	−10	2·8	B3p	B3 Ve	−0·20
6527	λ Scor	17 30·2	−37 04	320	− 4	1·7	B2	*(B2 IV)*	−0·34
6553	θ Scor	17 33·7	−42 58	315	− 8	2·0	Fo	Fo I–II	0·86
6556	α Ophi	17 32·6	+12 36	4	+21	2·2	A5	*(A5 III)*	0·30
6580	κ Scor	17 39·0	−39 00	319	− 6	2·3	B2	B2 IV	−0·32
6615	ι^1 Scor	17 44·1	−40 07	318	− 8	3·0	F5p	Fo I	1·15

TABLE II—*Continued*

B.S. No.	Star	R.A. 1950	Dec. 1950	Galactic coords. l	b	m_v	Spectral type H.D.	MKK	Gradient G
6743	θ Arae	18 02·7	−50 06	311	−16	3·8	B1p	B1 II	0·03
6879	ϵ Sgtr	18 20·9	−34 25	327	−12	1·9	A0	B9 IV	0·04
6897	α Tele	18 23·3	−46 00	316	−16	3·7	B3	B3 V	−0·21
7039	ϕ Sgtr	18 42·5	−27 03	336	−12	3·2	B8	B8 III	−0·07
7074*	λ Pavo	18 47·6	−62 14	301	−25	4·0	B2	B2 IIIe	Var
7107*	κ Pavo	18 51·8	−67 18	296	−27	4·2v	F5p	...	Var
7121	σ Sgtr	18 52·2	−26 22	337	−14	2·1	B3	(*B3 IV–V*)	−0·27
7194	ζ Sgtr	18 59·2	−29 57	334	−17	2·7	A2	A2 IV	0·14
7235	ζ Aqil	19 03·1	+13 47	15	+ 2	2·9	A0	A0 V	0·05
7236	λ Aqil	19 03·6	−04 58	358	− 7	3·3	B9	B8·5 V	−0·10
7264	π Sgtr	19 06·8	−21 06	344	−15	2·9	F2	(*F2 II*)	0·71
7342	v Sgtr	19 18·8	−16 04	350	−16	4·6	Aope	...	0·54
7446	κ Aqil	19 34·2	−07 08	0	−15	5·0	B0	...	0·26
7557	α Aqil	19 48·3	+08 44	15	−10	0·8	A5	(*A7 V*)	0·42
7665	δ Pavo	20 03·8	−66 19	297	−34	3·5	G5	G5 IV	1·43
7710	θ Aqil	20 08·7	−00 58	9	−19	3·3	A0	B9 IV	−0·07
7754	α^2 Capr	20 15·2	−12 42	359	−26	3·8	G5	G7 III	1·85
7790	α Pavo	20 21·7	−56 54	308	−36	2·0	B3	B3 IV	−0·25
7852*	ϵ Delf	20 30·8	+11 08	23	−18	4·0	B5	B5 V	0·01
7913	β Pavo	20 40·5	−66 23	296	−37	3·6	A5	A5 III	0·37
8204	ζ Capr	21 23·8	−22 38	355	−45	3·9	G5p	G4 Ib	1·84
8232	β Aqar	21 28·9	−05 48	16	−39	2·9	G0	(*G0 Ib*)	1·55
8322*	δ Capr	21 44·3	−16 21	6	−48	2·9	A5	A5 (met)	0·64
8353	γ Grus	21 50·9	−37 36	334	−53	3·1	B8	B8 III	−0·09
8414	α Aqar	22 03·2	−00 34	29	−43	3·1	G0	(*G1 Ib*)	1·82
8425	α Grus	22 05·1	−47 12	316	−54	2·1	B5	B5 V	−0·18
8634*	ζ Pegs	22 39·0	+10 34	47	−42	3·6	B8	B8·5 V	0·04
8675	ϵ Grus	22 45·5	−51 35	304	−58	3·6	A2	A3 V	0·22
8709	δ Aqar	22 52·0	−16 05	20	−62	3·4	A2	A2 III	0·16
8728	α Pisc A	22 54·9	−29 53	347	−66	1·3	A3	(*A3 V*)	0·11
8781	α Pegs	23 02·3	+14 56	58	−41	2·6	A0	(*B9 V*)	0·00

NOTES ON INDIVIDUAL STARS

897 θ Erid. Visual binary (8″). Mean gradient taken.

3207 γ^2 Velr. Wave-lengths λ 4660 and λ 5825, which coincided with emission bands, were omitted in measuring this Wolf-Rayet.

4133 ρ Leon. Gradient according to Stromlo −0·10; Greenwich +0·04; Barbier and Chalonge −0·06; Williams −0·20. The gradient equivalent of Williams' colours has been used, not the colours themselves.

4730/31 α Crux. The bluest star. Mean of two components.

4898 μ Crux. Bright component only.

5459/60 α Cent. Both components. Gradient for brighter estimated as +1·20.

6247 μ^1 Scor. Eclipsing binary. No evidence for periodic change of colour.

6262 ζ^1 Scor. One of the reddest of the brighter B stars.

7074 λ Pavo. Magnitude and colour both variable. See remarks in Section 11 of this paper.

7107 κ Pavo. Cepheid. Colour range (from seven observations) about +0·80 to +1·65.

7852 ϵ Delf. Gradient according to Mount Stromlo +0·01; Greenwich −0·12; Barbier and Chalonge −0·23; Williams −0·10. The gradient equivalent of Williams' colours has been used, not the colours themselves.

8322 δ Capr. Metallic line star. Gradient equivalent to F2.

8634 ζ Pegs. Gradient according to Mount Stromlo +0·04; Greenwich −0·11; Barbier and Chalonge +0·03; Williams −0·15. The gradient equivalent of Williams' colours has been used, not the colours themselves.

The following stars received less than three full-weight observations: 2282 ζ C Maj; 2451 v Pupp; 2456 15 Mono; 2550 α Pict; 2845 β C Min.

Consideration of the residuals from these mean gradients gives an internal figure on their accuracy. We find that for stars with G less than about 0·80, the mean s.e. of a gradient is about $\pm 0{\cdot}025$, and of one determination about $\pm 0{\cdot}05$. (The corresponding Greenwich figures quoted by Greaves (**11**) are $\pm 0{\cdot}03$ and $\pm 0{\cdot}06$.) For red stars, with G greater than about 0·80, the mean s.e. of a gradient is about $\pm 0{\cdot}04$, and of one determination about $\pm 0{\cdot}08$. The shorter base line (0·7 of the full base line) accounts for most of the increase in errors of the red stars.

7. *Comparisons with other observers.*—Three other observers have measured the colours of the brighter southern stars—King (**12**), Wallenquist (**13**) and E. G. Williams (**14**). King used extra-focal photometry and three plate-filter combinations to measure *Pg*, *Pv* and *Pr* (photographic, photovisual and photo-red) magnitudes. His well-known work covers the whole sky, except for the *Pr*, where he measured only the bright northern stars. Wallenquist made a visual match of the colours of his stars against the colour of a lamp, varying the latter with a movable blue wedge filter. Williams employed a Fabry lens and three plate-filter combinations to give him magnitudes at the effective wave-lengths $\lambda\lambda$ 4100, 5150 and 6200. His programme was limited for the most part to early B stars south of $-30°$.

Comparisons between these colours and the Mount Stromlo gradients look very like the comparisons found by the Greenwich observers between their gradients and various colour indices (**15**). We have little to add to their discussion and will not describe our results in detail. There are one or two anomalies, however, which should be mentioned. The first, and most important, arises when our gradients are compared with King's colour indices (*Pv–Pg*). The agreement is good, except for the bright stars α C Maj and α Cari, both of which we make appreciably bluer than does King. The possible systematic effect so suggested is discussed in detail in the next section. There is a good deal more scatter when the gradients are plotted against Wallenquist's "reciprocal temperatures"; in particular, our colours for ϵ Grus and τ Ceti are appreciably bluer than Wallenquist's, and for θ Scor, ι^1 Scor and α Aqar appreciably redder. The correlation between our measurements and Williams' is good, especially for the red (space-reddened) stars. The mean curve agrees well with that calculated from the effective wave-lengths quoted above, and, excluding a few stars with spectral peculiarities (γ^2 Velr), noticeable discrepancies exist only for ρ Leon and ζ Pegs, for which Williams' colours may be less accurate. Both these stars are discussed in the notes to Table II.

The very close relation between gradients and King's red indices (*Pr–Pg*) is worth mentioning. It is illustrated in Fig. 3. Most of the stars being in the north, we have had to use Greenwich gradients for more than half. α C Maj again stands off, as does δ Leon in the opposite sense. The Greenwich gradient for the latter is well confirmed by other spectrophotometric observers.

Turning now to the northern spectrophotometric work, we have made extended comparisons of our colours with those of Greenwich, Hall, and Barbier and Chalonge, all of whom were mentioned in connection with the standard stars. The comparisons are shown graphically in Figs. 4 and 5.

The mean absolute difference Mount Stromlo minus Greenwich for 23 stars in common is $\pm 0{\cdot}053$, appreciably larger than the $\pm 0{\cdot}025$ found in Section 5 for standard stars alone. The agreement can nevertheless be considered satisfactory.

These stars are far south at Greenwich; some do not rise more than 40° above the horizon there, and the Greenwich observers may well have had difficulty with extinction corrections. By the same token they are well north for us, and while the Mount Stromlo atmosphere should give less trouble, some of these stars, because of their relatively short observing season (curtailed for a number by a run of bad weather), were not observed as often as we would have liked. The worst discrepancies occur for ρ Leon (Stromlo minus Greenwich $= -0{\cdot}14$), ϵ Delf ($+0{\cdot}13$) and ζ Pegs ($+0{\cdot}15$). As it happens, our gradients for these three stars have quite good weight. All the five Orion stars we have in common with Greenwich we make bluer, by 0·04 in the mean, a trend in which we are supported by Stebbins and Whitford (**16**), who find δ, ϵ and ζ Orio among the bluest stars which they have measured. And the comparison with the 23 Greenwich stars, as opposed to that with the seven standard stars only, indicates a correction to our zero of $+0{\cdot}01$.

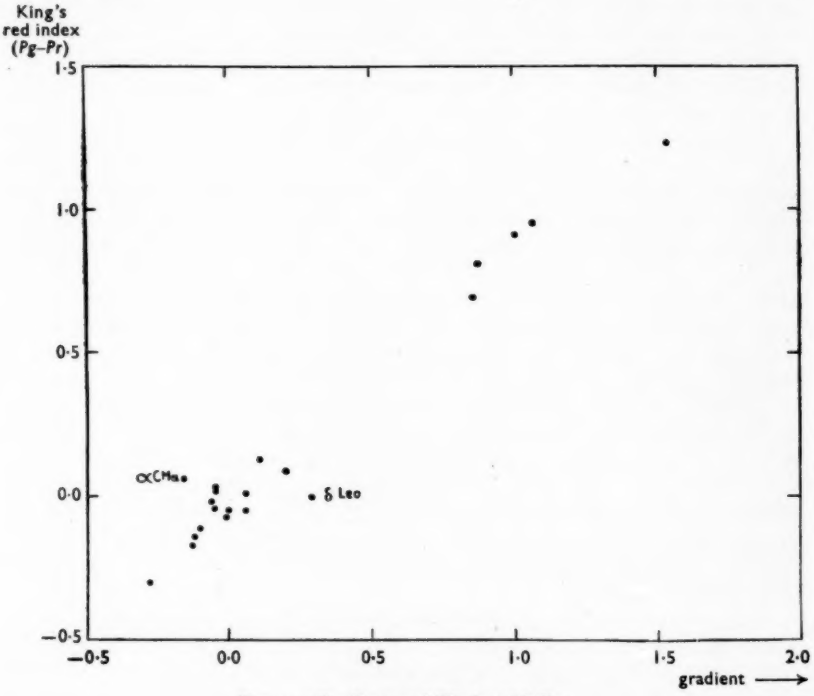

FIG. 3.—*Gradients and King's red indices.*

For the 17 stars we have in common with Hall we find a mean absolute difference $\pm 0{\cdot}038$. This is smaller than the mean absolute difference $-0{\cdot}044$ for Greenwich minus Hall. According to this comparison our zero should be increased by 0·017.

The comparison with Barbier and Chalonge shows good agreement except for a few rather large residuals and the comparatively big correction of $-0{\cdot}06$ indicated to our zero-point. The latter was unexpected after the good agreement

shown with Barbier and Chalonge in Table I for the standard stars. Closer examination shows that while the Barbier and Chalonge gradients for these are all of high weight (except perhaps for α Pisc A), this is not the case with many of the stars shown in Fig. 4, especially as less weight is given to those south of −15°. Perhaps over-correction by the French observers for atmospheric extinction for these southern stars is the reason for the discrepancy.

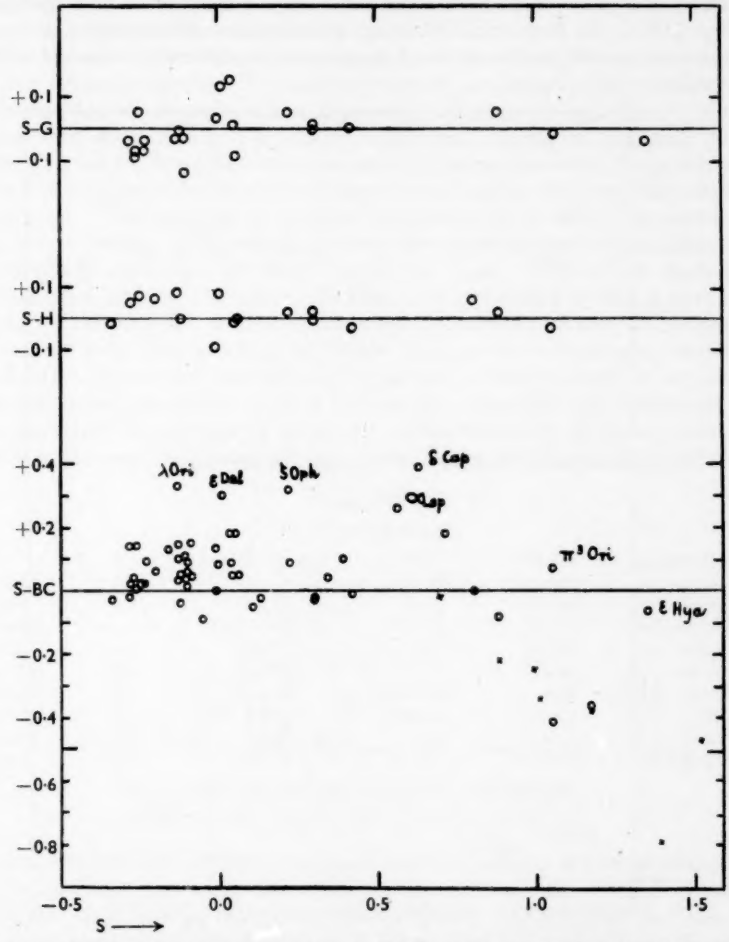

FIG. 4.—*Comparisons among gradients determined at Mount Stromlo (S), Greenwich (G), and by Hall (H), and Barbier and Chalonge (BC). Crosses are G–BC.*

Of the stars which stand off the main curve, λ Orio is of very early type (MKK O8) and various measurements of the colours of ε Delf disagree rather widely. (See note to Table II.) ζ Ophi is a strongly reddened star; its position on the figure is, as was first suggested by Greenstein (**17**) (see also references (**8**), (**11**) and (**16**)), a consequence of the fact that interstellar reddening, as measured by gradient excess,

increases with increasing wave-length, so that a reddened star is redder at λ5000 than at λ4250. α Leps is an Fo supergiant and δ Capr a well-known metallic line A. Beyond values of G of approximately 0·6 the correlation deviates from linearity, in the sense that the colour temperature then begins to increase with wave-length. A few Greenwich stars, indicated by crosses, have been added to illustrate the point. ε Hyda and π^3 Orio, both apparently normal, are now seen to stand off. But for these and the other stars mentioned in this paragraph, except ζ Ophi, the Barbier and Chalonge gradients are of low weight, with s.e.'s of the order ±0·08, so that too much importance should not be attached to these anomalies.

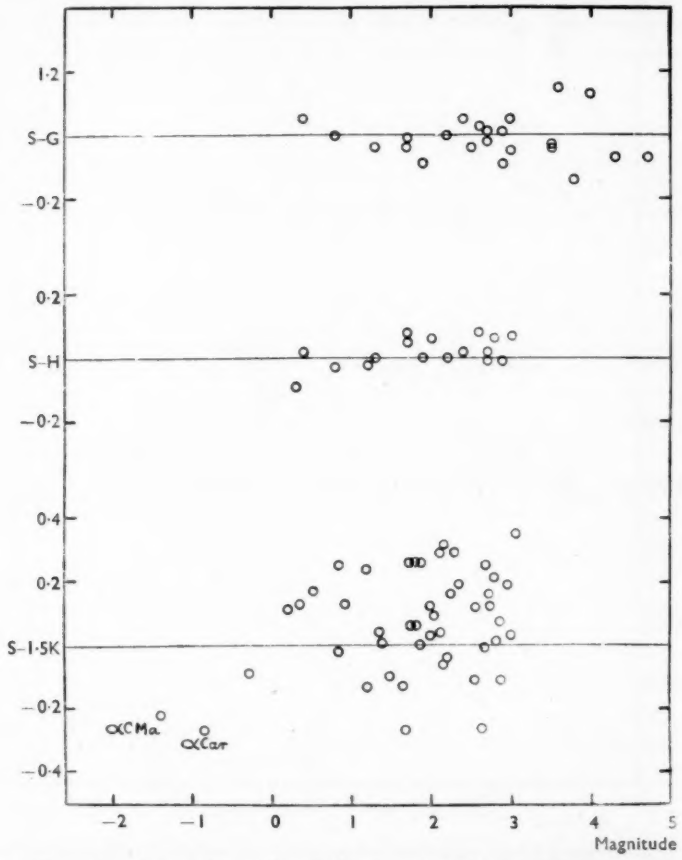

FIG. 5.—*Comparisons between Mount Stromlo (S), Greenwich (G), and Hall (H) gradients, and King's colour indices (K), to test for a possible magnitude affect.*

8. *The Gradients of Sirius and Canopus.*—According to these comparisons our real errors are not much in excess of the ±0·02 or ±0·03 calculated from the internal agreement of the individual observations, and hence no appreciable systematic effects were expected. It was therefore disconcerting to find that the two

brightest stars on the programme, Sirius (m_v −1·4; A1 V; G = −0·16) and Canopus (−0·7; Fo I; +0·25), were both much bluer than their spectral types would indicate, the more so as the comparison with King showed either that we were making these stars too blue or that King was making them too red. Further, the determination, by Dr Woolley and the writer (**4**), of 1·06 for the gradient of the Sun relative to Sirius implied that, if the gradient of Sirius is −0·16, that of the Sun is 0·90. Not only is this much too blue for a G2 V, but we are then also in difficulties with the stellar temperature scale.

The suggestion, that we are making the colours of the bright stars systematically too blue, is clearly serious. To examine it further, we plotted in Fig. 5 the colour differences Mount Stromlo minus Greenwich, Hall and King (King's colour indices were multiplied by 1·5) against magnitude. It can be seen that, apart from α Cari and α C Maj, there is no evidence for a magnitude effect in our colours.

In Table III we have assembled data concerning the brightest stars on the programme. This includes the gradient as determined at Mount Stromlo and, anticipating Section 9, that expected from the spectral type. Apart from the two brightest stars, the differences found are small. With α Cent both the measurements and the estimation of $G(Sp)$ are complicated by the presence of the K-type companion. β Orio must be slightly reddened, as one would expect. We make it bluer than does Hall (cf. Table I), but as it is a super-giant and also shows traces of emission, this difference is possibly a real indication of anomalies in its continuous spectrum. α Crux is certainly a very blue star, the bluest we have measured; but in view of its position as the nearest B1 in the sky, situated moreover in a very clear region of the galaxy, this is not altogether unexpected.

TABLE III

The Brightest Stars

	m_v	MKK type	$G(m)$	$G(Sp)$	$G(m)$–$G(Sp)$
α C Maj	−1·4	A1 V	−0·16	0·05	−0·21
α Cari	−0·8	Fo Ia	0·25	0·55	−0·30
α Cent	0·3, 1·7	G2 V + Ko V	1·27 :	1·35	−0·08 :
β Orio	0·3	B8 Ia	−0·01	−0·10	0·09 :
α C Min	0·4	F5 IV	0·88	0·90	−0·02
α Erid	0·6	B2 IV	−0·24	−0·25	0·01
β Cent	0·7	B1 II	−0·33	−0·35	0·02
α Aqil	0·8	A7 V	0·42	0·42	0·00
α Crux	0·9	B1 IV	−0·41	−0·35	−0·06

$G(m)$ is the gradient measured on this programme.
$G(Sp)$ is the gradient estimated from the spectral type.

It is certainly very difficult to account for the presence of a systematic error of this kind, and even more difficult to see how such an error should not affect the fainter stars, making them progressively redder. As reference to Table IV will show, some of our bluest stars were fainter than 3·0. And the good correlation found between our gradients and spectral type (Fig. 6) is a strong argument against systematic effects.

Two recent measurements of the colour of Sirius are now available *, although with Canopus the only colour we have, beside King's, is Wallenquist's, which neither disagrees with nor confirms ours. Danjon (**18**) has published visual

* Barbier and Chalonge's gradient for Sirius is omitted; they state that the gradients for their three brightest stars (α C Maj, β Orio and α Lyra) are unreliable.

measures of eight bright stars, in which he makes α C Maj definitely bluer than β Orio, and may be said to support our value. Seven of the eight stars are on Hall's programme, with whose figures Danjon agrees well. Eggen (**19**) has determined an accurate photoelectric colour of −0·07 for Sirius, on a scale which is near to, though not identical with, the International photographic scale*; −0·07 is near the International colour for spectral type A1.

To the writer, Dr Eggen's result is conclusive so far as Sirius is concerned. Meanwhile we can only repeat that, apart from these two stars, the evidence is against the presence of systematic effects, and we shall proceed on the assumption that they are in fact absent. Further observations of Sirius and Canopus are planned.

9. *The Spectrum-Colour Relation.*—The preponderance of bright B stars in the southern sky has been known for many years, and one of the objects of the present work was to find if the colours of these stars, a fair proportion of which might be near enough to avoid appreciable space-reddening, would help to fix more definitely the blue end of the spectrum-colour relation. It is the bluest stars which are of interest here, and a list of these is given in Table IV. Five are stated

TABLE IV

The Bluest Stars

B.S.	Star	Type	m_v	G	Distance (parsecs)
3447	*o* Velr	B3 V	3·6	−0·33	70
4199	θ Cari	Bo Vp	2·9	−0·32	120
4656	δ Crux	B2 IV	2·9	−0·32	130 (B)
4730/1	α Crux	B1 IV	0·9	−0·41	50
4853	β Crux	Bo III	1·4	−0·36	120 (B)
5056	α Virg	B1 III–IV	1·2	−0·34	90
5132	ε Cent	B1 IV	2·4	−0·30	180 (B)
5231	ζ Cent	B2 IV	3·0	−0·31	160
5267	β Cent	B1 II	0·7	−0·33	125
5695	δ Lupi	B2 IV	3·3	−0·31	180 (B)
5262	μ^2 Scor	B2 IV	3·7	−0·30	200 (B)
6508	*v* Scor	B2 IV	2·7	−0·33	135
6527	λ Scor	B2 IV	1·7	−0·34	90
6580	κ Scor	B2 IV	2·3	−0·32	115
G 39	γ Pegs	B2 V	3·0	−0·30	80
G 46	η Auri	B3 V	3·3	−0·22	70
G 113	η U Maj	B3 V	1·9	−0·23	40
G 221	β Ceph	B1 IV	3·3	−0·30	180

For stars with numbers prefixed with a *G* the gradients are from the Greenwich list (**2**) the number being the Greenwich number. Distances followed by (B) are from Blaauw's parallax for the Scorpio–Centaurus cluster (**20**).

by Blaauw (**20**) to be "certain" or "probable" members of the Scorpio–Centaurus cluster; his distances are given for these stars and are distinguished with a B. The distances of the remainder are from Miss Woods' luminosities, using the luminosity calibration in the Yerkes "Atlas". The possibility of a correction of +0·01 or +0·02 to our zero should be kept in mind, but will not affect any of our general conclusions. The four stars at the foot of the table are the two bluest

* The relations between the two scales will be described by Dr Eggen in a forthcoming paper in the *Astrophysical Journal*.

(γ Pegs and β Ceph) and the two nearest early B stars (η U Maj and η Auri) observed at Greenwich. In Fig. 6 we have plotted gradient against Yerkes spectral type, using only the nearest stars of each type. For F0 and earlier only Mount Stromlo gradients were used, and for B3 and earlier only those of Table IV. Later than F0 we included a number of Greenwich stars; these are not distinguished in any way. As one would expect from Morgan and Bidelmann's work (**21**), the correlation is extremely good. Indeed, earlier than about G0 the entire scatter may well be attributed to observational error. The one exception is γ Virg, an F0 V only about 100 parsecs away, in galactic latitude 61°. The Mount Stromlo gradient of 0·80 agrees well enough with Hall's mean of 0·74. On its colour this star could well be F3, or even F5.

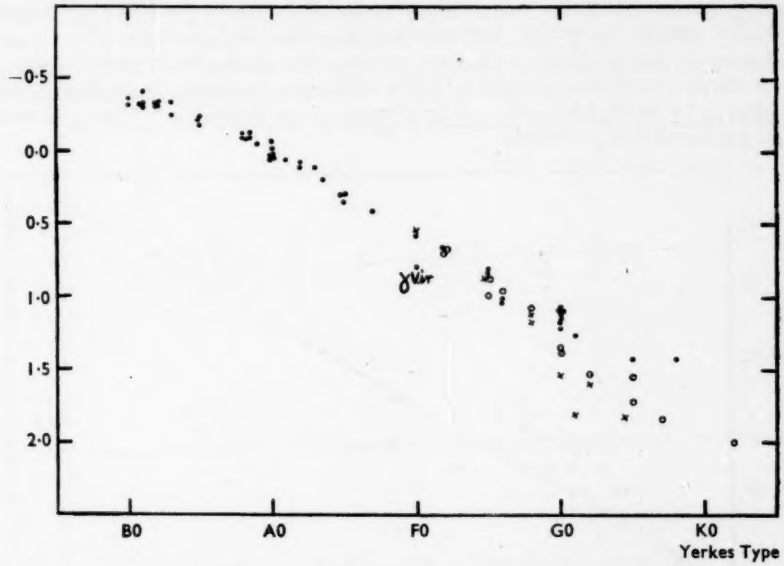

FIG. 6.—*Gradients and Yerkes spectral types. Filled circles represent dwarfs, crosses giants and open circles super-giants. No differentiation is made for stars earlier than F0.*

At about G0 the dwarf-giant differentiation can be observed setting in, in the customary way, though here as elsewhere one cannot be sure that space-reddening has been entirely eliminated. Space-reddening is in fact a major difficulty throughout this subject, well illustrated by η U Maj and η Auri. Though the two nearest in a table of early B stars, they are definitely the reddest. (We must not forget, however, the possibility of dispersion in the colours of the early B stars.) It is surprising that a star in such a low galactic latitude as α Crux should be so blue, and groups such as γ, λ and κ Scor must be in exceedingly transparent regions of space. (Yet σ Scor, just as near—it is also in the Scorpio–Centaurus cluster—is a B1 with a gradient of 0·48.) Stebbins and Whitford remark that the situation of α Virg, in galactic latitude 50°, might make it the bluest star in the sky. If this is so, then all the stars in Table IV are sensibly unreddened, and the intrinsic gradient of a B0 is no bluer than about −0·35.

At the same time the present work makes the early B stars at least as blue as $-0{\cdot}35$, and possibly as blue as, say, $-0{\cdot}40$. This question of the intrinsic colours of B stars is important for space-reddening and other problems, and it is of interest to find the equivalent of our colours in other systems. For instance, it has been suggested by Oort (**22**) and others that the normal C1 colours of Stebbins and Whitford should be corrected by $-0{\cdot}04$ (so that, for example, the C1 for an unreddened B1 should be $-0{\cdot}26$ and not $-0{\cdot}22$). In Fig. 7 C1 colours (taken from M.W.C. 621) are plotted against Greenwich and Mount Stromlo gradients. In choosing the line

$$G = 0{\cdot}76 + 4{\cdot}30\,\mathrm{C1}$$

to represent the relation, more weight has been given to the points at the blue end of the curve than to the intermediate ones; this seemed the better procedure for the present particular application. We then find that for $G = -0{\cdot}40$, $\mathrm{C1} = -0{\cdot}27$ and for $G = -0{\cdot}35$, $\mathrm{C1} = -0{\cdot}26$. Our work clearly supports Oort. Not enough observational material exists at present to enable the corresponding figures to be derived for other colour systems, in particular for the International and photo-red colour indices.

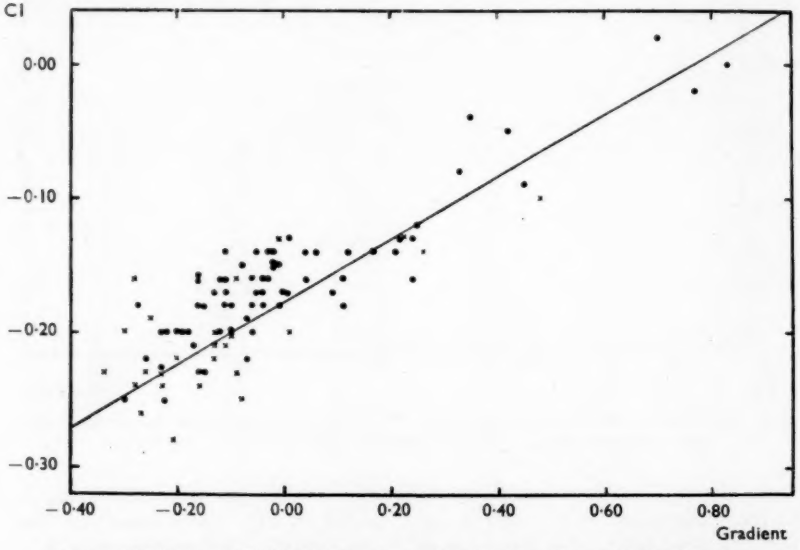

FIG. 7.—*Stebbins and Whitford's C1 colours plotted against Greenwich (dots) and Mount Stromlo (crosses) gradients. Early-type stars only are included; the red stars are space-reddened blue stars.*

In this general connection it is worth pointing out that different observers do not always agree on what are the bluest stars. Thus Stebbins and Whitford include among their half-dozen bluest V-I stars 10 Lacr (Greenwich $G = -0{\cdot}15$), δ Orio ($G = -0{\cdot}21$), β Ceph ($G = -0{\cdot}30$) and ϵ Pers ($G = -0{\cdot}23$). Of these only the short-period variable β Ceph has a really blue gradient, while both Greenwich and Mount Stromlo make δ Orio slightly but definitely reddened, as one would expect from the strength of its interstellar K line. Barbier and Chalonge make 10 Lacr very blue. These differences are outside the limits of observational

error, and are perhaps to be explained in terms of the deviations from black-body conditions noted by Stebbins and Whitford, and apparent in Fig. 3a of reference (16).

10. *The Stellar Temperature Scale.*—According to the preceding section the intrinsic colour of a main sequence Bo–B3 can be represented on the Greenwich system by a relative gradient of $-0{\cdot}35$. If the colour temperature at Ao is 16,000, that at Bo will then be 38,000 deg., which may be compared with the admittedly approximate value of 57,000 deg. found theoretically by Unsöld for τ Scor (23).

Stebbins and Whitford remark on a difficulty they experienced in adopting a temperature scale which would allow Ao and Go to agree with observation and at the same time not make Bo too hot. Thus if they assume 16,000 deg. for Ao, their $(V-I)$ values give them temperatures in the region of 100,000 deg. for Bo. And if, as our work suggests, and as they themselves realize was possible, even their bluest stars were slightly reddened, this difficulty is accentuated. But if gradients or $(V-R)$ colours are used the difficulty is not so apparent, and it is instructive to see how it comes about.

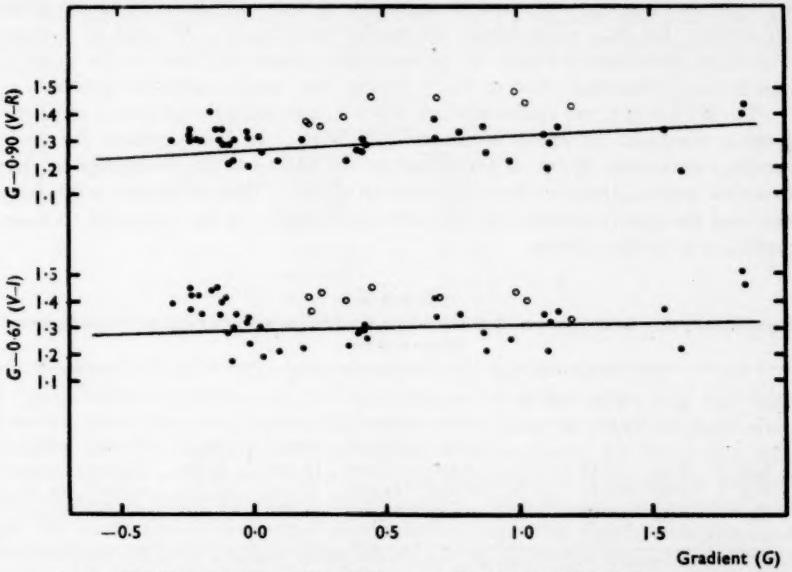

FIG. 8.—*Gradients plotted against Stebbins and Whitford's V–R and V–I colour indices. Open circles are space-reddened stars, and the full lines represent the relation between colours on each pair of systems and of a series of black bodies of differing temperatures.*

In Fig. 8 we plot $G-0{\cdot}67(V-I)$ and $G-0{\cdot}90(V-R)$ against G for the fifty-odd Stebbins and Whitford stars for which gradients are known. It will be recalled that V, R and I are heterochromatic magnitudes measured over fairly narrow spectral regions of effective wave-lengths λ4220, λ7190 and λ10,300 respectively. In Table 5 of (16) Stebbins and Whitford have computed (*inter alia*) the colour indices $(V-R)$ and $(V-I)$ as functions of black-body temperature, the colours having a common zero at $T=5500$ deg. The corresponding relation between gradient and temperature is set out in Table V of (1). These figures

enable us to draw the full lines of Fig. 8, relating in each pair of systems the colours of a series of black bodies of varying temperature. The zero has been chosen so that $T=6500$ deg. corresponds to $G=1{\cdot}15$, $(V-I)=-0{\cdot}25$ and $(V-R)=-0{\cdot}21$. This change of zero point necessitated the addition of 0·32 to the tabulated $(V-I)$ and of 0·21 to the tabulated $(V-R)$. From the plot of $(V-I)$ against G it is clear that departures from black-body conditions are present *, and, bearing in mind the more linear relation which evidently exists between $(V-R)$ and G, it seems safe to attribute the greater part of these to the I region, in particular to the Paschen discontinuity. Hall and Williams (**28**) have shown that the distribution of energy in the spectrum of Vega (A0) is quite closely that of a black body up to the Paschen limit, beyond which it shows an excess of energy of about 0·23 mag. And Hall (**7**) has shown that this behaviour is typical of stars in the region of A0, showing, as one would expect, close analogies to the Balmer discontinuity.

Some relevant figures are collected in Table V, which should be self-explanatory. The $(V-I)$ colour for B0 is rather arbitrary but cannot be far out. In one group we have adopted the common temperature of 6500 deg. for G0, in the other 30,000 deg. for B0. The better agreement between $(V-R)$ and G is clear. The lower temperature which the photoelectric colours attribute to G0 must be due to heavy line absorption in the V region; this would not affect gradients.

To the writer these considerations argue rather tellingly in favour of photographic methods for absolute temperature work. In this problem the lower accuracy obtainable is not as important as the ability of the photographic plate to isolate spectral regions a few angstroms in width. This, of course, is far from decrying the great accuracy and convenience brought by the photocell to many problems of stellar colours.

TABLE V

Variation of colour temperature with spectral type according to gradients and to two photoelectric colour indices

	G	$V-I$	$V-R$	G	$V-I$	$V-R$	G	$V-I$	$V-R$
				(deg.)	(deg.)	(deg.)	(deg.)	(deg.)	(deg.)
G0	1·15	−0·25	−0·20	6,500	6,500	6,500	6,350	6,000	6,150
A0	0·00	−1·85	−1·45	16,000	15,000	17,500	15,000	12,400	14,500
B0	−0·35	−2·60	−1·85	36,000	80,000	50,000	30,000	30,000	30,000

11. *Individual Stars of Interest.*—We will conclude this paper with a few remarks on individual stars of interest.

First γ^2 Velr, the brightest Wolf-Rayet star, has as common proper motion companion the apparently normal B3 γ^1 Velr. Not only can we determine the absolute magnitude of γ^2 Velr from the spectroscopic parallax of γ^1, but also we can use the colour of γ^1 to correct that of γ^2 for space absorption. We find γ^2 rather bluer than γ^1; intrinsically it must be a very blue star (**24**).

The following table contains data relative to four of our Be stars, selected because they appear to lie in very transparent directions of the galaxy. 205 G Cari is quite near in space to, and at about the same distance from the

* As otherwise there would be a random scatter of points about the solid line.

Sun as, θ Cari, of gradient −0·32. μ Cent is similarly only one degree away from ν Cent, of gradient −0·29. δ Cent is in a very transparent region, and α Arae is included as the bluest of the Be stars. For none of these stars would we expect space reddening to be appreciable, and taken as a group we consider that they present strong evidence in favour of the intrinsic reddening of Be stars (**25**).

TABLE VI

		Type	Gradient	Distance (parsecs)
4140	205 G Cari	B5 IVe	−0·08	80
4621	δ Cent	B2 Ve	−0·11	80
5193	μ Cent	B2 Ve	−0·10	90
6510	α Arae	B3 Ve	−0·20	60

Finally we have λ Pavo, an apparently normal B3 which, after the style of γ Cass, developed emission characteristics at some time in the last 20 years (**26**). As the accompanying journal of measurements shows, the colour of this star appears to vary. No obvious variations in emission-line intensities have been noticed.

TABLE VII

Measurements on λ Pavo

Date	Gradient
27/7/48	−0·03
1/8/48	0·07
3/8/48	0·04
12/10/48	0·18
24/10/48	0·21
29/10/48	0·16
23/6/49	−0·10

Cousins (**27**) and others have suspected this star of variability.

12. *Acknowledgments.*—Of the members of the Observatory staff who have assisted with this programme, the writer would like to thank in particular: Dr Woolley, for his generous encouragement and support; Mr Hogg and Miss Mason, for their cooperation in the use of the telescope and, in particular, for their determinations of the diaphragm transmissions; Miss Woods, for permission to use her spectral types in advance of publication; and Miss Lamb, who measured and reduced the great majority of the plates, for her very capable and conscientious assistance. He is also indebted to Dr Eggen, of the Lick Observatory, for permission to use his figures for the colour of Sirius.

Commonwealth Observatory,
Mount Stromlo,
Canberra, Australia:
1950 *January.*

References

(1) R. O., Greenwich, *Observations of Colour Temperatures of Stars*, 1926–1932.
(2) R. O., Greenwich, "Relative Gradients of 250 Stars," *M.N.*, **100**, 189, 1940.
(3) C. Davidson, *J. Sci. Instr.*, **5**, 238, 1928. J. H. Dowell, *ibid.*, **12**, 224, 1935.
(4) R. v. d. R. Woolley and S. C. B. Gascoigne, *M.N.*, **108**, 491, 1948.
(5) H. H. Plaskett, *Pub. D.A.O.*, **2**, 211, 1923.

(6) W. M. H. Greaves, *M.N.*, **96**, 825, 1936.
(7) J. S. Hall, *Ap. J.*, **94**, 71, 1941; **95**, 231, 1942.
(8) D. Barbier and D. Chalonge, *Ann. d'Ap.*, **4**, 30, 1941.
(9) W. W. Morgan, P. C. Keenan and Edith Kellman, *An Atlas of Stellar Spectra*, Chicago, 1943.
(10) W. B. Rimmer, *C.S.O. Memoir*, No. 2, 1930.
(11) W. M. H. Greaves, *M.N.*, **108**, 150, 1948.
(12) E. S. King, *H.A.*, **85**, Nos. 10 and 11, 1930.
(13) Ake Wallenquist, *Bosscha Ann.*, **5**, part 4, 1935.
(14) E. G. Williams and H. Knox-Shaw, *M.N.*, **102**, 226, 1942.
(15) R. d'E. Atkinson, A. Hunter and E. G. Martin, *M.N.*, **100**, 196, 1940.
(16) J. Stebbins and A. E. Whitford, *Ap. J.*, **102**, 318, 1945.
(17) J. L. Greenstein, *Ap.J.*, **87**, 151, 1938.
(18) A. Danjon, *B.A.*, **14**, 315, 1949.
(19) Olin J. Eggen, private communication.
(20) A. Blaauw, *Kapteyn Astr. Lab. Publ.*, No. 52, 1946.
(21) W. W. Morgan and W. P. Bidelmann, *Ap. J.*, **104**, 245, 1946.
(22) J. H. Oort, *B.A.N.*, No. 308, 1938.
(23) A. Unsöld, *Zeit. f. Ap.*, **21**, 229, 1942.
(24) But *cf.* W. Petrie, *D.A.O.*, **7**, 383, 1947.
(25) *Cf.* reference (11), pp. 145–150.
(26) S. C. B. Gascoigne, *Observatory*, **69**, 30, 1949.
(27) A. W. J. Cousins, *M.N.*, **103**, 154, 1943.
(28) J. S. Hall and R. C. Williams, *Ap. J.*, **95**, 225, 1942.

IC 4406: A DOUBLE NUCLEUS PLANETARY NEBULA

David S. Evans

(Received 1949 October 5)

Summary

IC 4406 is found to consist of an elongated mass of gas under the gravitational and radiative influence of two stars. The results of a photometric and spectroscopic investigation are presented. The system does not appear to form an equilibrium configuration and seems to resemble closely the type of model much discussed in connection with the theory of the origin of the solar system. It is hoped that the observations reported may be of interest to theoretical workers.

In the course of a survey of bright southern planetary nebulae attention was attracted to the system IC 4406, which, because of its unusual astrophysical interest, seemed to merit a detailed study. Dreyer * describes the system as "Planetary, stellar, 10 mag., extended in position angle 80°". Campbell and Moore † describe it as being of about 20″ diameter, slightly flattened on the east and west edges. These workers obtained three spectra showing no more than the N_1 and N_2 lines, and deduced a velocity of -22 km./sec. A drawing by Wilson shows an undifferentiated area of luminosity of the size and shape described above. There is no indication that a central star was observed. In the drawing a star is shown about 33″ to the west of the centre of the nebula. Fleming ‡ gives the magnitude of the nebula as 9·5.

The following plates of this object are on file at this observatory:—

TABLE I

IC 4406: R.A. $14^h\ 19^m{\cdot}3$; Dec. $-43°\ 55'$ (1950.0)
Galactic Long. 288°, Lat. +15°

No.	Date	Emulsion	Exposure (min.)	Filter	Calibration	Observer
A 304	1949 April 6	I.A.Z.	10, 3	...	−	ADT
A 315	April 19	I.A.Z.	15	...	−	DSE
A 316	April 19	I.A.Z.	10	...	−	DSE
A 317	April 19	K 103a–O	15	...	−	DSE
A 356	June 21	I.A.Z.	10, 5	...	−	DSE
A 369*	July 21	K 103a–O	15	...	+	DSE
A 369**	July 21	K 103a–O	15	...	+	DSE
A 374	July 22	K 103a–O	5	...	+	DSE
A 375	July 22	K 103a–E	15	W 25	+	DSE
A 376	July 23	K 103a–E	20	W 25	+	DSE
A 377	July 24	K 103a–E	10	W 25	+	DSE
A 378	July 24	I. HP_3	15	W 12	+	DSE
A 379	July 24	I. HP_3	15	W 12	+	DSE
A 380	July 26	I. HP_3	40	W 12	+	DSE
A 398	Aug. 23	K 103a–O	40	W 18a	−	DSE
A 399	Aug. 23	K 103a–E	20	W 25	−	DSE

I.A.Z.=Ilford Astronomical Zenith; K=Kodak; I=Ilford; W=Wratten.

Filters { W 25 : transmission, 6000 A. and to red.
W 12 : transmission, 5200 A. and to red.
W 18a : transmission (10 per cent +) 3300–3900 A.

* J. L. E. Dreyer, Second Index Catalogue, *Mem. R.A.S.*, **59**, 105, 1908.
† W. W. Campbell and J. H. Moore, *Lick Observatory Publications*, **13**, Part 4, 1918.
‡ Mrs Fleming, *Harvard Circular*, No. 60, 1901.

These plates were calibrated in the same way as those discussed in a previous paper.*

In the 74-inch telescope the object appears visually as a small almost rectangular blue smudge extended in an approximately east–west direction, sharply bounded to north and south, but somewhat blurred to east and west. No central star

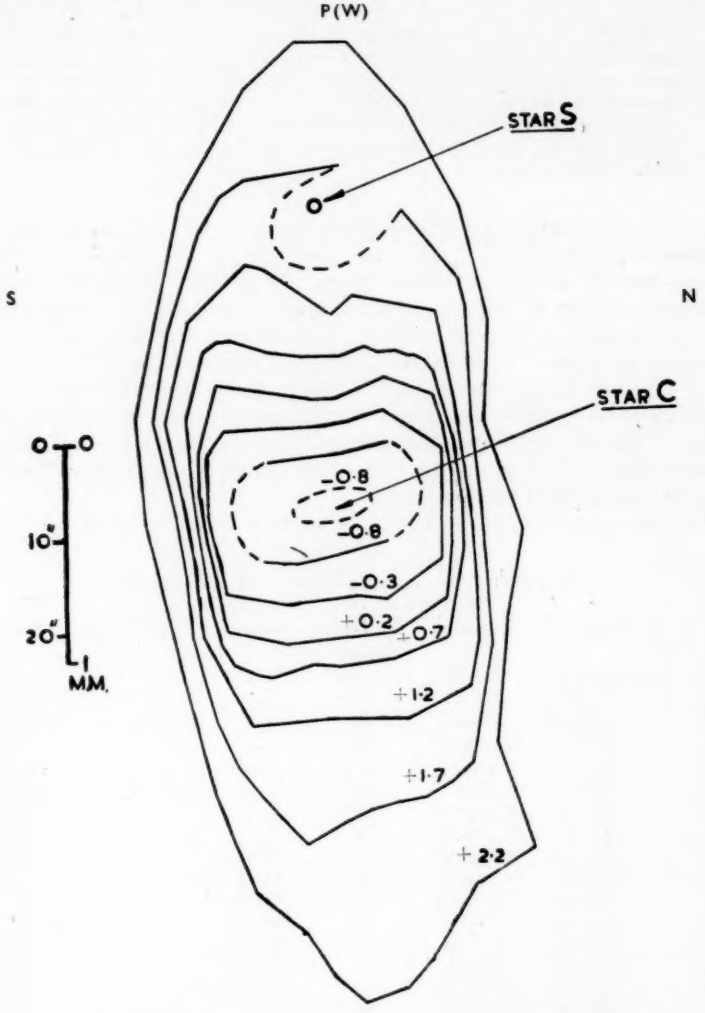

FIG. 1 (*a*).—*Blue.*

can be seen, but there is a prominent star to the west, lying apparently well outside the system.

On short-exposure red and blue plates, the central star (star C) is visible faintly. It appears to lie at the centre of a structure of oval shells, having an

* *M.N.*, **109**, 94, 1948.

axis ratio of about 1·5 : 1, the longer axis lying north and south, and the overall north–south diameter of the largest shell being about 34″. A small, rather asymmetrical dark area surrounds star C. The nebula has east–west symmetry about the central star, and on short-exposure plates its eastern and western ends appear slightly concave. On yellow plates star C can scarcely be seen.

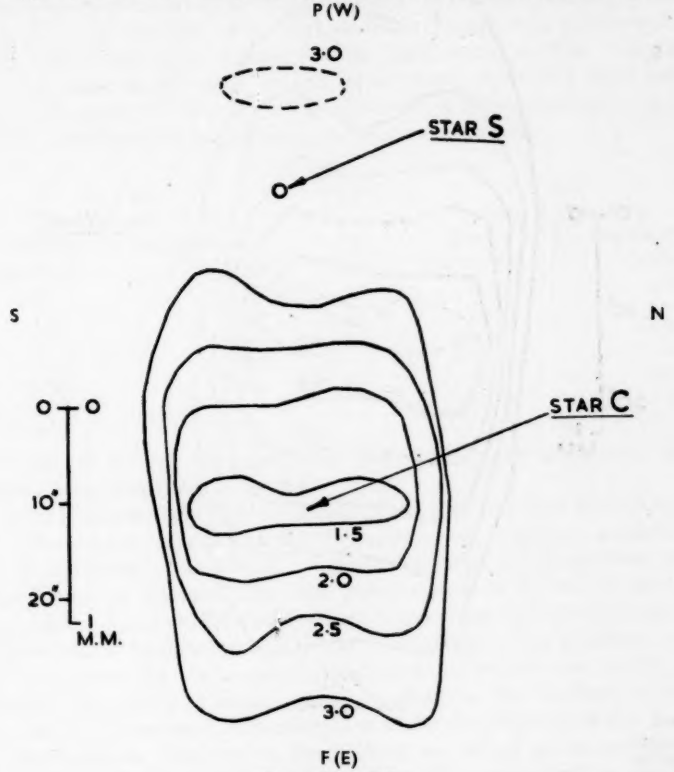

FIG. 1 (*b*).—*Yellow.*

As soon as the exposures are increased, star C disappears and the nebula can be traced as extending to greater and greater distances to east and west, remaining closely symmetrical about the position of the central star. The eastern and western ends remain slightly concave, until the exposures are sufficient to trace the parts of the nebula surrounding the second star (star S) lying 33″ to the west of the centre. A shell structure surrounding star S can now be seen, and this has the effect of making the western end of the nebula concave: at this stage the eastern end is somewhat irregular and slightly concave. Finally, it is possible to trace still greater faint extensions at both ends. To the west star S is surrounded, while on the east there is a rounded end. The whole nebula is shaped like a slightly curved elongated oval approaching a bean shape. In addition to this general structure there are a number of details to be described. On the east, short dark bays run inwards, while on the west, the form of the shell structure surrounding star S includes an asymmetrical tongue of brightness, issuing from the nebula and running close round the star to the south-west of it.

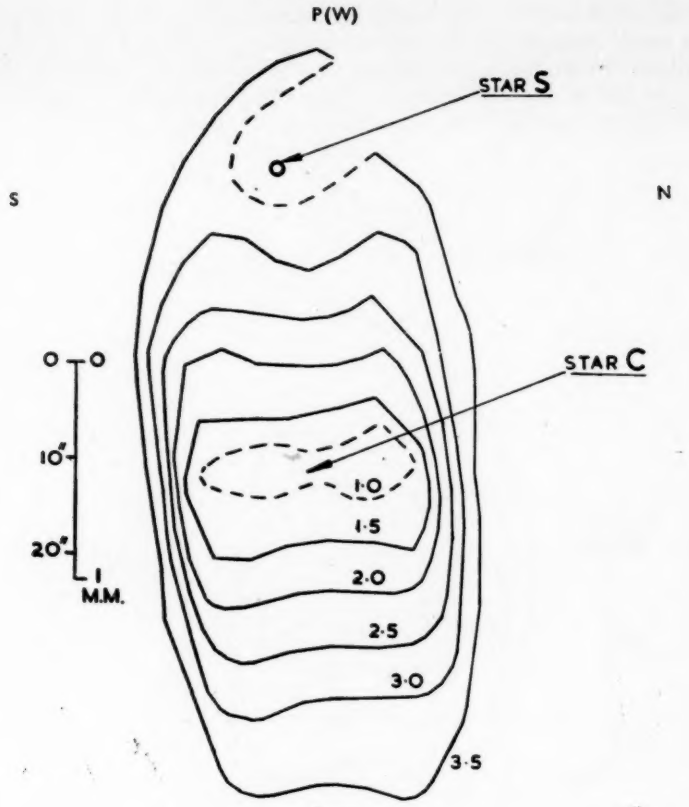

FIG. 1 (*c*).—*Red.*

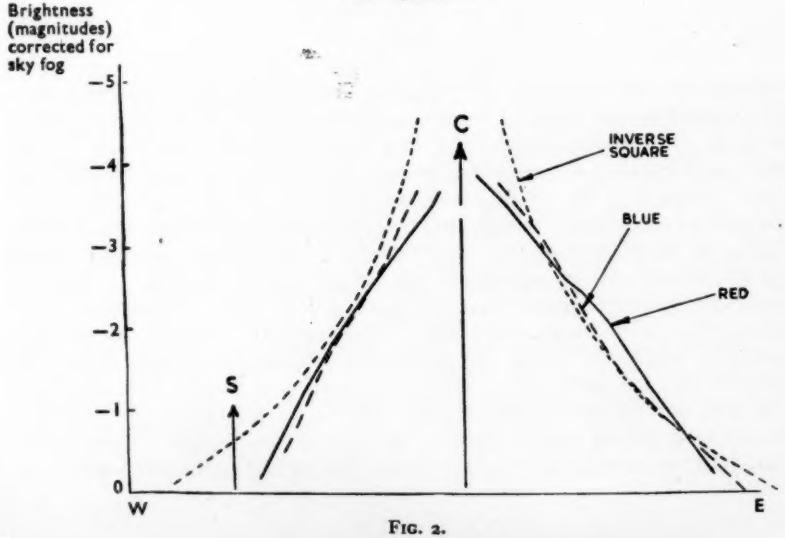

FIG. 2.

To the north-east of star S lie two small and slightly irregular fan-shaped dark areas centred on the star. The structures shown on the red, yellow and blue plates appear to be essentially the same, and it is believed that the material available does reveal the full extent of the system.

The surface of the nebula has been photometered, and the slightly smoothed version of the surface intensity variation which the method produces is illustrated in Fig. 1 (*a*), (*b*) and (*c*). Fig. 1 (*a*) shows half-magnitude isophotes for blue plates, A 369* and A 374, uncorrected for background sky fog. Similar plots for yellow plates A 378 and A 380 and for red plates A 376 and A 377 are shown in Figs. 1 (*b*) and 1 (*c*). For the red and blue plates, allowance for sky fog involves renaming the isophotes according to the following scheme :—

TABLE II

Blue		*Red*	
Plates A 369*, A 374		Plates A 376, A 377	
Sky-fog level : 2·43±0·045		Sky-fog level : 3·93±0·030	
Uncorrected	Corrected	Uncorrected	Corrected
2·20	4·01	3·50	4·72
1·70	2·48	3·00	3·60
1·20	1·63	2·50	2·84
0·70	0·95	2·00	2·20
0·20	0·35	1·50	1·62
−0·30	−0·21	1·00	1·08
−0·80	−0·74		

It will, of course, be appreciated that both these magnitude scales are arbitrary as to their zeros.

There is surprisingly little difference in the appearance of the system in light of various colours, except that the region near star C appears somewhat bluer than the periphery of the nebula. The red plates probably represent the distribution mainly in *Hα* light, the blue plates mainly in N_1 and N_2 and possibly λ3727 light. Fig. 2 shows a comparison, taken along the mid-line of the nebula, of the corrected brightnesses in red and blue light. The positions of stars C and S are shown by the arrows. The interesting features are: firstly, that the differences are relatively small; secondly, that the plot is closely symmetrical about star C and seems hardly affected at all by the presence of star S; thirdly, that the variation, especially in the blue, is not far off an inverse square law. By arguments similar to those advanced in a previous paper * we may probably attribute the nebular light to radiation originating in star C and scattered by the surrounding gas.

At my request Dr Thackeray was good enough to obtain a spectrum of IC 4406 with the Newtonian spectrograph, which gives a dispersion of 3·7 mm. between *Hβ* and *Hε*. The slit was placed longitudinally on the nebula, and the following lines were found :—

TABLE III

Spectrogram NS 106

1949 Aug. 25. Exp. 25m. Slit 10. Emulsion R 55

Line	N_1	N_2	*Hβ*	*Hγ*	*Hδ*	*Hε*+3967 (*NeIII*)	3869 (*NeIII*)
Strength	40	12	6	4	1	5	5
Length (seconds of arc)	55	53	29	23	16	19	21

The line λ 3727 unfortunately would fall precisely at the edge of the film and is therefore not recorded.

* *Loc. cit.*

The magnitude of star S could be estimated from image diameters on plate A317 by comparing it with plate A328 of selected area No. 132, taken by Dr Thackeray on April 23–24 on the same emulsion (K103a–O), with exposure times of 2^m, 6^m and 18^m. With an error of at most two to three-tenths of a magnitude, star S is estimated as having a photographic magnitude of 14·7. Star C shows two or three magnitudes fainter than this, but it is clearly much subject to absorption, and is hardly brighter than the nebular surface.

Plates taken at different wave-lengths show that while the transition from red to ultra-violet markedly alters the appearance of the surrounding star field, it hardly changes at all the appearance of the nebula and star S. It is clear that star S is of a very early type, and is hardly, if at all, redder than the nebula itself. No other information concerning the colour of star S is available at present.

To summarize, we have the following picture of the system: it is a mass of gas of a fairly uniform colour, of an elongated oval shape, measuring about $100'' \times 37''$, having a star, presumably of type W, but much dimmed by absorption, at its centre of symmetry. Star S, of early type and apparent photographic magnitude about 14·7, lies at a distance of $33''$ to the west of the central star, also on the mid-line of the nebula and within the nebulosity.

With the means at our disposal at present we cannot get an estimate of a spectroscopic parallax for star S, so that the distance and scale of IC4406 are unknown. However, we can consider the various possibilities which can be summarized in the following table:—

TABLE IV

Star S Hypothetical M	Distance (parsecs)	Distance CS (parsecs)
−5·3	10^5	16
−0·3	10^4	1·6
+4·7	10^3	0·16

Of these three guesses, the first makes star S intrinsically very luminous and puts it at a distance which, according to present ideas of galactic structure, should take it right outside the galaxy past its centre. There is no particular objection to the system IC4406 lying at a distance greater than the galactic centre, since the latitude is moderately large and so is the longitude difference from the centre. On the other hand, if there is a window here we should expect to find extra-galactic nebulae appearing on the plates. Even on plates which should have a limiting magnitude of, say, 18, no nebulae can be found. Thus, if there is no spatial absorption and even if IC4406 lies to one side and past the galactic centre, we must regard the first guess as giving a distance at least three times the possible reasonable maximum. This argument suggests that an upper limit for the distance CS is about 5 parsecs. The third guess, according to the classical Hertzsprung-Russell diagram would make star S of far too late a type. Guessing at a maximum possible value for M of, say, +1·7, the distance comes out at 2500 parsecs, giving $CS = 0{\cdot}4$ parsecs. Thus, assuming no absorption, we can probably place the distance CS as lying in the tenfold range from 0·5 to 5 parsecs.

The discussion of absorption effects falls into two parts. Either the system is very distant and lies clear of the central absorbing layer of the galaxy, or it is relatively near and lies within this layer. In the first case the absorption will be constant and may be taken as $0^m{\cdot}25$ cosec 15° or almost exactly 1 magnitude. With assumed values for M of −5·3 and −0·3, values of the distance, D, then come out

as $6{\cdot}3 \times 10^4$ parsecs and $6{\cdot}3 \times 10^3$ parsecs. The corresponding distances above the galactic plane, $D \sin 15°$, are then $1{\cdot}63 \times 10^4$ parsecs and $1{\cdot}63 \times 10^3$ parsecs, with CS being 10 parsecs and 1 parsec in the two cases.

The first estimate is probably much too large, for it makes IC 4406 an object lying well outside the galaxy and, just as in the unobscured case already discussed, we should be able to detect other extra-galactic objects on the plates. The second estimate is more reasonable. In this case IC 4406 lies more or less on the boundaries of the galaxy. It seems that we must retain as our rough upper limit for the distance CS the value of 5 parsecs already deduced for the unobscured case.

If however we assume a smaller absolute luminosity for star S, the system IC 4406 becomes a member of the galaxy, and the correct way to allow for the absorption is by reckoning a dimming of so many magnitudes per kiloparsec. The following table shows values of absorption computed on various assumptions:—

TABLE V

	$0^m{\cdot}5$ per kiloparsec				$0^m{\cdot}75$ per kiloparsec			
	D	$D \sin 15°$	CS	Total absorption	D	$D \sin 15°$	CS	Total absorption
$M=-2{\cdot}3$	6100	1580	0·98	$3^m{\cdot}1$	4800	1240	0·77	$3^m{\cdot}6$
$M=-0{\cdot}3$	4000	1030	0·64	$2^m{\cdot}0$	3250	840	0·52	$2^m{\cdot}4$
$M=+1{\cdot}7$	2300	590	0·37	$1^m{\cdot}2$	2000	520	0·32	$1^m{\cdot}5$

The last entry represents probably the low limit for the value of CS. The most probable values would seem to be $D=4000$ parsecs, $CS=0{\cdot}65$ parsecs, but there is a wide range of possibilities.

It is not the purpose of this paper to attempt a theoretical discussion, but it is possible to advance certain general physical arguments which may provide a pointer to the nature of the system. What seems of greatest importance is that although star S is involved in the system, the distribution is closely symmetrical about star C. If we consider a very artificial model consisting of two stationary point masses, m and m', surrounded by a tenuous cloud of gas, then eventually the gas will conform to the equipotential surfaces defined by these two masses. These are readily sketched out in bi-polar coordinates as the surfaces

$$m/r + m'/r' = \text{constant}.$$

For various values of the ratio m/m' they give a series of dumb-bell-shaped curves centred about the mass-centre of the two points. Some forms can be obtained which are reminiscent of IC 4406 but the centre of symmetry does not coincide with one of the point masses. Symmetry about m can only be secured by taking m/m' large, but then the surfaces approximate to spheres centred about m.

A physical possibility is that the two stars form a binary of long standing. In this case, neglecting radiation pressure, the equipotential surfaces will be somewhat modified, but still, in a general way, it is possible to maintain that the equilibrium form would have its centre near the mass-centre of the two stars and not coincide with one of them.

General considerations of radiation pressure seem to present the same dilemma. That is, if star C contributes all the radiation-pressure effects, it would be expected that the nebula would have spherical symmetry about this star. We know from the observational results that it is probable that star C does contribute most of the radiation exciting the nebula. One possibility still

remaining, of accounting for the state of the system *as one which is of long standing in its present form* would be to attribute all the radiation-pressure effects to star C while sharing out the gravitational effects between the two stars. It seems however that there are difficulties about this interpretation too, for the joint effect would be to leave the centre of symmetry lying between C and S, and, moreover, according to the mass-luminosity rule it is a highly artificial hypothesis to make star S both relatively faint and massive.

I am inclined to think that the solution of the dilemma lies in the hypothesis that IC 4406 is a system which has not yet reached equilibrium and which cannot therefore be of long standing. In fact, IC 4406 may represent a case of a stellar encounter. On this view star C would originally have been the central star of an ordinary planetary nebula having symmetry about the central star. Star S then produces tidal effects, which should give at any instant ellipsoidal equipotential surfaces centred about star C. This is, in fact, what we do find. Moreover, although there is a rough north–south symmetry about the line *CS* there are important detailed structures which show asymmetry. The whole nebula is slightly curved as if there were a component of transverse relative velocity in the plane of the sky. Moreover, the shell structure round star S shows the asymmetrical bright tongue already described, which suggests a modification of an originally spherical shell system due to relative motion.

In view of the possibility of changes I have consulted early descriptions of this object. Referring to the period 1898–1901 Delisle Stewart *, using the Bruce telescope at Arequipa, gives the description, "two nebulous stars make dumb-bell, remarkable". Innes †, writing in 1902, describes his observations with the Cape 7-inch:—"Is a fine planetary, 10 mag., about 20″ in diameter. Examined on the same night with the 18-inch it appeared dumb-bell shaped. With the 24-inch object-glass prism it was found to be a gaseous nebula. On *Carte du Ciel* Plate 3689 with 1 hour exposure are shown two very elongated spindle shaped nebulae of the same length, parallel to each other and in contact at their points of greatest condensation or brightness (angle of elongation 80°)".

There is a good deal which is puzzling about these descriptions. Even allowing for differences of scale and focal ratio it seems doubtful whether the nebula as now seen could fit Stewart's description. If it were not for the discrepancy of appearance in Innes' observations, to which he himself calls attention, one might be confident in saying that the appearance had changed, but the variety of the descriptions given casts some doubt on their reliability. The most that can be said is that there is a suspicion of change.

The investigation suggests that IC 4406 may represent a stellar encounter, and the system is clearly one which will repay not only an expert theoretical discussion but also more detailed spectroscopic examination when this becomes possible.

Acknowledgments.—I am much indebted to Dr Thackeray for the use of some of his material and for his critical comments on this paper, and to Dr Knox Shaw for comments on the manuscript.

Radcliffe Observatory,
Pretoria:
1949 *September.*

* D. Stewart, *Harvard Annals*, No. 60, p. 163.
† R. T. A. Innes, *M.N.*, **62**, 469, 1902.

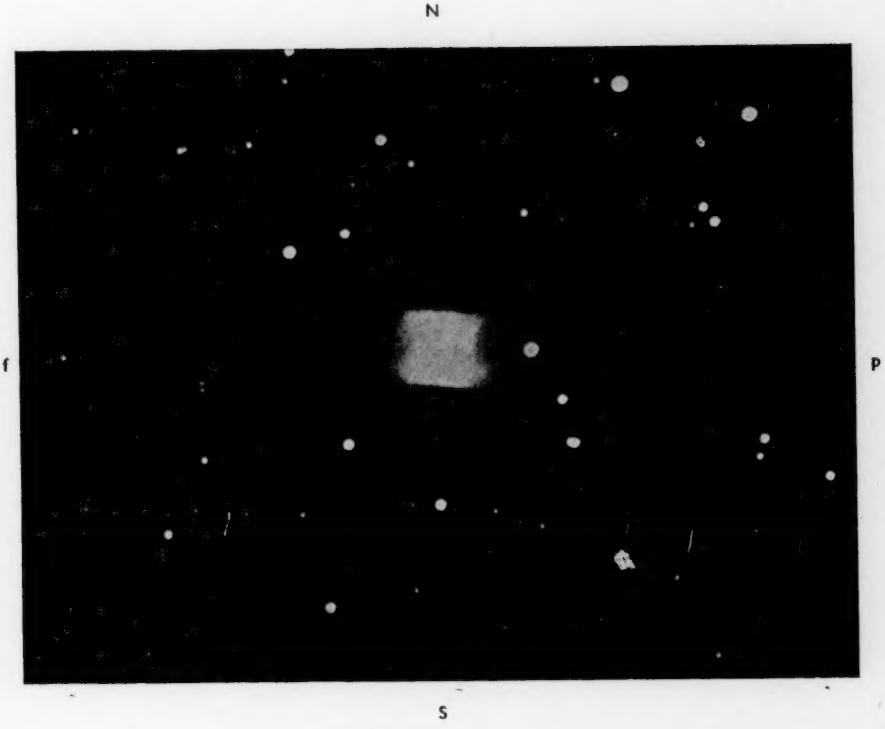

FIG. 3.—IC 4406.

Date: 1949 *April* 19; *Emulsion*: *Kodak* 103*a*—0; *Exposure*: 15 *minutes*; *Magnification*: × 10 *from original plate, giving* 2·25 *seconds of arc per mm. on this plate.*

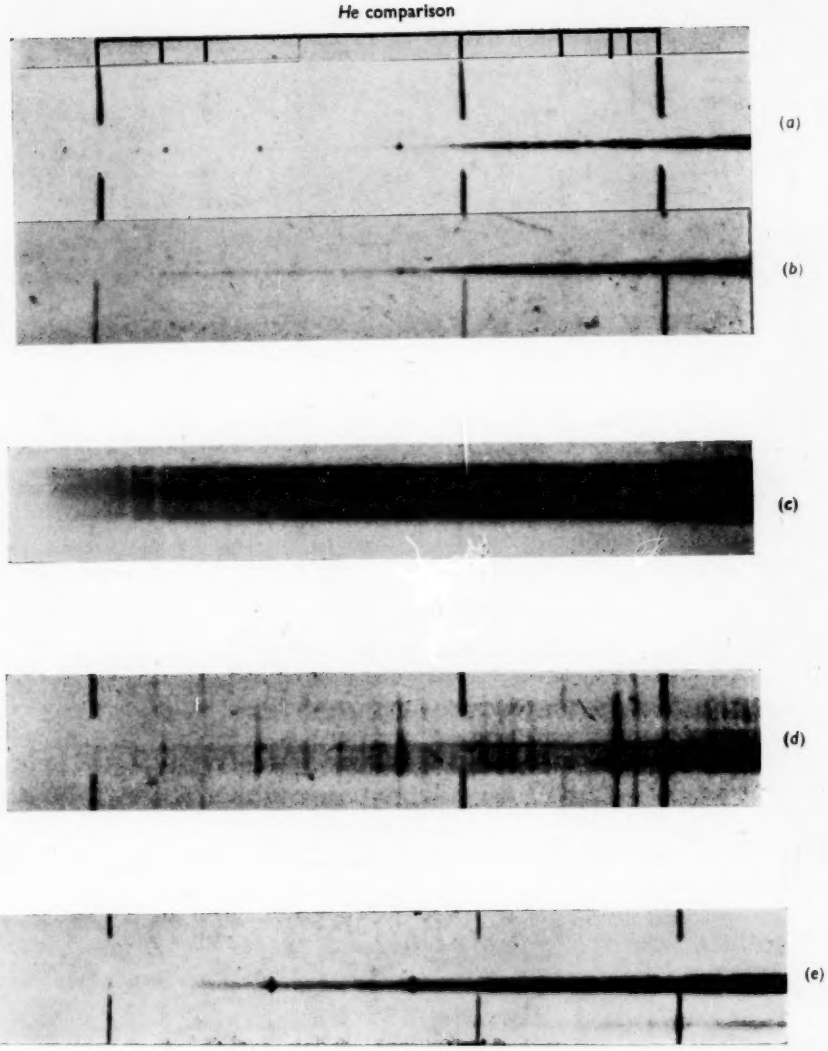

(*a*) *Proxima Centauri*, 1949 *July* 4 (*NS* 45).
(*b*) *Proxima Centauri*, 1949 *August* 3 (*NS* 78).
(*c*) *RR Telescopii*, 1949 *August* 8 (*NS* 89).
(*d*) *RR Telescopii*, 1949 *October* 7 (*NS* 121).
(*e*) 47 *Tuc. Var. No.* 1, *near maximum* (*NS* 97).

FIVE SOUTHERN STARS WITH EMISSION-LINE SPECTRA

A. D. Thackeray

(Received 1949 December 28)

Summary

Low-dispersion spectra showing bright lines of Proxima Centauri, RR Telescopii and of three long-period variables in 47 Tucanae are described. Proxima Centauri is of dMe type, the emission lines apparently varying in intensity. RR Telescopii underwent a rather abrupt transition from F-type absorption to emission plus continuous during the period 1949 August to September.

1. The Newtonian spectrograph at present in use on the 74-inch Radcliffe reflector is best suited for low-dispersion studies of faint extended sources such as diffuse nebulae, globular clusters and extra-galactic nebulae. In the absence of a spectrograph with higher dispersion it has also been used, chiefly at times of bright moon, for obtaining miscellaneous stellar spectra likely to be of interest. The dispersion (240 A./mm. at $H\gamma$) is too low for accurate spectral classification, but the instrument has proved useful for detecting emission-line spectra with which the present paper deals.

All the spectra here described were taken on R 55 Orthochromatic film covering the range 5700 to 3750 A., with the exception of two of RR Telescopii (at its brightest) for which a rather slower emulsion, Ansco Plenachrome, was used. The $f/1$ Schmidt camera gives a reduction factor of 4·2 and hence a wide slit could be tolerated.

2. *Proxima Centauri.*—Table I lists nine spectroscopic observations of this star which, as far as the writer is aware, has not been hitherto accessible to a slit spectrograph. In this and subsequent tables in the "Remarks" column, (*a*) denotes absorption, (*e*) emission.

TABLE I

Observations of Proxima Centauri

NS No.	Date JD 243+	Exp. (min.)	Slit (mm.)	Remarks
35	3088·301	60	0·22	*TiO*+*MgH*(*a*); no emission
45	3102·297	75	·20	*H*(*e*)!; Ca^+(*e*)!
75	3130·210	25	·20	*TiO* strong; no emission
78	3132·203	30	·15	*Hγ*, Ca^+(*e*)
82	3133·224	30	·15	*Hγ*(*e*); *Ca*, *Mn*(*a*)
84	3135·222	30	·15	*Hγ*, Ca^+(*e*)
87	3137·205	30	·13	? *Hγ*(*e*); some moon-fog
90	3139·202	32	·13	No emission
103	3153·210	30	0·15	No emission

The spectrum is of advanced dwarf M type with bands due to *TiO*. Comparison spectra were obtained of 20 C 923 and 20 C 1143 (dM5 and dM3 respectively according to Joy's list of standard types recommended to the I.A.U.). The *MgH* band at 5211 A., found strong in dwarfs relative to giants by Öhman *, has also

* Y. Öhman, *Stockholm Ann.*, Bd. 12, No. 8, 1936.

been measured. A rather strong diffuse structure extending to the violet from a measured wave-length 5567 ± 7 A. has been found on three spectra with correct exposure in this region; it is believed that the (1, 2) band of *MgH* with P and Q heads at 5568 and 5550 may be responsible. It is perhaps surprising that it appears stronger than the (0, 0) band at 5211, although the latter is masked by the strong *TiO* band at 5167. Öhman has also found absorption in this region in M dwarfs extending farther to the red and he has attributed it to the (0, 1) *MgH* band with P and Q heads at 5621 and 5609.

Line absorption due to *Ca* 4226 (apparently asymmetrical as found by Lindblad in dwarfs), *Mn* 4030 and *Fe* 5269 has been measured; Ca^+ H and K absorption is suspected on a weak continuous background on NS 82.

Emission lines due to hydrogen and Ca^+ H and K have been measured on five of the nine spectra. This is a common feature of late M dwarfs according to Joy *, who finds that late type rather than duplicity of the stars appears to be the determining factor. The emission lines appear remarkably strong on NS 45 (1949 July 4); see Plate 2(*a*). In this instance *Hβ*, *Hγ*, *Hδ*, *Hε* + H, K, *Hζ* and possibly two further Balmer lines appear bright, whereas on the other spectra *Hγ*, H and K were usually the only bright lines detected. The longer exposure given on this occasion compared with later spectra was probably more than offset by the fact that the later spectra were obtained with a freshly silvered mirror. The density of the continuous spectrum in the violet is much the same as on some of the later spectra with weak emission; see Plate 2(*b*). Two alternative conclusions suggest themselves: either (1) Proxima had undergone an abrupt physical change on 1949 July 4 perhaps analogous to that of the flares of Luyten's dwarf L–726–8 †, or (2) the origin of the bright-line spectrum does not coincide with that of the M-type continuum and a relatively greater proportion of the former region may have been transmitted by the slit on this single occasion. Unfortunately, the dispersion is too low to permit adequate measurement of radial velocity of the emission relative to the absorption or to the known velocity of the α Centauri system; further observations at the Cassegrain focus are urgently needed to settle this interesting point.

No accurate magnitude observations of Proxima are as yet available at the Radcliffe Observatory to test whether the star is liable to outbursts like those of L–726–8. The Cape observers have examined 58 plates of the star taken for parallax between 1932 and 1949 and have found no evidence of any variation in brightness exceeding 0·10 mag. However, the possibility of variations of about 0·2 mag. lasting less than an hour, such as have been observed ‡ recently for B.D. +20° 2465, is not excluded.

3. *RR Telescopii*.—This star was at one time suspected to be of U Geminorum type, but Kukarkin and Parenago's 1947 Catalogue lists it as "semi-regular", varying between 12·5 and less than 14 with a period of 387 days. Dr P. Kirchhoff of Johannesburg discovered that the star had brightened to 6·0 in 1948 July and photographs at the Cape Observatory showed that the brightening had taken place at least as early as 1946 September.§

* A. H. Joy, *Ap. J.*, **105**, 96, 1947.
† W. J. Luyten, *P.A.S.P.*, **61**, 179, 1949.
‡ K. C. Gordon and G. E. Kron, *P.A.S.P.*, **61**, 210, 1949.
§ R. P. de Kock, *M.N.A.S.S.A.*, **7**, 74, 1948. Harvard records show that the star was at mag. 10 and brightening towards the end of 1944 (M. W. Mayall, *H.B.*, No. 919, 16, 1949).

The star was placed on the observing list for the Newtonian spectrograph at the Radcliffe Observatory and spectra obtained on 1949 June 19 and 20 showed pure absorption apparently of supergiant F type with H and K three times as intense as *Hδ*. The only other element detected in absorption was *Ti*+ (five lines), though *Si*+ 4130 was suspected on both films. *Hβ* could not be detected but the strength of the other members of the Balmer series in absorption suggested that *Hβ* was lost due to a balance of absorption and emission as in some Be stars. This explanation receives some support from the next spectrum of 1949 August 8 which shows *Hβ* bright, *Hγ* undetectable, while *Hδ* and higher members of the series are fairly strong in absorption; see Plate 2 (*c*). In addition to *Hβ*, *Fe*+ 5018 and 4923 appear bright. As on June 20, *Ti*+ is well represented in absorption and *Fe*+ absorption is conspicuous by its absence. The next two spectra (taken on 1949 September 12 and October 7) show a remarkable change to a rich bright line spectrum superposed on a continuous background in which no absorption is measurable; see Plate 2 (*d*).* The dense September exposure shows the Balmer lines bright from *Hβ* to H 3750 at the limit of the film; *Ca*+ K is also bright with intensity approximately equal to H 3889. Nearly all the remaining lines are due to *Fe*+; multiplets 27, 28, 32, 37, 38, 42, 48 and 49 of the "Revised Multiplet Table" are all represented, lines with laboratory intensity equal to or greater than 4 appearing with very few exceptions. *Ti*+ 3913 and 3900 are weakly present; other strong *Ti*+ lines in the blue are lost in blends with *Fe*+. Further spectra taken on November 1 and December 4 show no marked change, though there has perhaps been some fading of the bright lines relative to the continuous.

TABLE II

Observations of RR Telescopii

NS No.	Date JD 243+	Exp. (min.)	Slit (mm.)	Remarks
31	3087·480	3	0·15	*H*, *Ca*+, *Ti*+(*a*); supergiant F spectrum
37	3088·45	3	·15	*H*, *Ca*+, *Ti*+(*a*); supergiant F spectrum
89	3137·429	5	·13	*Hβ*, ? *Fe*+(*e*): *Ca*+, *Ti*+(*a*)
111	3172·365	2	·10	*H*, *Fe*+, *Ca*+(*e*) ! !
121	3197·267	1·5	·15	*H*, *Fe*+, *Ca*+(*e*) ! !
131	3222·315	2·5	·10	*H*, *Fe*+, *Ca*+(*e*) ! !
132	3255·266	4·5	0·15	*H*, *Fe*+, *Ca*+(*e*) ! !

According to information supplied by Dr Kirchhoff the star began to fade in July. The transition to a pure emission spectrum is thus explicable in terms of a weakening of the continuous background which up till October 7 at least left the emission within the line cores relatively unaffected. The prominence of *Ti*+ in the absorption phase and of *Fe*+ in the emission phase recalls the differential behaviour of these two elements in the various shells of Nova Herculis. The spectra of RR Telescopii are of too low dispersion to state whether or not the emission lines are accompanied by violet absorption as in the usual nova, but the long period of maximum light and gradual fading which now seems to have set in suggest that the star should be classified as a "slow nova" with small velocity of expansion. The examples of Nova Pictoris and Nova Herculis show that the star merits the attention of double-star observers.

* This film shows very irregular trailing of the star along the slit due to the shortness of the exposure for such a bright star; but the reader should have no difficulty in distinguishing the stellar lines from the helium comparison.

4. *Long-Period Variables in 47 Tucanae.*—This well-known globular cluster, NGC 104, is remarkable for its apparent lack, despite searches, of typical short-period variables. Bailey's investigations revealed eight variables, apparently either irregular or of long period, of which numbers 1, 2, 3 have been shown by Shapley * to have definitive periods of 211, 203 and 192 days respectively and maxima of between 11·3 and 11·5 mag.

TABLE III

Observations of 47 Tucanae Variables

NS No.	Var. No.	Date JD 243+	Exp. (min.)	Slit (mm.)	Remarks
97	1	3144·463	45	0·15	*H*(*e*) !
105	1	3152·439	25	·15	*H*(*e*); star near maximum
112	3	3172·401	22	·15	*H*(*e*); star near maximum
116	1	3174·474	40	·10	Underexposed
120	1	3187·433	40	·15	
122	2	3197·332	30	·15	*H*(*e*)
123	1	3197·389	60	0·15	

All three of these stars have been photographed near maximum light with the Newtonian spectrograph (see Table III) and have been found to be of Me type, with *TiO* bands of only moderate strength, considerably weaker than in R Cent (M4e). $H\gamma$ and $H\delta$ have been found bright on all spectra with adequate exposure. The two lines are in most cases almost equal in strength, but the first two spectra of variable No. 1 taken at or perhaps a little before maximum show $H\delta$ somewhat stronger than $H\gamma$; see Plate 2(*e*). NS 97, a fairly dense spectrum, shows four Balmer lines beyond $H\epsilon$; $H\epsilon$ itself has not been observed on any of the spectra, presumably due to the usual obscuration by Ca^+ H. In all these features the three variables appear to be quite typical of long-period variables of Me spectra, despite the fact that according to Shapley they have absolute magnitudes at maximum some 5 magnitudes brighter than the average such star. (It is of interest to point out that if this estimate is correct Plates 2(*a*) and (*e*) correspond to stellar spectra, superficially not very dissimilar, but differing by 20 magnitudes in the absolute brightness of their sources.) Attempts to follow variable No. 1 some months after maximum, when other bright lines might be expected to appear if the analogy holds for the phases of decreasing light, have not as yet met with success.

Radcliffe Observatory,
Pretoria:
1949 *December* 13.

* H. Shapley, *P.N.A.S.*, **27**, 440, 1941; *Harv. Repr.*, No. 228, 1941.

SECULAR CHANGES OF STELLAR STRUCTURE AND THE ICE AGES

E. J. Öpik

(Received 1949 April 19)

Summary

A sudden increase in the rate of nuclear energy generation by a certain amount leads to expansion and to a decrease of the luminosity by nearly an equal amount (if measured in stellar magnitudes). Theoretical considerations are confirmed by actual calculations of expanding stellar models.

The corresponding changes of structure consist of two components :— (i) homologous changes, in which the release or absorption of gravitational energy is proportional to T/μ; (ii) pure changes of structure at constant potential energy, in which a certain energy of transition, w, is released in the central regions and absorbed in the outer regions, or vice versa. An approximate formula for w is given in terms of the variation of central density and temperature.

For homologous changes the time of relaxation, t_0, of a disturbance is inversely proportional to $s+3$, s being the temperature exponent of nuclear energy generation; for the Sun t_0 is about 5×10^5 years with $s \sim 15$; this falls well within the order of magnitude of the duration of the Quaternary glaciation.

A scheme of complex expansion, produced by a sudden increase of the intrinsic energy generation, is worked out by numerical integration; pure changes of structure and the boundary condition are schematically taken into account. As compared with homologous expansion, the drop in luminosity is delayed and reduced in depth.

Non-static changes of solar structure are suggested as a plausible cause of the recurrent ice ages on the Earth. An increase in the circumcentral hydrogen content in the Sun, produced by turbulence suddenly starting, may lead to an increased energy production and thus to a decreased luminosity.

Other existing theories of Quaternary climatic changes are briefly reviewed; it is shown that none of these is able to account for the observed size of the changes.

---

1. *Introduction.*—It has been formerly suggested by the writer* that a temporary expansion of the Sun may have caused a dimming of solar luminosity and a corresponding deterioration of the terrestrial climate known as the still lasting Quaternary glaciation, similar causes possibly being responsible for other ice ages which occurred on the Earth several times since the Archaean. After some disturbance in the energy balance the Sun is supposed to start re-adjusting itself toward a new equilibrium configuration; if this re-adjustment requires expansion, gravitational energy is absorbed at the expense of the radiative energy flux and the apparent luminosity is likely to decrease. The time intervals involved in such a re-adjustment agree more or less with the known duration of the Quaternary.

In the present paper a closer theoretical consideration is given to the above suggestion. This involves the theory of non-static stellar models.† As the

* E. Öpik, *Tartu Obs. Pub.*, **30**, No. 3, 1938; *Acta et Commentationes Univ. Tartu (Dorp.)*, Ser. A, **33**, 1938.

† F. Hoyle and R. A. Lyttleton, *M.N.*, **107**, 246, 1947, discuss non-static stellar models from a standpoint which, however, is hardly related to our present problem. The present theory was practically ready several years ago, but circumstances of the war prevented its publication.

time intervals involved in the changes considered here are large as compared with the period of free pulsations of the star (which is about a couple of hours for the Sun), the deviations from hydrostatic equilibrium are insignificant; therefore, all the ordinary equations of hydrostatic and radiative equilibrium remain practically valid in these non-static models. The only difference with respect to a static model consists in the distribution of the energy sources, gravitational energy sources being additionally active.

2. *The Model and the Disturbance.*—We will consider a typical stellar model, with the intrinsic (nuclear) energy sources confined to the central core (not necessarily a point-source); such a model consists of three main portions*: a convective core of radius r_1, mass M_1; an intermediate radiative equilibrium shell between r_1, M_1 and r_2, M_2; and a peripheral convective region, extending from r_2, M_2 outwards until the photospheric boundary is reached at the radius $r=R$ and total mass M of the star. In the core, the hydrogen content is supposed to decrease with time, as the result of nuclear reactions; in this way models with non-uniform chemical composition are formed. Several scores of different typical cases of such models have been calculated by the writer.† Cowling's model‡ is a particular case of uniform composition throughout and of a vanishing peripheral convective region. The different composite models are generally non-homologous with respect to one another.

In a real case, the type of the model is determined by the photospheric boundary condition (ρ_p, T_e); the density ρ_p at photospheric level depends upon the law of photospheric opacity; the effective temperature T_e must satisfy the condition of radiation to space equalling the heat transfer from the interior; the photospheric level itself may be practically identified as the level at optical depth $\frac{2}{3}$. The solution of the equations of hydrostatic, radiative and convective equilibrium is made to satisfy the boundary condition.

The boundary condition is extremely sensitive to the extent of the peripheral convective region, whereas for an equal extent of the latter it depends very little upon the conditions in the deep interior.§ Therefore we will symbolize the boundary condition by its practical equivalent, or by a certain ratio M_2/M, which is the relative mass inside the second (subphotospheric) interface. Cowling's model, with a "complete radiative outer shell", corresponds to $M_2/M=1$; from what we know of the photospheric opacity, the Sun's case probably does not differ much from that. Another extreme case is $M_2/M=M_1/M$, or when the two interfaces coincide, or the "complete adiabatic model". Most real cases of dwarf stars may be supposed to fall between these two extremes.

The boundary condition cannot be violated very much; but a slight increase in the extent of the peripheral convective region leads to a considerable decrease in the photospheric temperature and radiation, which means that a considerable fraction of the heat generated inside cannot be radiated any more to space; the extra heat becomes stored inside in the form of potential energy of gravitation and leads to expansion; as a consequence, the central temperature decreases, the nuclear energy sources are slowed down, and equality between energy

* E. Öpik, *Tartu Obs. Pub.*, **30**, No. 4, 1938.

† *Ibid.*, also **31**, No. 1, 1943 and recent material, in press or unpublished.

‡ T. G. Cowling, *M.N.*, **96**, 42, 1935.

§ Indirectly the boundary condition is also extremely sensitive to the conditions in the interior in so far as these affect the extent of the peripheral convective region; if, however, the latter is kept constant (by a suitable choice of the energy flux), the boundary condition varies little.

generation and radiation to space is approached again. This process of self-regulation of the energy balance is favoured by the circumstance that a decrease in the internal energy flux produces automatically a shrinking of the peripheral convective region, as an inherent property of the solution of the equations of radiative equilibrium; thus the boundary condition meets half-way the self-regulation of the energy sources.*

The disturbance of the energy balance can be imagined as a suddenly initiated convective mixing in the central regions of the star. The writer has calculated models† in which the hydrogen content increases outwards, starting from the boundary of the core, and which after continued transformation of hydrogen into helium are apt to develop a new convective region outside the core. The latter leads to a discontinuous change of structure, the local polytropic index changing by a finite amount from a value of $n=1{\cdot}2$–$1{\cdot}3$ to the adiabatic value near $n=1{\cdot}5$. The discontinuity is caused by the circumstance that the gradient of molecular weight which has installed itself during the radiative equilibrium stage is wiped out by the newly established convective equilibrium. Because of the discontinuity, the convective disturbance spreads out with finite speed, producing mixing of the material over a wide but limited range in the interior; a merging of the new convective zone and the original core is possible. In any case the result of such a disturbance will be a transport of hydrogen toward the exhausted central regions and thus a possible increase of the energy output. The detailed study of the processes involved is made elsewhere (unpublished). A surprising result is that the time intervals involved in the propagation of the convective disturbance are not so short, up to 10^7 years for solar dimensions, with major effects showing up after the lapse of some 10^6 years since the start. However, for the general way of treatment applied in the present paper the details are irrelevant. It suffices to admit the possibility of a "sudden"‡ increase in the intrinsic energy output. The consequences of this increase can be studied in a differential way, by comparing the disturbed model with an undisturbed one, both models being built upon exactly the same set of differential equations and physical constants but for the changed distribution of the energy sources. For the differential study almost any type of a radiative equilibrium model is well adapted, but for the sake of simplicity we will use for this purpose models of uniform composition (constant molecular weight throughout), namely the writer's series of models numbered from 1 to 7§ which are representative of the static composite models of the entire range of boundary condition from $M_2/M=M_1/M$ (No. 1) to $M_2/M=1$ (No. 7)‖, the last case differing from Cowling's¶ but slightly (in taking into account radiation pressure and electron scattering).

3. *The Luminosity of Slowly Expanding or Contracting Models.*—The integration of the equations of radiative equilibrium of a static model can be

* For boundary condition *cf.* also H. N. Russell, *M.N.*, **97**, 127, 1937, and L. Biermann (jointly with T. G. Cowling), *A.N.*, **267**, 131, 1938.

† *Proc. Roy. Irish Acad. A*, **53**, 1, 1949; *Armagh Obs. Contr.*, No. 3, 1950 (in press).

‡ Sudden as compared with a time-scale of the order of 10^9 years.

§ *Loc. cit.*

‖ Outside these extreme values of M_2/M the boundary condition may still vary, leading to "super-radiative" photospheres at $M_2/M=1$ (early-type stars), or to "super-convective" structures with $M_2/M=M_1/M$ (perhaps red dwarfs) in which the convective transport of heat does nowhere vanish; for stars around the solar mass these cases hardly do occur.

¶ *Loc. cit.*

performed by assuming an arbitrary value for the intrinsic energy generation, E (core-source); each value of E leads to one definite boundary condition and vice versa. Actually the range of E (for a given mass of the model) which leads to a more or less reasonable boundary condition is rather narrow. In nature the boundary condition (although unknown to us) is fixed by the behaviour of photospheric opacity and, therefore, the value of E is also precisely fixed, $E=E_0$ being the static value leading to the prescribed boundary condition. In the static model (core-source) the radiative flux outside the core is constant and equal to $Q=E_0$; this is also identical with the luminosity $L_0=E_0$, representing the energy radiated to space. A deviation of E from the equilibrium value E_0, at the imposed boundary condition, is incompatible with a static solution; it requires an expanding ($E>E_0$) or contracting ($E<E_0$) model. For the non-static model let Q_r be the variable radiative flux in the radiative equilibrium zone, H_r—the gravitational energy generated inside r per unit of time; evidently

$$Q_r=E+H_r. \tag{1}$$

Let Q_1, H_1 correspond to the boundary of the convective core, Q_2, H_2 to the top of the radiative equilibrium zone, and let H be the total gravitational energy generated by the model, so that its luminosity is given by

$$L=E+H. \tag{2}$$

Consider a small deviation $E-E_0$ from the static value; the principle of continuity and average quantities require that, at the same boundary condition, in the non-static model a certain average value of the radiative flux intermediate between Q_1 and Q_2 be equal to the static value E_0,

$$Q_1 \gtrless E_0 \gtrless Q_2.$$

This may be written also as

$$E_0=kQ_1+(1-k)Q_2, \tag{3}$$

where k is a positive fraction. In the solution of the equations of radiative equilibrium a variation of the radiative flux affects the boundary condition the more the deeper it is situated; therefore the relative weight of Q_1 in (3) exceeds the weight of Q_2, $k>1-k$ or $k>\frac{1}{2}$; the semi-empirical value $k=\frac{2}{3}$ fits well actual stellar models as shown below.*

Substituting Q_1 and Q_2 according to (1) into (3), setting $h_1=H_1/H$, $h_2=H_2/H$ and with

$$a=kh_1+(1-k)h_2, \tag{4}$$

it is easy to obtain

$$E-E_0=-aH; \tag{5}$$

also, substituting H from (5) into (2) we get the deviation of the luminosity of the non-static model from the static value as

$$L-L_0=L-E_0=-\frac{(1-a)}{a}(E-E_0). \tag{6}$$

As h_1 and h_2 by their definition are reasonably positive fractions, the characteristic factor a is by (4) also a positive fraction. Hence (5) tells us that an increase of E requires a negative value of H, which means expansion, and vice versa. From (6) we infer that the change of luminosity is always of opposite sign to the change of the nuclear energy generation.

* *Cf.* Addendum.

Assuming with Eddington that the release of gravitational energy per unit of mass and time is proportional to the temperature (actually to T/μ for non-homogeneous composition), an assumption strictly corresponding to homologous changes of structure but which turns out to be an excellent approximation for the actual non-homologous changes likely to occur, we find that for Models Nos. 7, 6, 5, representing possible configurations of a solar mass with a relative mass of the core about 0·14, about 22–23 per cent of the gravitational energy is released inside the core. We assume the round value $h_1 = 0{\cdot}25$, further $h_2 = 1$ and $k = \frac{2}{3}$; this yields $a = \frac{1}{2}$ and from (5) and (6)

$$H = -2(E - E_0), \tag{5'}$$

$$L - L_0 = -(E - E_0). \tag{6'}$$

The expected change in luminosity is opposite in sign and equal in amount to the change in the energy generation, and the release of gravitational energy is the double of that. The value of a may vary with the type of the model; however, for widely different models the above equations are changing but insignificantly.

These general considerations are substantiated by actual calculations of expanding models. To the usual equations of hydrostatic and radiative equilibrium the differential equation of the release of gravitational energy is added:

$$dH_r = CT\,dM_r; \tag{7}$$

the constant C, negative in the case of expansion, is chosen arbitrarily; E is then determined from an integration over the whole convective core according to equation (1):

$$Q_1 = E + C\int_0^{M_1} T\,dM_r. \tag{8}$$

Q_1, the radiative flux at the boundary of the core, is given independently by the assumed structure of the core (polytrope $n = 1{\cdot}5$) and the law of opacity; continuity of the radiative flux at the boundary of the core is assumed.

The comparison between a certain set of non-static and static cases for the same boundary condition is given in Table I. The non-static models of this

TABLE I

Expanding and Static Models at Same Boundary Condition and Constant Central Temperature

M_2/M	0·297	0·386	0·491	0·682	0·824	0·929	0·969	1·000
M_1/M Exp.	0·297	0·297	0·295	0·289	0·284	0·279	0·277	0·277
M_1/M Stat.	0·224	0·188	0·165	0·151	0·144	0·140	0·139	0·138
R Exp.	1·000	1·000	1·000	1·014	1·048	1·105	1·185	1·423
R Stat.	1·000	1·000	1·009	1·037	1·086	1·186	1·286	1·576
ρ_c/ρ_m Exp.	6·00	6·03	6·10	6·60	7·58	9·19	11·49	19·96
ρ_c/ρ_m Stat.	6·00	6·06	6·50	7·69	9·5	13·0	16·9	31·3
$-2{\cdot}5 \log \frac{E}{E_0}$	−0·20	−0·36	−0·59	−0·79	−0·88	−0·95	−0·95	−0·95
$-2{\cdot}5 \log \frac{L}{L_0}$	+0·26	+0·53	+0·78	+0·91	+0·97	+0·99	+1·01	+1·02

table have been built all on the same core, corresponding to $z = 1{\cdot}5$ (Emden's reduced radius), all the range of M_2/M being obtained by varying the parameter C in (7); the results were reduced to constant mass and central temperature with the aid of homologous transformations (using mean values of the radiation pressure); the values for the static models are interpolated according to M_2/M from the actually calculated set of Nos. 1–7. In the table, M_1/M is the relative mass of the core, R the relative radius of the model, ρ_c/ρ_m the ratio of central to mean density. The last two lines of the table give the change of the energy output and of the luminosity, both expressed in stellar magnitudes; from a comparison of these two lines it appears that, for the present finite and rather large changes, the simple relation (6′) deduced in the present section is of course no more valid, but that a similar relation referring to the logarithmic changes is approximately fulfilled: the logarithm of the luminosity varies by about the same absolute amount but in the opposite direction as compared with the logarithm of the energy production. For the first two cases of small changes the infinitesimal relation (6′) is, however, almost exactly fulfilled:

M_2/M	$= M_1/M$	0·386	0·491
$(E-E_0)/E_0$	+0·20	+0·39	+0·72
$(L-L_0)/E_0$	−0·21	−0·39	−0·51

4. *Changes of Structure.*—Any change of stellar structure can be considered as consisting of two components: a general homologous transformation in which the potential energy changes inversely as the radius; and a non-homologous transition at constant potential energy which we will call further a "pure change of structure".

In usual notations the potential energy of a spherically symmetrical body is given by*

$$\Omega = G\int_0^M \frac{M_r\,dM_r}{r}, \tag{9}$$

also

$$\Omega = 3\int_0^M PV\,dM, \tag{10}$$

with

$$PV = \frac{\mathfrak{R}T}{\beta\mu} = (\gamma-1)c_v T, \tag{11}$$

where $\gamma = c_p/c_v$ refers to the mixture of gas plus radiation. When the molecular weight is constant and when $1-\beta$ is small, an average value of β over the whole model can be used and (10) may be represented as

$$\Omega = \frac{3\mathfrak{R}}{\bar{\beta}\mu}\,\overline{T}M, \tag{12}$$

where

$$\overline{T} = \frac{\int_0^M T\,dM}{M}. \tag{13}$$

* *Cf.* A. S. Eddington, *Internal Constitution of the Stars*, Cambridge, 1926, and various other sources.

For a true polytrope of index n (9) is reduced to

$$\Omega = \frac{3}{(5-n)} \frac{GM^2}{R} . \tag{14}$$

Table II represents a sequence of pure changes of structure along true polytropes; for these $\bar{\beta}$ = const. or $\bar{\beta} = 1$ is to be assumed somewhat artificially; for $n = 3{\cdot}25$ the data are based on Chandrasekhar's* calculations, the rest on Emden's.† According to (12), Ω = const. implies $\overline{T}$ = const., whence the relative central temperature is determined from

$$\frac{T_c}{\overline{T}} = \frac{R'(5-n)}{M'(n+1)} \tag{15}$$

and the relative central density is

$$\rho_c \sim (5-n)^3 . \frac{\rho_c}{\rho_m} ;$$

R' and M' are Emden's reduced radius and reduced mass (Eddington's notations).‡

The table shows that a pure change of structure with increasing n requires an increasing central density and a decreasing central temperature. Both these changes mean a release of heat at the centre. As the potential and the total energy of the model remain constant, an equal amount of heat must be absorbed in the outer regions. Thus a pure change of structure requires a certain "energy of transition", w, to be transferred from the central regions to the outer regions (increasing n, positive w) or in the opposite direction (decreasing n, negative w).

TABLE II

Polytropes at Constant Mass and Potential Energy

n	R relative	$T_c/\overline{T}$	T_c relative	ρ_c relative
1·5	1·0000	1·884	1·0000	1·000
2·0	1·1667	1·806	0·9582	1·196
2·5	1·4000	1·758	0·9332	1·462
3·0	1·7500	1·710	0·9080	1·690
3·25	2·0000	1·693	0·8989	1·836
4·0	3·5000	1·661	0·8815	2·423
4·9	35·0000	1·655	0·8784	3·632

This remains true for all kinds of pure change of structure, whether polytropic or not. As shown below, the energy of transition for the composite non-polytropic models of the above-described type is considerably smaller than for true polytropes and amounts to a small fraction of the potential energy, practically of the order of 10^{-3}, 10^{-2} at the utmost. Therefore, instead of using the laborious method of numerical integration in each particular case, a differential formula can be derived. The formula yields the energy of transition in units of the potential energy with sufficient accuracy (to quantities of second order) for transitions between two arbitrary models when the variations of T_c, ρ_c at constant potential energy are given.

* S. Chandrasekhar, *Ap. J.*, **89**, 116, 1939.
† R. Emden, *Gaskugeln*, Leipzig, 1907.
‡ A. S. Eddington, *op. cit.*

The energy released per unit mass in a change of state is

$$dq = -(P\,dV + c_v\,dT). \tag{16}$$

Assuming $\bar{\beta} = 1$, $P = p_g$ (gas pressure), $\gamma = \frac{5}{3}$ (monatomic gas), an approximation admissible for stars of about the solar mass and even larger, with the aid of (11) and (12) it is easy to obtain with $\rho = 1/V$, when for dq, $d\rho$, dT the small finite quantities q, $\Delta\rho$, ΔT are substituted

$$q = \tfrac{1}{2}\frac{\Omega}{M}\frac{T}{\bar{T}}\left(\frac{2}{3}\frac{\Delta\rho}{\rho} - \frac{\Delta T}{T}\right), \tag{17}$$

which gives the heat released per unit mass in the finite but small change of state.

For homologous transitions $\Delta\rho/\rho$ and $\Delta T/T$ are constant, whence $q \sim T$; for non-homologous changes this is no more true, but the absolute value of q remains a quantity of the order of T; we may assume

$$q/T \sim \tfrac{2}{3}\frac{\Delta\rho}{\rho} - \frac{\Delta T}{T} \sim a - bx,$$

where $x = M_r/M$ is the relative mass and

$$a = \tfrac{2}{3}\frac{\Delta\rho_c}{\rho_c} - \frac{\Delta T_c}{T_c}. \tag{18}$$

On a broad line $u = T/T_c$ does not very essentially differ from $1 - x$, as shown by the run of these quantities for the composite model No. 7:

$1-x$	1·000	0·862	0·624	0·407	0·295	0·121	0·000
u	1·000	0·793	0·606	0·473	0·400	0·277	0·000

This is typical for all models which may come into question. Therefore (17) may be represented fairly well as a quadratic wave

$$q = \tfrac{1}{2}\frac{\Omega}{M}\frac{T_c}{\bar{T}}(1-x)(a-bx).$$

For pure changes of structure

$$\int_0^M q\,dM = M\int_0^1 q\,dx$$

must vanish, which yields $b = 3a$.

The energy of transition represents the maximum absolute value of

$$M\int_0^x q\,dx$$

which is attained evidently at

$$q = 0, \qquad x = x_0 = \frac{a}{b} = \tfrac{1}{3};$$

x_0 separates the region of positive q from that of negative q. Performing the integration, further assuming as a broad average $T_c/\bar{T} = 1{\cdot}7$ (*cf.* Table II, around

$n=3$–$3{\cdot}25$), and substituting (18) for a, we get an expression for the energy of transition

$$w=\frac{\Omega}{8}\left(\frac{2}{3}\frac{\Delta\rho_c}{\rho_c}-\frac{\Delta T_c}{T_c}\right), \tag{19}$$

which can be used irrespective of the type of model. Table III contains collected data for the seven typical composite models.*

The effective value of the polytropic index in the sixth line of the table is chosen to satisfy the potential energy in equation (14); as compared with the true polytropes of Table II, at constant potential energy the range in radius corresponds more or less to n (effective); the range in T_c and ρ_c, however, is much smaller than for true polytropes of an equal range in n; moreover, there is an "inversion" in the trend of T_c between No. 6 and No. 7. As a consequence, the energies of transition between these core-source composite models are considerably smaller than for true polytropes.

TABLE III

Potential Energy and Energy of Transition of Composite Models

[μ=const.]

Model No.	1	2	3	4	5	6	7
M_2/M	0·250	0·358	0·478	0·684	0·820	0·943	1·000
M_1/M	0·250	0·189	0·167	0·150	0·143	0·139	0·138
ρ_c/ρ_m	6·00	6·06	6·42	7·70	9·51	13·96	31·27
Ω, 10^{48} erg $\left(\begin{matrix}M=M_\odot\\R=R_\odot\end{matrix}\right)$	3·235	3·245	3·283	3·408	3·583	4·006	5·205
n, effective	1·50	1·51	1·55	1·68	1·84	2·18	2·83
Ω, 10^{48} erg $\left(\begin{matrix}M=M_\odot\\\bar{\epsilon}\sim T_c^{20}\end{matrix}\right)$	3·235	3·225	3·218	3·205	3·190	3·173	3·161
$-2{\cdot}5\log L+$const.	−0·84	−0·83	−0·68	−0·40	−0·21	−0·04	0·00
At Constant Mass and Potential Energy							
T_c relative	1·0000	0·9970	0·9922	0·9838	0·9804	0·9779	0·9795
ρ_c relative	1·0000	0·9998	1·0235	1·0980	1·1631	1·2257	1·2514
R relative	1·000	1·003	1·015	1·053	1·109	1·238	1·609
Transition	1→2	2→3	3→4	4→5	5→6	6→7	...
w/Ω, 10^{-5} units	+35	+257	+694	+525	+471	+153	...

In Table III, the seventh line gives the potential energy on the assumption that the average release of nuclear energy per unit of mass and time is proportional to the 20th power of the central temperature, with the relative luminosities as in the eighth line (stellar magnitudes); this case, which may be near to the actual conditions for dwarf stars, yields an almost constant potential energy for the different composite models.

* E. Öpik, *Tartu Obs. Pub.*, **30**, No. 4, 1938.

5. *Decay of the Disturbance through Homologous Transitions.*—For a first approximation we neglect the pure changes of structure and changes in the boundary condition which actually should accompany every disturbance; the type of structure and the boundary condition we regard as rigidly imposed on the model during all the changes it is likely to undergo; similarly, we assume the equilibrium luminosity $L_0 = E_0$ to be independent of the radius, disregarding thus factors of the order of $R^{-0.5}$ which would follow from Kramers' law of opacity. We remain thus within the frame of Section 3 of the present paper, assuming the response of the rate of expansion and of luminosity to a disturbance in the energy generation to take place instantaneously according to the simple formulae (5′) and (6′).

We assume a law of energy generation $E = C(1+\lambda)\rho_c T_c^s$ and assume that the disturbance consists in λ changing suddenly from zero to a certain finite value and remaining constant after that. The equilibrium luminosity is thus $E_0 = C\rho_0 T_0^s$, ρ_0, T_0, R_0 and Ω_0 being central density, central temperature, radius and potential energy of the initial undisturbed model. By homology $T_c \sim R^{-1}$, $\rho_c \sim R^{-3}$ and it is easy to verify that after the disturbance has started

$$E = E_0(1+\lambda)\left(\frac{R_0}{R}\right)^{s+3}. \tag{20}$$

The output of gravitational energy is a fraction

$$\frac{\gamma - \frac{4}{3}}{\gamma - 1} = \tfrac{1}{2}$$

of the variation of the potential energy when $\gamma = \frac{5}{3}$; hence

$$H = \tfrac{1}{2}\frac{d\Omega}{dt} = -2(E - E_0)$$

by (5′); as

$$\Omega = \Omega_0 \frac{R_0}{R},$$

we obtain the differential equation (t = time)

$$\frac{R_0}{R^2}\frac{dR}{dt} = \frac{4E_0}{\Omega_0}\left[(1+\lambda)\left(\frac{R_0}{R}\right)^{s+3} - 1\right]. \tag{21}$$

The expansion ($\lambda > 0$) or contraction ($\lambda < 0$) proceeds according to this formula, approaching asymptotically the new equilibrium state $E_1 = E_0$ which, according to (20), corresponds to an equilibrium radius

$$R_1 = R_0(1+\lambda)^{1/s+3}. \tag{22}$$

For small changes (21) may be simplified, by setting $x = R/R_0 - 1$ and by retaining only members of the first order with respect to x and λ; this gives

$$\frac{dx}{dt} = \frac{4E_0}{\Omega_0}[\lambda - (s+3)x],$$

or, setting $t = 0$ at $x = 0$, we get

$$x = \frac{\lambda}{(s+3)}(1 - e^{-t/t_0}), \tag{23}$$

where

$$t_0 = \frac{\Omega_0}{4E_0(s+3)} \tag{24}$$

represents the time of relaxation of the disturbance. Assuming a solar luminosity $E_0 = 3{\cdot}8 \times 10^{33}$ erg/sec. and a potential energy of $\Omega_0 = 4 \times 10^{48}$ (Table III, Model No. 6), with $s = 15$ we get $t_0 = 4{\cdot}4 \times 10^5$ years as a probable figure for the Sun.

The disturbance of the luminosity decays with the same period, in agreement with (6′) and (20),

$$L - E_0 = -\lambda E_0 e^{-t/t_0}. \tag{25}$$

6. *Complex Decay of Disturbance.*—The above assumption of an instantaneous response of the luminosity to a disturbance, with homologous changes, is rather schematical. The expanding model does not undergo exactly homologous changes (*cf.* Table I), wherefore a certain energy of transition appears as a delaying factor; also, the boundary condition will be violated to a certain extent. Here an attempt is made at a second approximation in which the changes of structure and of the photospheric temperature are taken into account, although still rather schematically. As the initial type of static model we assume No. 7; according to Section 3, expansion requires an increase of M_1/M, the relative mass of the core; from Table III we infer that this would correspond to a shift of structure from No. 7 toward the earlier numbers; we therefore assume conventionally that the structure may undergo a continuous displacement along the composite models of Table III. As a continuous coordinate of structure we assume the relative energy of transition $y = w/\Omega$, starting from No. 7; this is found as follows from the last line of Table III:

TABLE IV

Model No.	7	6	5	4	3	2	1
$y \times 10^5$	0	−153	−624	−1149	−1843	−2100	−2135
$T_e(\rho_p = \text{const.})$	5800	4880	4650	4557	4465	4396	4350

The last line gives T_e, the photospheric temperature which follows from the numerical solution of the models, assuming a constant value of the photospheric density, ρ_p, chosen so as to give $T_e = 5800$ deg. for Model No. 7. The external radiation is prescribed by T_e (and radius). Instead of the actual figures, the luminosity as function of the structural parameter y is represented by an empirical interpolation formula

$$L = \tfrac{10}{9} E_0[1 - (-y + 10^{-10})^{1/10}], \tag{26}$$

satisfactorily corresponding to T_e of Table IV; E_0 is the equilibrium luminosity of Model No. 7 ($y = 0$).

The equilibrium luminosity E_0' of different structures ($y \neq 0$) differs, however, from E_0. The actual deviations $\log E_0'/E_0$ are identical with the figures of the eighth line of Table III. According to formula (3), $E_0' = \bar{Q}$ is identical with a certain average value of the radiative flux inside the radiative equilibrium zone for the given set of models. This is well represented by the empirical formula

$$E_0' = \bar{Q} = E_0[1 + 197(-y)^{4/3}]. \tag{27}$$

The actual luminosity of the expanding model differs from $\bar{Q}$ and is given by (26).

The radiative flux has to take care of the following components: the energy from nuclear sources, E (positive); the gravitational energy, H_r (negative for expansion), of the homologous component in the change of structure; and the flow of the energy of transition, the maximum value of which is given by

$$J = \frac{dw}{dt} = \Omega \frac{dy}{dt}, \tag{28}$$

a negative quantity for the transitions from No. 7 toward the earlier numbers.

The radiative flux at the first interface will be

$$Q_1 = E + 0{\cdot}25H + J,$$

with respect to E and H in agreement with Section 3 ($H_1 = 0{\cdot}25H$), whereas for J the coefficient should really be somewhat less than 1 (Section 4).

The flux at the second interface will be

$$Q_2 = L = E + H^*;$$

according to formula (3), $k = \frac{2}{3}$, we obtain

$$\bar{Q} = E + \tfrac{1}{2}H + \tfrac{2}{3}J. \tag{29}$$

This expression, being comparable with (27), is of fundamental importance for the solution of our problem.

In agreement with formulae (5′) and (6′) we assume

$$E = E_0 - \frac{H}{2}, \tag{a}$$

$$L = E_0 + \frac{H}{2}. \tag{b}$$

Differentiation of (*a*) yields

$$\frac{dE}{dt} = -\tfrac{1}{2}\frac{dH}{dt}. \tag{c}$$

On the other hand, assuming for the homologous component of the change of structure the formulae of Section 5 for small changes, (*b*) with (25) yields

$$H = 2(L - E_0) = -2\lambda E_0 e^{-t/t_0},$$

whence by differentiation

$$\frac{dH}{dt} = -\frac{H}{t_0}. \tag{d}$$

Substituting (*d*) into (*c*), we get the last of our differential equations required for the solution

$$\frac{dE}{dt} = +\frac{H}{2t_0}. \tag{30}$$

The above system of equations is conveniently reduced to relative variables: $\tau = t/t_0$; $y = w/\Omega$ as before; $z = E/E_0$; $h = H/E_0$; $j = J/E_0$. Setting

$$a = \frac{L_0 t_0}{\Omega_0} = \frac{1}{4(s+3)},$$

* Practically correct for transitions between Nos. 7 and 6 which alone come into question here, as shown below.

we obtain:

$$\left.\begin{aligned} \frac{dy}{d\tau} &= aj; \\ \frac{dz}{d\tau} &= \tfrac{1}{2}h; \\ z+\tfrac{1}{2}h+\tfrac{8}{3}j &= 1+197(-y)^{4/3}; \\ z+h &= \tfrac{10}{9}[1-(-y+10^{-10})^{1/10}]. \end{aligned}\right\} \qquad (31)$$

Table V represents the result of a numerical integration, for $s=15$, $a=\frac{1}{72}$; for $\tau=0$ the relative energy generation is assumed to increase suddenly from $z_0=1$ to $z=1{\cdot}5(\lambda=0{\cdot}5)$.

The first column gives the time in years, assuming for a solar mass the time of homologous relaxation equal to half a million years; the third column gives L/E_0, the relative luminosity; the fourth column gives $2-z=2-E/E_0$ which would be the march of luminosity in the case of instantaneous response, according to formula (6′); the last column gives the effective radiative flux inside, which is seen to change very little. Remarkable is the great stability in the type of structure as revealed by y; the maximum change (at $t=1{\cdot}5\times10^5$) corresponds to only about one-sixth of the interval No. 7→No. 6. On the other hand, the variation of the luminosity is very much influenced by the "inertia of structure and boundary condition", as follows from a comparison of columns 3 and 4 and as is shown in Fig. 1.

TABLE V

Decay of Disturbance by Simultaneous Expansion and Change of Structure

t years ($t_0=5\times10^8$)	y	L/E_0	$2-z$	h	j	$\bar{Q}/E_0$
<0	0	1·000	1·000	0	0	1·000
0	0	1·000	0·500	−0·500	−0·375	1·000
0·005	$-5{\cdot}2\times10^{-11}$	0·995	·500	− ·505	− ·370	1·000
0·05	$-4{\cdot}8\times10^{-10}$	·979	·500	− ·521	− ·359	1·000
0·5	$-4{\cdot}8\times10^{-9}$	·947	·500	− ·553	− ·335	1·000
5	$-4{\cdot}5\times10^{-8}$	·907	·500	− ·593	− ·305	1·000
50	$-4{\cdot}0\times10^{-7}$	·857	·500	− ·643	− ·269	1·000
500	$-3{\cdot}5\times10^{-6}$	·796	·500	− ·704	− ·222	1·000
5000	$-2{\cdot}75\times10^{-5}$	·722	·504	− ·774	− ·163	1·000
5×10^4	$-17{\cdot}5\times10^{-5}$	·643	·540	− ·817	− ·073	1·002
$\cdot\times10^5$	$-24{\cdot}7\times10^{-5}$	·627	·581	− ·792	− ·030	1·003
$1{\cdot}5\times10^5$	$-26{\cdot}6\times10^{-5}$	·622	·620	− ·758	+ ·003	1·003
2×10^5	$-24{\cdot}5\times10^{-5}$	·627	·657	− ·716	+ ·027	1·003
$2{\cdot}5\times10^5$	$-19{\cdot}5\times10^{-5}$	·638	·692	− ·670	+ ·044	1·002
3×10^5	$-12{\cdot}9\times10^{-5}$	·658	·724	− ·618	+ ·051	1·001
$3{\cdot}5\times10^5$	$-6{\cdot}0\times10^{-5}$	·690	·754	− ·556	+ ·048	1·000
4×10^5	$-1{\cdot}2\times10^{-5}$	0·753	0·780	−0·467	+0·020	1·000

The complex decay (A) yields a very broad minimum, the lowest luminosity of 0·622 being attained $1{\cdot}5\times10^5$ years after the start; the first approximation ($B=2-z$) starts much deeper, at 0·5, then rises steadily. For $t>4\times10^5$ both curves approach the curve of exponential decay and merge into each other.

As to the response of luminosity at the beginning of the disturbance in case A, although not instantaneous it is nevertheless catastrophically rapid, noticeable already during the first year and exceeding one-half of the largest effect after 500 years.

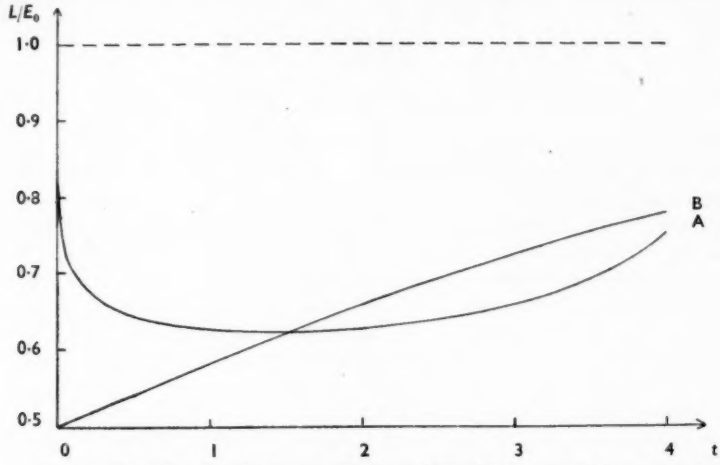

FIG. 1.—*Variation of luminosity caused by a 1·5-fold sudden increase in the energy output.*
Abscissae: time in 10^8 years, for a solar mass.
Ordinates: relative luminosity.
A: complex decay (second approximation).
B: instantaneous response (first approximation).
Broken line: original (equilibrium) luminosity.

7. *The Ice Ages.*—The problem can only be very briefly reviewed here. It is gratifying to notice that the standpoint assumed earlier by the writer with respect to paleoclimatic changes* coincides essentially with the views expressed by many leading modern geologists†: namely, that the normal average temperature of the Earth is higher than it is at present; that we are still inside a period of general deterioration of the terrestrial climate, a period already lasting for about a million years and connected with the phenomenon of Quaternary glaciation; and that the theories of continental drift and of the migration of the poles cannot be made responsible for this, as well as for earlier disturbances of the terrestrial climate. The writer pointed out that a general increase of solar radiation, due to the decreasing hydrogen content of the Sun, would be responsible for a gradual "secular" increase of the mean temperature of the Earth which apparently may be traced between the Cambrian and the Tertiary. This normal trend is interrupted by more or less short periods of glaciation, spaced about as follows‡:—

Glaciation	Algonkian	Cambrian	Ordovician§	Silur-Devonian*	Carbo-Permian	Quaternary
Time, 10^8 years from our era	−5·6	−4·8	−3·8	−3·1	−2·3	0

* E. Öpik, *Tartu Obs. Pub.*, **30**, No. 3, 1938.
† J. H. F. Umbgrove, *The Pulse of The Earth*, The Hague, 1947 (2nd edition).
‡ The list of the main glaciations is the same as quoted by the writer in 1938, but the epochs are assumed according to Umbgrove.
§ "Mountain glaciation" according to J. H. F. Umbgrove, *loc. cit.*

It is proposed to account for these climatic anomalies by certain repeated disturbances in the energy balance of the Sun as outlined in Sections 1 and 2 of the present paper. The theory of a single disturbance is expounded in Section 6. The phenomena of the Quaternary glaciation are, of course, rather complicated. The smooth curve of solar radiation of Fig. 1 cannot explain the repeated advance and retreat of the glaciers known to have happened on a large scale at least four times during the Quaternary. However, even the warmer interglacial periods (to which our era belongs, too) are definitely colder than the preceding Tertiary or Cretaceous; for the latter Urey * finds, from the relative abundances of oxygen isotopes in deposited lime, a temperature at formation from +17·5 deg. to +26·5 deg. C., the average for the six studied specimens being +21·6 deg. C. in Hampshire, England. Even assuming this to refer to the summer temperature, it differs significantly from the present summer average of the sea temperature about +15·5 deg. C. near the surface. The fluctuations of Quaternary glaciation are thus secondary waves superposed upon a major general depression. For the major depression the above picture of the complex decay of a disturbance in the solar interior may be advocated. The fluctuations may be produced by complications from the outer shell, the inner disturbance affecting the extent of the peripheral convective region.† Repeated, or continuous disturbances (long-enduring propagation of the disturbance in the interior) may explain the slight deterioration of climate which is characteristic of the end of the Tertiary preceding the start of the first "acute" glaciation.

Terrestrial causes seem to be generally inadequate to produce overall changes of climate to such a scale. The apparent (but loose) connection of past glaciations with the periods of mountain building (Holmes) may well be accidental, in view of the small number of coincidences; especially when we consider that mountain glaciation is possible only when mountains are present. The amount of carbon dioxide in the air as a climatic factor cannot have any influence because absorption by water vapour covers more effectively all the regions of the spectrum where carbon dioxide may exert its "greenhouse" effect. Moreover, vegetation is so efficient in removing CO_2 from the air‡ that, since the time when plants came into existence, the CO_2 content in the terrestrial atmosphere could hardly ever have exceeded the present amount, which actually approaches the minimum at which plants can exist (on Mars, according to Kuiper, the pressure of CO_2 is about the same as on the Earth, a very significant fact suggestive again of vegetation). A different distribution of the areas covered by land and sea may be more efficient in producing climatic changes all over the Earth's surface. The effect of an increased water surface would be a general lowering of the temperature, because of greater cloudiness, a smoothing out of seasonal changes and a smaller difference between pole and equator. However, the two hemispheres of the Earth, representing a difference in the land and sea distribution which is certainly larger than the possible fluctuations of the mean conditions on the Earth in the geological past have been, set an upper limit to the expected effect: the southern hemisphere is indeed cooler, but only by about two degrees (Hann); seasonal differences of temperature are largely smoothed out; but the maritime softening of the

* H. Urey, *Science*, **108**, 489, 1948.

† F. Hoyle has recently advocated an external cause for such fluctuations which perhaps is not quite so open to objections which are adduced at the end of this paper against meteoric effects.

‡ The present amount can be removed by the photosynthesis of plants within but a few hundred years.

climatic difference in latitude is hardly perceptible. There is hardly more of an ice age in the southern hemisphere than in the northern. From this it appears that systematic transgressions or regressions of the sea on a world-wide scale are still inadequate to account for the large climatic changes of the past. Besides, the warm period of the Tertiary differs from the present not only by an elevated average temperature, but also by a smaller climatic difference, the warming up being the most pronounced in the polar regions; this is hardly compatible with a more continental climate, whereas an increase in solar radiation alone explains it: at the elevated average temperature the moisture content, thus also the heat content of the air, is considerably increased, and the atmospheric circulation is more efficient in the convective transport of heat; as a result the temperature differences between the climatic zones are reduced.

It seems difficult to escape the conclusion that the main cause of these climatic changes is to be sought outside the terrestrial globe.

There have been several attempts to advocate changes in the eccentricity of the Earth's orbit and in the obliquity of the ecliptic as a cause of the ice ages; since the older work of Adhemar (1842) and James Croll (1864–1889), this idea has been considered repeatedly; the most detailed treatment is by Milankovitch *; a calculation of the perturbations of the Earth's orbit and obliquity has been made for a similar purpose by Pilgrim † for the past 800,000 years. All these considerations have the same weak point in common, namely, in ascribing to small causes large consequences out of any proportion. The obliquity of the ecliptic influences the annual distribution of heat received at different latitudes, greater obliquity corresponding to increased insolation at latitudes above 45°; the annual effect according to Milankovitch amounts to +0·78 per cent at latitude 60° per degree of obliquity and, as the extreme range of obliquity is from 22°·2 to 24°·5 according to Pilgrim, a maximum range of insolation of ±0·8 per cent results from this cause; the range in the black-body radiative temperature corresponding to this is ±0·6 deg. C.; the average temperature of the Earth is not influenced by this cause, a rise in high latitudes being counterbalanced by a decline within the tropics and vice versa. Nothing of the size of the actual climatic changes can be explained by such a minute effect. The eccentricity of the Earth's orbit affects the *intensity* of insolation in different seasons, by small amounts about as the above, but the total quantity of heat received during the year remains unaffected by it; only a second-order effect can be expected from that, largely smoothed out by the Earth's predominantly maritime climate: the result is doubtless nil.

Even if we admit with Milankovitch and others that the advancing and retreating pulse of Quaternary glaciation reflects the combined fluctuations in the eccentricity ‡ (e) and obliquity (ϵ) of the Earth's orbit, the absence of glaciation in the Tertiary and earlier remains still unexplained; the fact that Pilgrim did not dare to push his calculations back farther than 800,000 years before our era does not mean that the fluctuations did not exist before that; the variations of e and ϵ depend upon planetary perturbations and are continuing certainly all the time the Earth and the solar system exists. Obviously something

* M. Milankovitch, *Théorie mathématique des phénomènes thermiques, etc.*, Paris, 1920; *Kalorische Jahreszeiten und deren Anwendung im paläoklimalen Problem*, Beograd Akad., 1923.

† L. Pilgrim, *Versuch einer rechnerischen Behandlung der Eiszeiten*, Stuttgart, 1904.

‡ Combined with the precession of the equinoxes and the motion of the perihelion.

of a more fundamental change has occurred at the end of the Tertiary, and unless an explanation is given for the mere start of the first glaciation it may seem superfluous to argue about its subsequent course.

The most elaborate, and probably the most futile, attempt to devise a theory of the ancient climatic changes on the Earth has been made by W. Köppen and A. Wegener.* Of the 256 pages of this treatise 99 deal with the Quaternary. The authors accept Milankovitch's and Pilgrim's astronomical data for a basis; however, they are confronted with the insufficiency of the astronomical cause. They do not realize that the true fluctuations in temperature will always be smaller than those calculated from a black-body radiative equilibrium formula, because for a constant annual amount of heat received by the whole Earth local or seasonal anomalies will be counterbalanced by the store of heat in the oceans and by atmospheric circulation having an equalizing effect; the theoretical amplitude of $\pm 0{\cdot}6$ deg. C. should be reduced to from one-half to one-third of that amount. Köppen and Wegener take an opposite course, applying to the small figures a certain numerical amplification. Moreover, they restrict themselves to the summer solstice when the fluctuations are the largest, and instead of using directly the data for insolation, they convert them into effective shifts of latitudes. Because the curve of insolation runs rather flat with latitude at the solstice†, small changes of insolation are represented as big shifts in latitude, and the shifts in latitude so obtained are converted into temperature changes by using mean temperatures for the corresponding latitudes. Such a method yields final changes which are 10–20 times larger than the actual variation in the radiative equilibrium temperature, thus up to 50 times exceeding the probable variations expected. But this amplification is still insufficient, and Wegener's theory of continental drift is introduced: the northern continents have to be displaced by about 1000 km. in half a million years. This is not enough, and so the pole of rotation of the Earth is to be moved by 20 degrees of latitude during 600,000 years. And now one might expect that after having adjusted arbitrarily so many factors everything fits well into the scheme, but this is not so. Numerous facts which do not fit are either dismissed or *ad hoc* explanations are produced. As to the displacement of the pole of rotation, the apparent changes in the barycentre hitherto observed during half a century are entirely explained by errors in the stellar proper motions used and by changes in the observing programme.‡ But assuming the changes as they stand, they imply a motion of the pole of only $0''{\cdot}06$ per century, or $600''$ in one million years, 200 times less than assumed by Köppen and Wegener. Also all hitherto announced directly observed continental shifts are traced to systematic errors.§ Leading paleontologists strongly oppose the conception of continental drift as proposed by Wegener and it has been stressed "that the continents were essentially stable throughout the whole time involved in mammalian history (i.e. since the Triassic)".‖ All the elaborate edifice of Köppen and Wegener breaks down, as not one of their arguments has a real foundation. Since the beginning of the Tertiary at least, and very likely for the

* W. Köppen and A. Wegener, *Die Klimate der geologischen Vorzeit*, Berlin, 1924.

† The curve of geometrical insolation even rises toward the pole; however, Milankovitch introduces a correction for atmospheric absorption (rather primitively) and obtains a slow decline toward the pole.

‡ T. Nicolini, *Draft Reports of I.A.U.*, Zürich, 1948, Commission 19, p. 36.

§ *Ibid.*, p. 39, and Wm. Markowitz, *Trans. Amer. Geophys. Union*, **26**, 197, 1945.

‖ G. G. Simpson, *Amer. J. Sci.*, **241**, 1, 1943; also *Bull. Geol. Soc. Amer.*, **58**, 613, 1947.

earlier periods, we may assume that the climatic changes recorded in the terrestrial rocks reflect chiefly the changes in the intensity of solar radiation, only partially modified by local factors.

The radiative equilibrium of the Earth may be influenced by other cosmic factors also. For example, meteoric dust has been many times advocated as a possible cause of the ice ages. There is a fundamental misunderstanding about this point. Meteoric particles by their impact will produce extra heat on the surfaces of the Sun and the Earth, but any absorption of solar radiation will be more than compensated by the re-radiation of solar heat from the dust cloud inside and outside the Earth's orbit. A thorough discussion by V. Riives * settles definitely this point in the sense that from such a cloud only a warming effect can be expected. If the problem is inverted and it is assumed that the "normal" state corresponds to a meteoric medium sufficiently dense to increase the solar radiation by 10–20 per cent, an impossibly high space-density of galactic matter must be postulated.

It seems therefore that disturbances in the energy balance and internal structure of the Sun, perhaps complicated by secondary disturbances in the hydrogen (or hydrogen + helium) content of the subphotospheric convective region and leading to temporary disturbances in solar radiation, offer the most plausible explanation for the phenomenon of the recurrent ice ages on the Earth.

Armagh Observatory,
Northern Ireland:
1949 *March* 1.

ADDENDUM

The behaviour of the luminosity of a non-static model, considered in Section 3, may be commented upon also in the following way. In a static model with a core-source of energy the radiative flux between r_1 and r_2 (Fig. 2) is constant, being a definite function of the parameters and boundary conditions involved:

$$Q = f(M, T_c, \rho_c, T_c, \rho_p, \mu, \kappa_0, \ldots) = E_0. \qquad (1)$$

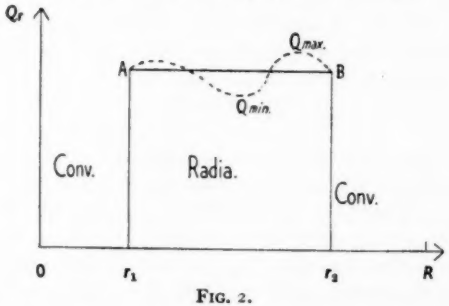

FIG. 2.

This function cannot, of course, be expressed explicitly, but it is a definite outcome in the process of numerical integration and may be called the "radiative" equilibrium function". In Fig. 2 the straight line AB represents the behaviour of $Q_r = Q = Ar_1 = \text{const.}$ over the radiative equilibrium zone.

* V. Riives, *Tartu Obs. Pub.*, 30, No. 7, 1940.

Let us now abandon the condition of the constancy of the radiative flux. This may be done by interposing arbitrary positive and negative energy sources, and Q_r may be represented by the dotted line in Fig. 2. Under unchanged conditions (parameters, etc.), and when the deviations are infinitesimal, the average value of the radiative flux will equal the static value, $\bar{Q}_r = Q = E_0$. Now, the mean value theorem requires that $Q_{max} > \bar{Q}_r > Q_{min}$ or $Q_{max} > E_0 > Q_{min}$. This is true also for finite small changes and, as calculations indicate (Table I), remains valid even for large finite changes.

Let us now consider the case of an expanding model. Negative gravitational energy sources are present and the radiative flux is steadily decreasing outwards ($Q_1 \to Q_2$, Fig. 3); $Q_{max} = Q_1$, $Q_{min} = Q_2$; thus, according to the above,

$$Q_1 > E_0 > Q_2. \tag{2}$$

This is the principal inequality used.

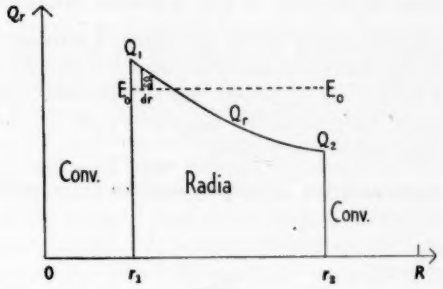

FIG. 3.

In an actual model the parameters of (1) are changing with the change of structure, and therefore the value of Q in (1) will somewhat change also and instead of (2),

$$Q_1 > Q > Q_2 \tag{2'}$$

should be written. Actual integrations, however, indicate that the deviation of Q from E_0 is so small that (2) remains always valid.

Let us consider the transition from a static case $Q_r = E_0 = \text{const.}$ toward the non-static case $Q_1 Q_r Q_2$ to be obtained by the cumulative effect of single perturbations $\delta Q = Q_r - E_0$, each covering the range dr (Fig. 3); a single perturbation $\delta Q\, dr$ will, in the process of outward integration, produce in the boundary condition a variation $F(r) . \delta Q\, dr$. As the radiative equilibrium solution in outward integration is divergent, the character of the divergence being an exponential one*, and as the region between r_2 and R is irrelevant as governed by a fixed adiabatic equation of state, $F(r)$ will represent a rapidly increasing function of $r_2 - r$, such that $F(r_1) : F(r_2)$ may be of the order of 10^4 and more. The total perturbation in the boundary condition will be

$$\delta B = \int_{r_1}^{r_2} \delta Q \, . \, F(r)\, dr. \tag{3}$$

* E. Öpik, *cf. Tartu Obs. Pub.*, **30**, No. 3, 1938.

Setting $\delta B = 0$, which is justified because the physical boundary condition (T_e, ρ_p) is extremely stable, being limited by the laws of photospheric opacity and radiation*, we have a condition

$$\int_{r_1}^{r_2} \delta Q \,.\, F(r)\, dr = 0 \qquad (4)$$

which, by the theorem of mean value, implies at once

$$Q_1 > E_0 > Q_2.$$

In the practical application E_0 has been assumed a weighted mean of the extreme values,

$$E_0 = kQ_1 + (1-k)Q_2,$$

which is formula (3) of the paper. The actual shape of the function Q_r as the sum of a constant core-energy and the negative energy of expansion proportional to $\int_0^{M_r} T\, dM_r$ is about as pictured in Fig. 3, convex toward the r-axis, and the weight $F(r)$ of the perturbation δQ in (4) increases strongly toward r_1; under such circumstances the fraction k exceeds $\frac{1}{2}$ in any case, and for the core-source models considered here it can be shown that k fluctuates within a narrow range around $\frac{2}{3}$. The actual integrations for models of uniform molecular weight and of moderate ρ_c/ρ_m lead to $k = \frac{2}{3}$ very closely.

* This differs from a mathematical boundary condition which may be varied at will.

THE EFFECT OF TURBULENCE ON A MAGNETIC FIELD

P. A. Sweet

(Communicated by the Director of the University Observatory, Glasgow)

(Received 1949 December 14)

Summary

The work of a previous paper (1) by the author on the effect of steady large scale convection currents on a magnetic field is extended to include turbulent convection. It is shown that turbulence reduces the effective electrical conductivity of a gas, in some cases to a small fraction of its normal value.

---

1. *Introduction.*—It has already been suggested by Cowling (2) that the decay of the Sun's general magnetic field might be accelerated by the turbulence in the convective core breaking up the field into small pieces which could decay independently. This, however, cannot be the actual mechanism of the decay, for however large a number of pieces were broken from a given set of tubes of force in a given region, the tubes of force themselves must still thread the region as a whole. They would in general merely be displaced from their original positions and compressed, as the volume they occupied was diminished by the volume occupied by the broken pieces. In general a field can only decay as the complete closed tubes of force constituting it disappear by contracting to a point. It will be shown that the effect of turbulence is to facilitate this contraction.

A representation of the field in a conducting medium in motion is established in Section 2, which makes it possible to see qualitatively why turbulence should reduce the effective conductivity. The mathematical treatment is then given in Section 3.

2. *A physical representation of a magnetic field in a conducting medium.*—Alfvén (3) has given an excellent picture of the lines of force of a magnetic field in a perfectly conducting medium, as elastic strings embedded in the medium. This picture can be extended to allow for the finiteness of the conductivity. In this case it is possible for material to flow across the field, thus introducing a definite velocity of the medium relative to the lines of force. It is necessary therefore to make a clear definition of the velocity of the lines of force.

Let $\boldsymbol{K}$ and $\boldsymbol{B}$ be a solenoidal vector field and its vector potential, respectively; the stream-lines of $\boldsymbol{K}$ are merely the mathematical family of lines given by Lagrange's differential equation

$$\frac{dx}{K_x} = \frac{dy}{K_y} = \frac{dz}{K_z}. \tag{2.1}$$

Any particular line can be labelled at a given instant by stating the point in which it intersects some reference surface S_0 intersected once by all the stream-lines in the region considered. The physical conception of a velocity can be attached to a stream-line only by assigning a velocity to its point of intersection with S_0. No physical significance can be attached to velocity along the line; the velocity,

denoted by $\boldsymbol{u}$, will therefore be taken as perpendicular to the line. It can be determined in terms of $\boldsymbol{K}$ and of its values on S_0, as follows:—

The ordinary theory of differential equations (**4**) shows that, in general, two independent families of surfaces can be found to satisfy (2.1). Let $\phi(xyzt) = \text{const.}$ and $\psi(xyzt) = \text{const.}$ be two such independent families of surfaces containing the stream-lines. Now $\boldsymbol{K}$ can be expressed in the form

$$\boldsymbol{K} = F \operatorname{grad}\phi \wedge \operatorname{grad}\psi, \tag{2.2}$$

where F is some function of position and time. Since

$$\operatorname{div}\boldsymbol{K} = 0,$$

$\operatorname{grad} F . (\operatorname{grad}\phi \wedge \operatorname{grad}\psi)$ vanishes, and F is therefore a function of ϕ and ψ. The vector potential can therefore be written

$$\boldsymbol{B} = \int^{\varphi} F\, d\phi \operatorname{grad}\psi + \operatorname{grad} W, \tag{2.3}$$

where W is an arbitrary function.

Consider now a stream-line defined by $\phi = \lambda$, $\psi = \mu$, where λ, μ are constants. Adopting Lagrange's treatment, select any point on a stream-line (λ, μ) at time $t = 0$, and let (x, y, z) be the position of this point at a subsequent time t. Hence $x = x(\lambda, \mu, \nu, t)$, etc., where ν is a parameter determining the distance of the original point along the line (λ, μ). We can therefore write

$$\partial\phi/\partial t + \boldsymbol{u} . \operatorname{grad}\phi = d\lambda/dt = 0, \tag{2.4}$$

where $\boldsymbol{u} = (\partial x/\partial t, \partial y/\partial t, \partial z/\partial t)$ is the velocity of the stream-line. Similarly

$$\partial\psi/\partial t + \boldsymbol{u} . \operatorname{grad}\psi = d\mu/dt = 0. \tag{2.5}$$

Thus

$$\begin{aligned} \boldsymbol{u} \wedge \boldsymbol{K} &= F\boldsymbol{u} \wedge (\operatorname{grad}\phi \wedge \operatorname{grad}\psi) \\ &\equiv F(\boldsymbol{u} . \operatorname{grad}\psi) \operatorname{grad}\phi - F(\boldsymbol{u} . \operatorname{grad}\phi) \operatorname{grad}\psi \\ &= F\partial\phi/\partial t \operatorname{grad}\psi - F\partial\psi/\partial t \operatorname{grad}\phi, \end{aligned} \tag{2.6}$$

on substituting from (2.4) and (2.5). Finally, on taking the *curl* of both sides, while noting that $F = F(\phi, \psi)$, this equation reduces to

$$\operatorname{curl}(\boldsymbol{u} \wedge \boldsymbol{K}) = \partial\boldsymbol{K}/\partial t, \tag{2.7}$$

which is the required relationship determining $\boldsymbol{u}$ in terms of $\boldsymbol{K}$ and the boundary conditions on S_0. In order to show that the boundary conditions on S_0 are sufficient to determine a unique solution, suppose it were possible for two distinct solutions $\boldsymbol{u}_1$, $\boldsymbol{u}_2$ to exist, taking the same values on S_0. The vector $\boldsymbol{w} = \boldsymbol{u}_1 - \boldsymbol{u}_2$ would vanish on S_0, and would satisfy the equation

$$\operatorname{curl}(\boldsymbol{w} \wedge \boldsymbol{K}) = 0 \tag{2.8}$$

everywhere. On noting that $\boldsymbol{w}$ is perpendicular to $\boldsymbol{K}$, it will be shown by the following lemma, that $\boldsymbol{w}$ vanishes everywhere, thus proving the uniqueness of the solution.

Lemma.—If $\boldsymbol{w}$ is a vector satisfying $\operatorname{curl}(\boldsymbol{w} \wedge \boldsymbol{K}) = 0$ in a given region, and is such that $\boldsymbol{w} \wedge \boldsymbol{K}$ vanishes on a surface S_0 intersected by all the stream-lines of $\boldsymbol{K}$ passing through the region, then $\boldsymbol{w} \wedge \boldsymbol{K}$ vanishes throughout the whole region.

Since $\operatorname{curl}(\boldsymbol{w} \wedge \boldsymbol{K}) = 0$, there must be a potential function W such that

$$\boldsymbol{w} \wedge \boldsymbol{K} = -\operatorname{grad} W.$$

Both $\boldsymbol{w}$ and $\boldsymbol{K}$ lie in the surfaces $W=$ const., hence $W=$ const. on a stream-line of $\boldsymbol{K}$. But grad $W=0$ on S_0, hence $W=$ const. throughout the whole region considered, which proves the lemma.

The boundary values of $\boldsymbol{u}$ over S_0 cannot, however, be assigned arbitrarily, as the variations of $\boldsymbol{u}$ over S_0 must always satisfy (2.7), or strictly, the component of (2.7) normal to S_0, since it is only this component which involves exclusively the derivatives of $\boldsymbol{u}$ in the surface S_0. Now the general solution of (2.7) can be written

$$\boldsymbol{u}\wedge\boldsymbol{K}=\boldsymbol{u}_0\wedge\boldsymbol{K}-\text{grad}\,W, \tag{2.9}$$

where $\boldsymbol{u}_0$ is a particular solution, and W is a function which can be assigned arbitrarily on S_0. W is then uniquely determined everywhere because, in virtue of grad W being perpendicular to $\boldsymbol{K}$, W is constant on the stream-lines. On taking the vector product of both sides of (2.9) with $\boldsymbol{K}$, and noting again that $\boldsymbol{u}$ has been defined as being perpendicular to $\boldsymbol{K}$, the explicit general solution is thereby seen to be

$$\boldsymbol{u}=\boldsymbol{u}_0+\text{grad}\,W\wedge\boldsymbol{K}/K^2, \tag{2.10}$$

where K is the magnitude of $\boldsymbol{K}$. This also shows that the boundary conditions for $\boldsymbol{u}$ can always be expressed in terms of a particular allowable set of values $\boldsymbol{u}_0$ on S_0, together with an arbitrary function W, given on S_0.

It can be shown, by a generalization of Kelvin's theorem concerning the circulation of fluid round any closed curve moving with the fluid, that

$$\text{curl}\,(\boldsymbol{v}\wedge\boldsymbol{K})=\partial\boldsymbol{K}/\partial t \tag{2.11}$$

is the necessary and sufficient condition for the flux of $\boldsymbol{K}$ through any closed curve moving according to a velocity field $\boldsymbol{v}$, to be constant in time. Equation (2.7) shows that, in particular, the velocity $\boldsymbol{u}$ of the stream-lines of $\boldsymbol{K}$ satisfies this condition. The flux of $\boldsymbol{K}$ through any curve moving with the stream-lines of $\boldsymbol{K}$ is therefore constant. This justifies the physical picture of tubes of magnetic induction which can only vanish by contracting to a point, or by converging on some limiting line and disappearing into it in the manner of a line sink, and vice versa. In a decaying magnetic field, for example, the tubes of magnetic force can only disappear by contracting to a point on a null line of the field, while if, on the other hand, the field is being built up by, say, a current flowing down the length of a cylindrical shell, tubes of magnetic force will appear from the shell, already formed.

By taking $\boldsymbol{K}$ to be a magnetic field $\boldsymbol{H}$, (2.11) is the same as the electromagnetic equation for a perfectly conducting material of unit permeability, moving with velocity $\boldsymbol{v}$ and carrying no externally impressed E.M.F.'s, provided $\boldsymbol{v}$ does not vary rapidly enough to produce an appreciable electromagnetic radiation. The above-mentioned extension of Kelvin's theorem, applied to magnetic fields, therefore gives the well-known result that, for a perfectly conducting medium in motion, the flux of magnetic force through any closed curve moving with the medium is constant in time. This property gives rise to the usual picture of a field frozen into the material carrying it.

This picture can be developed to include the effect of the finiteness of the conductivity. Consider further the equation $\text{curl}\,(\boldsymbol{v}\wedge\boldsymbol{H})=\partial\boldsymbol{H}/\partial t$ for a perfect conductor. Equation (2.7), which holds for any solenoidal vector, shows that if $\boldsymbol{u}$ is the velocity of the lines of magnetic force, then $\text{curl}\,(\boldsymbol{u}\wedge\boldsymbol{H})=\partial\boldsymbol{H}/\partial t$, since

$\boldsymbol{H}$ is solenoidal. (It is assumed here and throughout this paper that the material carrying the field has unit permeability.) Thus if $\boldsymbol{v}-\boldsymbol{u}=\boldsymbol{w}$, the velocity of the material relative to the lines of force, then curl $(\boldsymbol{w}\wedge\boldsymbol{H})=0$. The lemma then shows that, by defining $\boldsymbol{u}$ as the component of the material velocity normal to $\boldsymbol{H}$ on the reference surface S_0, $\boldsymbol{u}$ is equal to this component throughout the whole region. The lines of force therefore move with the material, which completely justifies the picture of a frozen field.

In the case of finite conductivity, the electromagnetic equation is

$$\operatorname{curl}\boldsymbol{H}/4\pi\sigma=\boldsymbol{v}\wedge\boldsymbol{H}+c\boldsymbol{E}^{\text{ext}}-c\operatorname{grad}V-\partial\boldsymbol{A}/\partial t, \tag{2.12}$$

where σ is the electrical conductivity expressed in e.m.u., $\boldsymbol{E}^{\text{ext}}$ the impressed E.M.F., due for example to thermal effects, $\boldsymbol{A}$ the vector potential, and V an arbitrary function. Now (2.7) shows that $\partial\boldsymbol{A}/\partial t$ can be written as

$$\partial\boldsymbol{A}/\partial t=\boldsymbol{u}\wedge\boldsymbol{H}+\operatorname{grad}U, \tag{2.13}$$

where U is an arbitrary function of position and time. On substituting for $\partial\boldsymbol{A}/\partial t$, (2.12) then becomes

$$\operatorname{curl}\boldsymbol{H}/4\pi\sigma=\boldsymbol{w}\wedge\boldsymbol{H}+c\boldsymbol{E}^{\text{ext}}-c\operatorname{grad}V, \tag{2.14}$$

where U has been absorbed into the function V.

In cases where curl $\boldsymbol{H}$ and $\boldsymbol{E}^{\text{ext}}$ are perpendicular to $\boldsymbol{H}$, such as, for example, the Sun's general magnetic field or sunspot fields neglecting currents circulating in meridian planes, $\boldsymbol{u}$ can be defined so that $\boldsymbol{w}\wedge\boldsymbol{H}=\operatorname{curl}\boldsymbol{H}/4\pi\sigma-c\boldsymbol{E}^{\text{ext}}$ on the reference surface S_0. The work of the earlier part of the section then shows that

$$\operatorname{curl}\boldsymbol{H}/4\pi\sigma=\boldsymbol{w}\wedge\boldsymbol{H}+c\boldsymbol{E}^{\text{ext}} \tag{2.15}$$

everywhere, while the component of $\boldsymbol{w}$ normal to the lines of force can be written explicitly as

$$\boldsymbol{w}_n=\boldsymbol{H}\wedge(\operatorname{curl}\boldsymbol{H}/4\pi\sigma-c\boldsymbol{E}^{\text{ext}})/H^2. \tag{2.16}$$

The first term of this expression admits of a semi-geometrical interpretation, as follows:—

Put $\boldsymbol{H}=H\boldsymbol{t}$, where $\boldsymbol{t}$ is the unit tangent to the line of force. Hence

$$\boldsymbol{H}\wedge\operatorname{curl}\boldsymbol{H}=H^2\boldsymbol{t}\wedge\operatorname{curl}\boldsymbol{t}+H\boldsymbol{t}\wedge(\operatorname{grad}H\wedge\boldsymbol{t}).$$

By ordinary vector theory it can be shown that

$$\boldsymbol{t}\wedge\operatorname{curl}\boldsymbol{t}=\tfrac{1}{2}\operatorname{grad}\boldsymbol{t}^2-(\boldsymbol{t}.\operatorname{grad})\boldsymbol{t}=-(\boldsymbol{t}.\operatorname{grad})\boldsymbol{t},$$

since $\boldsymbol{t}^2=1$. But $(\boldsymbol{t}.\operatorname{grad})\boldsymbol{t}=-\kappa\boldsymbol{n}$, where κ is the curvature of the line of force, and $\boldsymbol{n}$ the unit normal drawn outwards from the convex side of the line. We therefore have

$$\boldsymbol{w}_n=\kappa\boldsymbol{n}/4\pi\sigma+\boldsymbol{t}\wedge(\operatorname{grad}H\wedge\boldsymbol{t})/4\pi\sigma H+c\boldsymbol{E}^{\text{ext}}\boldsymbol{H}/H^2, \tag{2.17}$$

which gives a clearer interpretation for $\boldsymbol{w}_n$ than the expression in (2.16).

Consider now the effect of the magnetic field on the motion of the material carrying it. The equations of motion are

$$\rho\frac{D\boldsymbol{v}}{Dt}=-\operatorname{grad}p+\rho\boldsymbol{g}+\boldsymbol{F}^m,$$

where $\boldsymbol{F}^m$ is the mechanical force exerted by the magnetic field on the material. Now $\boldsymbol{F}^m=-\boldsymbol{H}\wedge\operatorname{curl}\boldsymbol{H}/4\pi$, which can be substituted from (2.16) to give

$$\boldsymbol{F}^m=-\sigma H^2\boldsymbol{w}_n+\sigma c\boldsymbol{E}^{\text{ext}}\wedge\boldsymbol{H}. \tag{2.18}$$

The equations of motion can therefore be put in the form

$$\rho \frac{D\boldsymbol{v}}{Dt} = -\operatorname{grad} p + \rho \boldsymbol{g} - \sigma H^2 \boldsymbol{w}_n + \sigma c \boldsymbol{E}^{\text{ext}} \wedge \boldsymbol{H}. \tag{2.19}$$

In the absence of any external E.M.F. $\boldsymbol{E}^{\text{ext}}$, the magnetic field can therefore be regarded as a porous elastic material allowing free movement parallel to the field, but resistant to motion across it, with a coefficient of resistance σH^2/cm.^{3}/unit relative velocity.

With regard to the decay of a field in a stationary medium, (2.17) shows that the velocity of the lines of force contracting through the medium decreases as the conductivity of the medium increases. This is another aspect of the well-known property that the rate of decay of a field decreases with increasing conductivity. The conductivity may therefore be regarded as a measure of viscosity in the medium in resisting motion of the lines of force through it. If the lines of force are distorted by turbulence of the medium, thereby increasing their curvature, (2.17) shows also that their general mobility may possibly be increased, with a consequent lowering of the effective conductivity. This cannot, of course, be taken as a proof that such a reduction actually occurs because, although the numerical value of the curvature at any point is increased by the turbulence, the effective contribution to the mean relative velocity $\boldsymbol{w}_n$ has different signs at different points. The theory in this section has been developed principally as an introduction to the theory of turbulent conductivity given in Section 3.

3. *The theory of turbulent conductivity.*—Consider a field such as the Sun's general magnetic field, symmetrical about an axis, and distorted by a meridian-plane circulation velocity. Using cylindrical polar coordinates as in a previous paper (1) by the author, the meridian-plane components of the field $\boldsymbol{H}_0$ which would be produced in the absence of turbulence are given by

$$H_{0\varpi} = -\frac{1}{\varpi}\frac{\partial B_0}{\partial z}, \qquad H_{0z} = +\frac{1}{\varpi}\frac{\partial B_0}{\partial \varpi},$$

where $B_0 = B_0(\varpi, z, t)$ is a stream function constant on the lines of force. If the lines of force are represented by the family of curves $u_0(\varpi, z, t) = \lambda$, then $B_0 = B_0(\lambda, t)$ and $H_0 = G_0/h_{u_0}\varpi$, where $h_{u_0}\Delta\lambda$ is the distance between adjacent curves $u_0 = \lambda$, $u_0 = \lambda + \Delta\lambda$, and $G_0 = \partial B_0/\partial\lambda$.

The effect of turbulence is to distort the lines of force about their mean positions $\bar{u} = \text{const.}$ Assuming that it does not affect the essence of the problem, the turbulence will be taken for simplicity to occur as tight folds in surfaces of revolution about the axis, thereby admitting a two-dimensional treatment. The distorted lines of force will be denoted by $u(\varpi, z, t) = \text{const.}$, so that any line $\bar{u} = \lambda$ is distorted into the line $u = \lambda$. The distorted field $\boldsymbol{H}$ is given by

$$H_\varpi = -\frac{1}{\varpi}\frac{\partial B}{\partial z} = -\frac{G}{\varpi}\frac{\partial u}{\partial z}, \qquad H_z = +\frac{1}{\varpi}\frac{\partial B}{\partial \varpi} = +\frac{G}{\varpi}\frac{\partial u}{\partial \varpi},$$

so that $H = G/h_u\varpi$. Here $G = \partial B/\partial\lambda$, where $B = B(\lambda, t)$ but is not the same function as B_0. The mean field $\boldsymbol{H}_m$ is therefore given by

$$H_{m\varpi} = -\frac{G}{\varpi}\frac{\partial \bar{u}}{\partial z}, \qquad H_{mz} = +\frac{G}{\varpi}\frac{\partial \bar{u}}{\partial \varpi},$$

so that $H_m = G/h_{\bar{u}}\varpi$.

B is determined by the ϕ-component of the electromagnetic equation in the form developed in Section 2, viz.,

$$\frac{1}{4\pi\sigma}\operatorname{curl}\boldsymbol{H}=\boldsymbol{w}\wedge\boldsymbol{H}+c\boldsymbol{E}^{\text{ext}}-c\operatorname{grad}V, \tag{3.1}$$

where $\boldsymbol{E}^{\text{ext}}$ is as usual the impressed E.M.F., V is a function which is uniquely determined once the velocities of the lines of force are assigned, as in Section 2, and $\boldsymbol{w}$ again is the velocity of the medium relative to the lines of force. All the functions are independent of ϕ, hence B is given by

$$-\left[\varpi\frac{\partial}{\partial\varpi}\left(\frac{1}{\varpi}\frac{\partial B}{\partial\varpi}\right)+\frac{\partial^2 B}{\partial z^2}\right]\Big/4\pi\sigma\varpi=-\left[w_\varpi\frac{\partial B}{\partial\varpi}+\omega_z\frac{\partial B}{\partial z}\right]\Big/\varpi+cE_\varphi^{\text{ext}}. \tag{3.2}$$

On multiplying both sides of this equation by $\rho\varpi^2$, where ρ is the density of the medium, and integrating over a finite narrow strip ΔS in the (ϖ, z)-plane between two adjacent lines of force $u=\lambda$, $u=\lambda+\Delta\lambda$, it follows that

$$\begin{aligned}-\frac{1}{4\pi}\iint_{\Delta S}\frac{\rho\varpi}{\sigma}&\left[\varpi\frac{\partial}{\partial\varpi}\left(\frac{1}{\varpi}\frac{\partial B}{\partial\varpi}\right)+\frac{\partial^2 B}{\partial z^2}\right]dS\\&=-\iint_{\Delta S}\rho\varpi\left[w_\varpi\frac{\partial B}{\partial\varpi}+w_z\frac{\partial B}{\partial z}\right]dS+c\iint_{\Delta S}\rho\varpi^2E_\varphi^{\text{ext}}\,dS.\end{aligned} \tag{3.3}$$

The left-hand side of this equation and the first term on its right-hand side may be transformed into line integrals by Stokes' theorem. After some reduction and rearrangement of terms, while noting that $\boldsymbol{H}$ is normal to, and $\boldsymbol{w}$ parallel to the short ends of the strip, this results in the equation

$$\begin{aligned}&\left\{G(\lambda+\Delta\lambda)\int_{u=\lambda+\Delta\lambda}\frac{\rho\varpi}{\sigma h_u}\,ds-G(\lambda)\int_{u=\lambda}\frac{\rho\varpi}{\sigma h_u}\,ds\right\}\Big/4\pi\\&\qquad+\frac{1}{4\pi}\iint_{\Delta S}\frac{1}{\varpi}\left[\frac{\partial B}{\partial\varpi}\cdot\frac{\partial}{\partial\varpi}\left(\frac{\rho\varpi^2}{\sigma}\right)+\frac{\partial B}{\partial z}\cdot\frac{\partial}{\partial z}\left(\frac{\rho\varpi^2}{\sigma}\right)\right]dS\\&=-\{B(\lambda+\Delta\lambda)-B(\lambda)\}\int_{u=\lambda+\Delta\lambda}\rho\varpi\,\omega\,ds\\&\qquad-\iint_{\Delta S}(B(\lambda)-B)\varpi\operatorname{div}\rho\boldsymbol{w}\,dS+c\iint_{\Delta S}\rho\varpi^2E_\varphi^{\text{ext}}\,dS,\end{aligned} \tag{3.4}$$

where $w=|\boldsymbol{w}|$, and ds is an element of length of a distorted line of force. On dividing by $\Delta\lambda$ and proceeding to the limit $\Delta\lambda\to0$, while noting that $dS=h_u\Delta\lambda\,ds$, this equation can be written

$$\begin{aligned}\frac{1}{4\pi}\frac{\partial}{\partial\lambda}&\left(G\int_{u=\lambda}\frac{\rho\varpi}{\sigma h_u}\,ds\right)+\frac{1}{4\pi}\int_{u=\lambda}\frac{1}{\varpi}\left[\frac{\partial B}{\partial\varpi}\cdot\frac{\partial}{\partial\varpi}\left(\frac{\rho\varpi^2}{\sigma}\right)+\frac{\partial B}{\partial z}\cdot\frac{\partial}{\partial z}\left(\frac{\rho\varpi^2}{\sigma}\right)\right]h_u\,ds\\&=-G\int_{u=\lambda}\rho\varpi\omega\,ds+c\int_{u=\lambda}\rho\varpi^2E_\varphi^{\text{ext}}h_u\,ds.\end{aligned} \tag{3.5}$$

Now

$$\left[\frac{\partial B}{\partial\varpi}\cdot\frac{\partial}{\partial\varpi}\left(\frac{\rho\varpi^2}{\sigma}\right)+\frac{\partial B}{\partial z}\cdot\frac{\partial}{\partial z}\left(\frac{\rho\varpi^2}{\sigma}\right)\right]h_u=-G\frac{\partial}{\partial n}\left(\frac{\rho\varpi^2}{\sigma}\right), \tag{3.6}$$

where $\partial/\partial n$ denotes differentiation along the normal to the curve $u=\lambda$ in the direction of increasing λ. Moreover, since the strip is long compared with the dimensions of the turbulence, then

$$\int_{u=\lambda} \frac{1}{\varpi}\frac{\partial}{\partial n}\left(\frac{\rho\varpi^2}{\sigma}\right) ds = \int_{\bar{u}=\lambda} \frac{1}{\varpi}\frac{\partial}{\partial \bar{n}}\left(\frac{\rho\varpi^2}{\sigma}\right) ds, \qquad (3.7)^*$$

where $\partial/\partial\bar{n}$ denotes differentiation along the normal to the mean curve $\bar{u}=\lambda$ in the direction of increasing λ. Hence

$$\int_{u=\lambda} \frac{1}{\varpi}\left[\frac{\partial B}{\partial \varpi}\cdot\frac{\partial}{\partial \varpi}\left(\frac{\rho\varpi^2}{\sigma}\right) + \frac{\partial B}{\partial z}\cdot\frac{\partial}{\partial z}\left(\frac{\rho\varpi^2}{\sigma}\right)\right] h_u\, ds = -G\int_{\bar{u}=\lambda} \frac{1}{\varpi}\frac{\partial}{\partial \bar{n}}\left(\frac{\rho\varpi^2}{\sigma}\right) ds$$

$$= \int_{\bar{u}=\lambda} \left\{\boldsymbol{H}_m \wedge \operatorname{grad}\left(\frac{\rho\varpi^2}{\sigma}\right)\right\}_\varphi h_{\bar{u}}\, ds. \qquad (3.8)$$

Some of the remaining integrals can be expressed in terms of certain mean values characterizing the turbulence, but independent of the strength of the field. Put

$$\int_{u=\lambda} ds \Big/ \int_{\bar{u}=\lambda} ds = \kappa \quad \text{and} \quad \int_{u=\lambda} h_u ds \Big/ \int_{\bar{u}=\lambda} h_{\bar{u}} ds = \kappa/\gamma, \qquad (3.9)$$

where the integrals are taken along sections which are long compared with the dimensions of the turbulence but short compared with the distance of variation of the mean field. Here κ is the ratio of the length of a distorted line of force to the corresponding section of the corresponding mean line; thus $\gamma = h_{\bar{u}}/\overline{h_u}$, where $\overline{h_u}$ is the mean value of h_u in the region concerned. γ is thus a measure of the constriction of the tubes of force consequent on the distortion; hence $\gamma \gg 1$ in a highly turbulent region. It should be noted also that $h_{\bar{u}}/h_u = H/H_m$, hence $\gamma = \overline{H}/qH_m$, where $\overline{H}$ is the mean value of the scalar strength of the distorted field, while $q = \overline{H}[1/\overline{H}]$, and is thus a mean function of the turbulence of order unity.

In order to examine κ further, consider a strip of area ΔS, between two mean curves $\bar{u}=\lambda_0$, $\bar{u}=\lambda_0+\Delta\lambda$, and small compared with the area of variation of the mean field while large compared with the area of a turbulent eddy. Now

$$\Delta S = \int_{\lambda_0}^{\lambda_0+\Delta\lambda}\int_{\bar{u}=\lambda} h_{\bar{u}}\, ds\, d\lambda = \frac{\gamma}{\kappa}\int_{\lambda_0}^{\lambda_0+\Delta\lambda}\int_{u=\lambda} h_u\, ds\, d\lambda = \frac{\gamma}{\kappa}\Delta S, \qquad (3.10)$$

hence $\kappa=\gamma$.

Consider now the mass in the region between the moving lines $u=\lambda$, $\bar{u}=\lambda$. The rate of flow of mass out of the region across a strip of the surface of revolution formed by rotating the line $u=\lambda$ about the axis of symmetry is $2\pi\int_{u=\lambda}\rho\varpi w\, ds$, while the rate of flow into the region across the corresponding strip of the surface of revolution of the mean line $\bar{u}=\lambda$ is $2\pi\int_{\bar{u}}\rho\varpi\bar{w}\, ds$, where $\bar{w}$ is the normal component of the mean mass velocity of the material across this mean line. But the total effective area of the region vanishes, since areas cut off by $u=\lambda$ on opposite sides

* By Stokes' theorem we have

$$\iint_S \left[\frac{\partial}{\partial\bar{\omega}}\left\{\frac{1}{\bar{\omega}}\frac{\partial}{\partial\bar{\omega}}\left(\frac{\rho\bar{\omega}^2}{\sigma}\right)\right\} + \frac{1}{\bar{\omega}}\frac{\partial^2}{\partial z^2}\left(\frac{\rho\bar{\omega}^2}{\sigma}\right)\right] dS = \int_{\bar{u}=\lambda}\frac{1}{\bar{\omega}}\frac{\partial}{\partial\bar{n}}\left(\frac{\rho\bar{\omega}^2}{\sigma}\right) ds - \int_{u=\lambda}\frac{1}{\bar{\omega}}\frac{\partial}{\partial n}\left(\frac{\rho\bar{\omega}^2}{\sigma}\right) ds,$$

where S is the region between the curves $\bar{u}=\lambda$, $u=\lambda$. The left-hand side vanishes since the mean area between the curves vanishes. (3.7) then follows.

of the mean line make contributions of opposite sign to the total rate of increase of mass in the region, hence

$$\int_{u=\lambda} \rho\varpi w\, ds = \int_{\bar{u}=\lambda} \rho\varpi\overline{w}\, ds. \tag{3.11}$$

By taking the length of the mean strip to be small compared with the typical distance of variation of the mean field, but still large compared with the dimensions of the turbulence, (3.5) can now be written

$$\frac{1}{4\pi}\frac{\partial}{\partial\bar{\lambda}}\left(\int_{\bar{u}=\lambda}\frac{\rho\varpi^2}{\sigma}q\gamma^2 H_m\, ds\right) + \frac{1}{4\pi}\int_{\bar{u}=\lambda}\left\{\boldsymbol{H}_m \wedge \operatorname{grad}\left(\frac{\rho\varpi^2}{\sigma}\right)\right\}_\varphi h_{\bar{u}}\, ds$$
$$= \int_{\bar{u}=\lambda}\rho\varpi^2\{\boldsymbol{w}\wedge\boldsymbol{H}_m\}_\varphi h_{\bar{u}}\, ds + c\int_{\bar{u}=\lambda}\rho\varpi^2 E_\varphi^{\text{ext}} h_{\bar{u}}\, ds, \tag{3.12}$$

where it has been noted that $\kappa=\gamma$ and $\overline{H}=q\gamma H_m$. On making a retransformation by Stokes' theorem, and noting that $\boldsymbol{H}_m$ is normal to the curves $\bar{u}=\lambda$, $\bar{u}=\lambda+\Delta\lambda$ bounding the mean strip $\Delta\bar{S}$ at its short ends, we can write

$$\frac{\partial}{\partial\bar{\lambda}}\left(\int_{\bar{u}=\lambda}\frac{\rho\varpi^2}{\sigma}q\gamma^2 H_m\, ds\right) = \frac{1}{\Delta\bar{\lambda}}\iint_{\Delta\bar{S}}\left\{\operatorname{curl}\left(\frac{\rho\varpi^2}{\sigma}q\gamma^2\boldsymbol{H}_m\right)\right\}_\varphi dS, \tag{3.13}$$

Equation (3.12) can then be written

$$\frac{1}{4\pi\Delta\bar{\lambda}}\iint_{\Delta\bar{S}}\left\{\operatorname{curl}\left(\frac{\rho\varpi^2}{\sigma}q\gamma^2\boldsymbol{H}_m\right)\right\}_\varphi dS + \frac{1}{4\pi}\int_{\bar{u}=\lambda}\left\{\boldsymbol{H}_m\wedge\operatorname{grad}\left(\frac{\rho\varpi^2}{\sigma}\right)\right\}_\varphi h_{\bar{u}}\, ds$$
$$= \int_{\bar{u}=\lambda}\rho\varpi^2\{\overline{\boldsymbol{w}}\wedge\boldsymbol{H}_m\}_\varphi h_{\bar{u}}\, ds + c\int_{\bar{u}=\lambda}\rho\varpi^2 E_\varphi^{\text{ext}} h_{\bar{u}}\, ds. \tag{3.14}$$

Finally, on dividing by $h_{\bar{u}}\Delta\bar{s}$, where $\Delta\bar{s}$ is the length of the mean strip, while noting that $dS = h_{\bar{u}}\Delta\lambda\, ds$, (3.14) can be written

$$\frac{1}{4\pi}\left\{\operatorname{curl}\left(\frac{\rho\varpi^2}{\sigma}q\gamma^2\boldsymbol{H}_m\right)\right\}_\varphi + \frac{1}{4\pi}\left\{\boldsymbol{H}_m\wedge\operatorname{grad}\left(\frac{\rho\varpi^2}{\sigma}\right)\right\}_\varphi = \rho\varpi^2\{\boldsymbol{w}\wedge\boldsymbol{H}_m\}_\varphi + c\rho\varpi^2 E_\varphi^{\text{ext}}. \tag{3.15}$$

Now $\boldsymbol{w}=\overline{\boldsymbol{v}}_n-\overline{\boldsymbol{u}}$, where $\overline{\boldsymbol{v}}_n$ is the component of the mean mass velocity $\overline{\boldsymbol{v}}$ of the material normal to $\boldsymbol{H}_m$, and $\overline{\boldsymbol{u}}$ is the velocity of the mean line of force. Hence on substituting $\{\overline{\boldsymbol{u}}\wedge\boldsymbol{H}_m\}_\varphi = \partial A_{m\varphi}/\partial t$, where $A_{m\varphi}$ is the ϕ-component of the mean vector potential $\boldsymbol{A}_m$, (3.15) becomes

$$\frac{1}{4\pi}\left\{\operatorname{curl}\left(\frac{\rho\varpi^2}{\sigma_T}\boldsymbol{H}_m\right)\right\}_\varphi + \frac{1}{4\pi}\left\{\boldsymbol{H}_m\wedge\operatorname{grad}\left(\frac{\rho\varpi^2}{\sigma}\right)\right\}_\varphi$$
$$= \rho\varpi^2\{\overline{\boldsymbol{v}}\wedge\boldsymbol{H}_m\}_\varphi + c\rho\varpi^2 E_\varphi^{\text{ext}} - \rho\varpi^2\partial A_{m\varphi}/\partial t, \tag{3.16}$$

where

$$\sigma_T = \sigma/q\gamma^2. \tag{3.17}$$

(3.16) is therefore the electromagnetic equation determining the mean field $\boldsymbol{H}_m$, and is best considered by reducing it to a more normal form by multiplying by $4\pi\sigma_T/\rho\varpi^2$. The equation is now

$$\frac{\sigma_T}{\rho\varpi^2}\left\{\operatorname{curl}\left(\frac{\rho\varpi^2}{\sigma_T}\boldsymbol{H}_m\right)\right\}_\varphi + \frac{\sigma_T}{\rho\varpi^2}\left\{\boldsymbol{H}_m\wedge\operatorname{grad}\left(\frac{\rho\varpi^2}{\sigma}\right)\right\}_\varphi$$
$$= 4\pi\sigma_T\{\overline{\boldsymbol{v}}\wedge\boldsymbol{H}_m\}_\varphi + 4\pi\sigma_T c E_\varphi^{\text{ext}} - 4\pi\sigma_T\partial A_{m\varphi}/\partial t. \tag{3.18}$$

In highly turbulent regions $\gamma \gg 1$; consequently $\sigma_T \ll \sigma$, and (3.18) can be written approximately as the ϕ-component of

$$\operatorname{curl} \boldsymbol{H}_m + \frac{\sigma_T}{\rho\varpi^2} \operatorname{grad}\left(\frac{\rho\varpi^2}{\sigma_T}\right) \wedge \boldsymbol{H}_m \simeq 4\pi\sigma_T \bar{\boldsymbol{v}} \wedge \boldsymbol{H}_m + 4\pi\sigma_T c\boldsymbol{E}^{\text{ext}} - 4\pi\sigma_T \partial \boldsymbol{A}_m/\partial t. \quad (3.19)$$

Except for the second term on the left-hand side this is the same equation, in every respect, as for the field in a medium of conductivity σ_T. σ_T is therefore the reduced effective conductivity of the turbulent medium, at least with respect to the meridian-plane component of the field.

The theory just given does not apply to the meridian-plane components of (3.19), but it is tempting to extend the principle of the reduction of conductivity to these components also. Such an extension would enormously increase the difficulty of the analysis, and it will not be attempted in this work. A statistical method might be more tractable, although it is questionable whether such an approach is fundamentally possible.

The effect of the mean mass velocity $\bar{\boldsymbol{v}}$ of the meridian-plane circulation can be examined by the method given by the author in a previous paper (1). It was shown there that a mean circulation velocity in meridian planes merely tends to distort the field to follow the lines of flow, without seriously affecting the strength of the field.

If, as just mentioned, (3.19) could be taken to hold with respect to its meridian-plane components, then the effect, on the field, of differential angular velocity could be examined as in the author's previous paper (1). The lowering of the conductivity would allow a greater measure of differential angular velocity along the lines of force of the meridian-plane component. The results of this previous paper show, however, that in the reversing layer the transverse component H_φ which would result from a variation in angular velocity of the observed order, along the the lines of force, would be of the order of 10^6 times the strength of the meridian-plane component. The effective conductivity would therefore need to be reduced by a similar factor before any appreciable angular velocity variation would be possible along the lines of force of the meridian-plane component. The actual extent of the reduction of conductivity due to turbulence is discussed in the next section.

Illustrative example.—Since the results of this section represent a great departure from the classical concept of conductivity, an illustrative example will be taken in which the problem is reduced to its bare essentials.

Consider the magnetic field in a long circular cylinder of uniformly conducting incompressible material, produced by a uniform E.M.F. E impressed along the length of the cylinder. If the material of the cylinder were not in motion the lines of force of the resulting field would be concentric circles about the axis of the cylinder, with a field strength H_0 at distance r from the axis given by

$$H_0 = 2\pi r\sigma c E. \quad (3.20)$$

The effect of turbulence is to distort the lines of force into crinkled curves following mean concentric circles. The turbulence considered takes the form of steady motion in small cells where, although the velocity varies rapidly from point to point over a right cross-section, it is constant in time at a given point and is constant along the length of the cylinder. The electromagnetic equation is therefore

$$\operatorname{curl} \boldsymbol{H} = 4\pi\sigma \boldsymbol{v} \wedge \boldsymbol{H} + 4\pi\sigma c\boldsymbol{E}, \quad (3.21)$$

where $\boldsymbol{v}$ is the velocity of the gas and $\boldsymbol{E}$ is a vector of strength E parallel to the axis of the cylinder. Only the axial component of this equation is non-vanishing, the vector form being retained for clarity. If the integral of this equation is taken over the area S enclosed by a distorted line of force C we have

$$\iint_S \operatorname{curl} \boldsymbol{H} . d\boldsymbol{S} = 4\pi\sigma \iint_S \boldsymbol{v} \wedge \boldsymbol{H} . d\boldsymbol{S} + 4\pi\sigma c \iint_S \boldsymbol{E} . d\boldsymbol{S}. \tag{3.22}$$

Since $\boldsymbol{H}$ is solenoidal we can write

$$\iint_S \boldsymbol{v} \wedge \boldsymbol{H} . d\boldsymbol{S} = \iint_S \boldsymbol{v} . \operatorname{grad} B \, dS, \tag{3.23}$$

where B is a stream function for $\boldsymbol{H}$, constant on the lines of force. On expressing $\boldsymbol{v} . \operatorname{grad} B = \operatorname{div}(B\boldsymbol{v}) - B \operatorname{div} \boldsymbol{v}$, transforming the $\operatorname{div}(B\boldsymbol{v})$ term into a line integral, noting that $B = \text{const.}$ (B_0 say) on the bounding line of force, and subsequently retransforming into a surface integral, we have

$$\iint_S \boldsymbol{v} . \operatorname{grad} B \, dS = \iint_S (B_0 - B) \operatorname{div} \boldsymbol{v} \, dS. \tag{3.24}$$

But $\operatorname{div} \boldsymbol{v} = 0$ everywhere since the material is incompressible, hence

$$\iint_S \boldsymbol{v} \wedge \boldsymbol{H} . d\boldsymbol{S} = 0. \tag{3.25}$$

After transforming its left-hand side by Stokes' theorem, while noting that E is uniform, (3.22) can now be written

$$\int_C H \, ds = 4\pi\sigma c E \iint_S dS. \tag{3.26}$$

For a line of force whose mean circle radius is r, (3.26) becomes

$$2\pi r \kappa \overline{H} = 4\pi\sigma c E \pi r^2, \tag{3.27}$$

where, as in the preceding theory, κ is the ratio of the length of a distorted line of force to the corresponding section of the mean line, while $\overline{H}$ is the mean value of H along a section of the line which is long compared with the distance of variation of the velocity. The mean field H_m can then be written

$$H_m = 2\pi\sigma_T c E r, \tag{3.28}$$

where $\sigma_T = \sigma q (H_m/\overline{H})^2$, while $q = \overline{H}[1/H]$ as before.

It will be noticed that σ_T is not a constant of the material but depends also on the strength of the mean field. Equation (3.28) provides a simple example of how the whole character of the electromagnetic equation is changed by this circumstance. On substituting from (3.20), (3.28) can be written

$$q H_m H_0 = \overline{H}^2, \tag{3.29}$$

where H_0 is the field which would be produced in the absence of turbulence. Now since $H_m \ll \overline{H}$, (3.29) shows that $H_m \ll \overline{H} \ll H_0$, so that in cases where the source of the field is in a turbulent region even the mean scalar distorted field strength $\overline{H}$ is reduced to below the normal field strength H_0. Equation (3.29) alone is not sufficient to determine H_m. However, in anticipation of a result obtained in the next section we can quote an additional relation

$$\overline{H} = \lambda^{1/2} H_m, \tag{3.30}$$

where $\lambda = O(4\pi\sigma vd)$, v and d being the typical velocity and diameter, respectively, of the turbulent eddies. In the Sun's convective core for example we have $\sigma \sim 7 \times 10^{-4}$ e.m.u., while Cowling has estimated (**7**) $v \sim 2 \times 10^3$ cm./sec. and $d \sim 10^9$ cm., giving $\lambda \sim 2 \times 10^{10}$. Now, $H_m = qH_0/\lambda$, $\overline{H} = qH_0/\lambda^{1/2}$, hence the mean field resulting from a given E.M.F. in the convective core would be reduced by a factor of order 10^{10} by turbulence.

This effect must not be confused with the distortion of a field originating in some remote non-turbulent region, such as the distortion, in the hydrogen convection zone, of a given field emanating from the radiative envelope. Here $\overline{H}$ can be very much greater than, while $\boldsymbol{H}_m$ is of the same order of magnitude as, the field in the radiative envelope. For intense turbulence the conductivity in the turbulent layer would be negligible, so that $\boldsymbol{H}_m$ is simply the irrotational completion of the field at the boundary of the radiative envelope, and as such is easily calculated without further knowledge of the turbulence.

4. *The turbulent conductivity in the convective core and in the surface layers.*— The problem is to find the order of magnitude of the ratio of the mean scalar field strength to the strength of the mean field, in these regions. It will be assumed that turbulence takes the form of a combination of two types of motion, pure rotatory motion, or eddying, in small cells, and rapid translation of small portions of the gas which on moving from point to point isolate themselves from their initial surroundings. This distinguishes turbulence from the type of motion in a system of quasi-steady convection currents in the form of long filaments, where the material at any point is not isolated from the material on either side of it along the filament, although the filament itself may be constantly changing its surroundings. Even in this case, of course, there may be turbulence at the surface of the filaments.

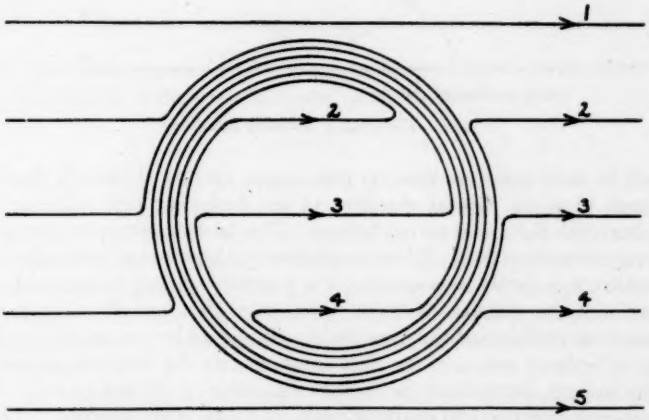

FIG. 1.—*The effect of an eddy in turning through one revolution.*

The effect of eddying on the field is to wind up the lines of force like clock springs, as illustrated diagrammatically in Fig. 1.

The effect of turbulent translation is as indicated in Fig. 2. As the cell isolates itself from the material initially surrounding it, so also does the field it carries isolate itself from the surrounding field. As the cell moves through the

field it wraps lines of force round itself which break away in succession from the parent lines as the surrounding material closes in behind the cell. Fig. 2 shows the correspondence between the lines of force of the isolated field inside the cell and their parent lines in the general field; the limiting line of force about to be broken away is shown by the heavy line. The point B on this line where the two fields are attached is a null point of the field, as is also the point A within the cell.

A finite solenoidal vector such as a magnetic vector can only vanish on closed lines, although in special cases these lines may coalesce into surfaces. In Fig. 2 the null line involved is a line through B perpendicular to the plane of the figure. This is the line of attachment of the broken piece to the main field, and it joins up with a similar line through A running inside the cell, thereby completing a closed curve as required.

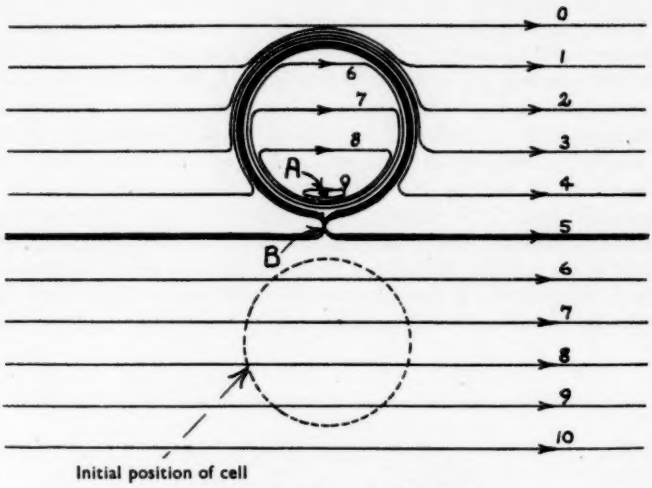

FIG. 2.—*The effect of turbulent translation.*

It will be seen therefore that, on this model, no line of force is displaced by much more than the typical diameter of the turbulent cells, although pieces broken from the field may travel farther. The broken pieces do not of course contribute to the mean field. These considerations justify that step in the previous section where it is tacitly assumed that it is possible to select strips which are long compared with the dimensions of the turbulence, although short compared with the distance of variation of the mean field. It should be remarked here that the presence of isolated pieces of the field must modify the detailed analysis of the preceding section, particularly as regards equations (3.10) and (3.11). It is the writer's opinion that the final result as given by (3.19) is not affected. The result may not be very accurate, however, where the turbulence is reduced to a system of convection currents as is apparently the case in the hydrogen convection zone, and possibly also in the convective core and in the chromosphere. Hoyle's theory (**5**) of the chromosphere, for example, is based on a study of long convection columns driven by the accretion of interstellar material. However, even in long convection filaments, where material is constantly being interchanged between

filaments, it may still happen that no one portion of material actually travels very far along a filament before crossing to an adjacent filament, thereby becoming isolated from its surroundings.

The intensity of distortion of the lines of force is limited by one of two factors. It has been shown that the mean scalar field strength is increased by the turbulence, as compared with the strength of the mean field. This scalar intensity cannot increase far beyond the point where the field begins to affect the dynamics of the turbulence. This occurs when the magnetic energy density $\overline{H}^2/8\pi$ of the distorted field is comparable with the kinetic energy of the turbulence. Alfvén, for example, has suggested (**6**) that a scalar intensity of between 160 and 500 gauss may be present in the photosphere, owing to convection there. The second possible limiting factor depends on the normal conductivity. Bearing in mind the picture developed in Section 2, together with equation (2.17), it can be seen that, as the curvature consequent on the distortion increases, the lines of force, in attempting to straighten themselves, slip back faster through the gas distorting them. A point will be reached when the lines straighten themselves as fast as the gas eddies tend to distort them and no further distortion takes place. The intensity, when limited in this way, would be a very large multiple of the initial mean intensity. (2.17) shows that the maximum mean curvature of the lines is given, in order of magnitude, by

$$\kappa = 4\pi\sigma w, \tag{4.1}$$

where κ is the mean scalar curvature. Since any small bulge in a line of force is straightening as fast as the turbulence is distorting it, w must therefore be the velocity of the gas in that bulge relative to the velocity in adjacent bulges. Now the turbulent velocity v of the gas varies over a typical distance of the order of the diameter d of the eddy cells, hence

$$w \sim vl/d, \tag{4.2}$$

where l is the typical diameter of the bulges in the lines of force. But $l \sim 1/\kappa$, hence on eliminating w between (4.1) and (4.2) we have

$$l \sim d/\lambda^{1/2}, \tag{4.3}$$

where $\lambda = 4\pi\sigma vd$. Hence in any distance L along a mean line of force the corresponding distorted line of force doubles back on itself $\lambda^{1/2}L/d$ times. It has been shown that the amplitude of the distortion of the lines as a whole is of order d. Consider then a region of diameter d as traversed by a certain tube of force. The contribution to the mean field from this tube is simply the strength of the tube. But in a distance d the tube doubles back on itself $\lambda^{1/2}$ times, hence the total contribution of the tube to the mean scalar strength of the distorted field is $\lambda^{1/2} \times$ *strength of tube*. Hence

$$\overline{H} \sim \lambda^{1/2} H_m. \tag{4.4}$$

As was mentioned in the previous section $\lambda^{1/2} \sim 10^5$ in the convective core. The largest field yet accountable for theoretically is of order 10^{-4} gauss in the core, as given in a theory (**2**) by Cowling. Thus, neglecting factors such as turbulence tending to reduce it, the field could not be less than this. The limit which would be imposed by the conductivity is therefore of order 10 gauss. This, as is shown later, is less than the limit imposed by the available energy of the turbulence.

In the surface layers the factor $\lambda^{1/2}$ would not exceed 10^3 owing to the lower conductivity. Cowling's field is of order 10^{-6} gauss in strength at the surface; the distorted scalar strength of this field would therefore be limited to about 10^{-3} gauss by the conductivity, which again is less than the limit imposed by the energy of the turbulence. However, since it is generally thought that a mean field of order 30 gauss, of unknown origin, is present in the surface layers, it will be assumed that the scalar distorted intensity is limited in the surface layers and in the core by the energy of the turbulence.

The turbulent conductivity is therefore best expressed as

$$\sigma_T = \sigma q \left(\frac{H_m}{\overline{H}}\right)^2, \tag{4.5}$$

where $\overline{H}$ is a function of the turbulence only. σ_T thus depends on the mean field, which greatly complicates the study of the electromagnetic equation. It should be noted, however, that the expression in (4.5) only holds where the strength of the mean field is less than the scalar intensity available from the turbulence. Larger mean fields than this tend to prevent turbulence in any case, allowing motion only parallel to the field. Sunspot fields in particular exceed the level of the turbulent intensity in the photosphere as assessed by Alfvén (**6**) and are therefore not appreciably affected by it. In spot-free areas of the photosphere where it is assumed that the mean field is of order 30 gauss and the turbulent intensity of the order of 300 gauss, (4.5) shows that the effective conductivity is reduced by about 100 : 1, to a value of order 10^{-11} e.m.u. A reduction of this order of magnitude is of little importance; it would allow a drift velocity of gas across the field of the order of 100 times the amount accepted hitherto, but still smaller than the drifts observed.

If, however, the mean field were found to be considerably less than the classical value of 30 gauss, say about 1 gauss, as recently measured by Thiessen, the conductivity would be reduced by about 10^5 : 1. Latitude drifts of up to 10^3 cm./sec. would then be possible without appreciably affecting the field. The results of the author's previous paper (**1**), however, show that a reduction of 10^7 or more in the effective conductivity would be necessary to permit an appreciable variation in angular velocity along the mean field.

In the convective core, also, the turbulent intensity is probably much greater than the mean field. Following Cowling's theory (**7**) of the convective core, the kinetic energy $\frac{1}{2}\rho v^2$ of the turbulence is of the order of 2×10^9 ergs/cm.^{3}. This would produce a scalar intensity of the order of 70,000 gauss; thus if the mean field were taken as 10^4 gauss, the effective conductivity would be reduced by about 50 : 1. Such a reduction has two main consequences; first, in theories seeking to explain the Sun's field by E.M.F.s in the core, the E.M.F. to be searched for must be greater than previously supposed, as was shown at the end of Section 3, and secondly, the decay time of the field, if decaying from a field built up at some remote epoch, must be somewhat less than that derived from calculations based on the normal value of the conductivity. This calculation is made difficult by the non-uniformity of the conductivity throughout the Sun. Using Rayleigh's principle, Cowling (**2**) calculated this decay time to be approximately 10^{10} years, and the eigenstate distribution corresponding to an intensity of 25 gauss at the equator at the surface, to give 2000 gauss at the centre. With this value of the central field the conductivity in the core would be reduced by the turbulence,

from its normal value of about 7×10^{-4} e.m.u. to approximately 6×10^{-7} e.m.u. These rough considerations show that the decay time depends, not on the core, but on the inner part of the radiative envelope surrounding it, and that the field in the core must decay relatively quickly to an irrotational completion of the field in the radiative envelope. The actual calculation of the decay time of the whole field will not be attempted in this paper.

5. *Conclusion.*—(i) Turbulence reduces the effective conductivity in the core and in the outer layers of the Sun. Sunspot fields are not affected however.

(ii) The decay time of the Sun's general magnetic field is somewhat less than the figure of 10^{10} years given by Cowling (**2**), although not by a factor of any great consequence, while the mean field in the core, if the general field is decaying from some initial state, is irrotational.

(iii) No system of meridian-plane convection currents in the Sun can provide a general amplification of a field produced by a given E.M.F., while turbulence in fact reduces the field.

I would like to thank Professor T. G. Cowling for his invaluable criticism of the paper. I am also indebted to him for suggesting the short proof given of the lemma in Section 2.

University Observatory,
Glasgow:
1949 *December* 5.

References

(1) P. A. Sweet, *M.N.*, **109**, 507, 1949.
(2) T. G. Cowling, *M.N.*, **105**, 166, 1945.
(3) H. Alfvén, *Ark. f. Mat. Ast. o. Fys.*, Bd. **29B**, No. 2, 1942.
(4) A. R. Forsyth, *A Treatise on Differential Equations*, art. 189, Macmilllan, 1914.
(5) H. Bondi, F. Hoyle and R. A. Lyttleton, *M.N.*, **107**, 184, 1947.
(6) H. Alfvén, *M.N.*, **107**, 211, 1947.
(7) T. G. Cowling, *M.N.*, **96**, 42, 1935.

ERRATA

M.N., **109**, No. 4, 1949, J. G. Porter's paper:

P. 411, equation (12), third line, *for* $a \cos EdE$ *read* $a \cos Ede$.

M.N., **109**, No. 4, 1949, G. Merton's paper:

P. 425, equation (13), *for* $-2r\zeta_1$ *read* $-2r\xi_1$.

P. 426, line 7, *for wn read w/n.*

P. 427, equation (22), *for* the first term on the right-hand side *read* $'f(x)\, s - \frac{1}{2}$.

M.N., **109**, No. 6, 1949, Harold Jeffreys' paper:

P. 678, equations (27) and (28), *for L read L/n.*

ADJUSTMENTS WITHIN SHELLS AND ASYMMETRIC EJECTA FROM Z ANDR, ζ AURI, β LYRA, ρ CASS AND γ CASS

Martin Johnson

(Received 1949 December 30)

Summary

Equations due to McCrea are applied to distinguishing between (*a*) the amoun tof radial separation allowed by viscous drag among circumstellar gases under different radiation pressures, and (*b*) the more common interpretation of " stratified atmosphere " as a radial variation in stages of optical excitation due to screening and attenuation of radiation without separation of materials. A range in variation of radiation pressure for McCrea's theory is obtained by adapting the equations of Gerasimovic. Asymmetric ejections of gases are classified where they can present spectra of high and low excitation together and thus simulate a stratified shell. Using Grotrian's time for an absorbing envelope to adjust itself to change in radiation, as well as McCrea's time for gases to adjust their velocities, some limits are found to the delay in spectral changes imposed by rate of uncovering of radiation in a binary system, and by the rate of penetration of a screen. Simple application is made to some features of Z Andr, ζ Auri, β Lyra, ρ Cass and γ Cass, as elucidated by Struve and Swings, Merrill, Kuiper, Kopal, Baldwin and others, preliminary to studying the more violent motions in W binaries and novae.

---

1. *Movements in circumstellar gases contributing to rates of spectral change.*— Among the problems of non-steady stars, some of the most complex arise from the presentation of spectra implying high and low excitation simultaneously or in rapid succession. The term "stratification", frequently used in discussing such problems, does not always leave certain whether it means (*a*) that differential gas motions have enforced a radial distribution in composition, or (*b*) that dilution or screening has provided radial differences in the stages of excitation without necessarily any chemical separation. But this distinction is itself incomplete if the simultaneous spectra arise not merely at different radial distances from a star but from different portions of the area presented; so the alternatives (*a*) and (*b*) involve the additional possibility (*c*) of asymmetry due to equatorial or local extrusions in a single star or to interference between the atmospheres of a binary pair. The degree of such symmetry can range from the prominence localized in all dimensions in Kopal's suggestion for ζ Auri, to include the spiralling stream from Kuiper's model for β Lyra, and then the separated rings around RY Pers or the optical structure in the equator of γ Cass; even a shell of P Cygn type, when as small as that said to surround Z Andr, must exhibit some slighter asymmetry if its source is a component of a binary.

Any rate of change of the spectrum may either denote development and decay of the conditions underlying (*a*), (*b*) or (*c*), or, if the object is binary, may be controlled mainly by the orbital motion giving atmospheric eclipses. Single instances of minima in the light-curve may be due to random drift of interstellar cloud, suggested as one of the alternatives in discussion of N Herc (1934) but an unlikely coincidence for frequent repetition; asymmetric ejecta allow more chances of repeated interposition of a screen from rotating stars and binaries.

Interposition of a short-lived prominence may never recur, whereas inequality in recurrence of abnormal opacity in β Lyra has been attributed to the gradual development of a ring from a jet with a maximum density in the second convolution. Rotation of the inner portion of a shell around Z Andr or α Scor, relative to its now detached nebulosity, offers fluctuations even more unequal in repetition if the object is a binary or a single source of asymmetric ejecta. On the other hand, ascription of fluctuating opacity to local association and dissociation *in situ* is attempted in ter Haar's model of N Herc (1934), also for ρ Cass in 1947, and in explanations of changing shell transparency for Z Andr.

A complete discrimination between these possibilities must ultimately account for duration and rate of extinction and repetition of any spectral change, in terms of geometrical factors of rotation and orbit and physical factors of local change in composition, density and excitation. But that task awaits two types of decision: (i) Can gases acquire such differential impulses, e. g. by selective radiation pressure, as to maintain separation as shells without degenerating into common motion by viscous drag? (ii) What time elapses (*A*) during establishment or decay of such separation, (*B*) during adjustment to changes in radiation, (*C*) during the emergence into line of sight of one or other portions of a rotating and asymmetrically erupting atmosphere or one of the components of an eclipsing binary?

Preliminary exploration into some aspects of this complex problem seems possible by applying McCrea's (**1**) criteria of gas separation, and Grotrian's (**2**) "time of relaxation of a system exposed to changing radiation", to some of the published evidence on complex variable stars; from these we assemble a set of examples. It is hoped that a tentative decision on some of the above ambiguities in these well-known stars may enable progress to be made towards the even more complicated simultaneous spectra of novae, e. g. where Stratton and Gaposchkin postulate jet models of N Herc (1934), and in the W binaries of Beals, Wilson, and Gaposchkin, where the greatest elaboration is to be expected in the penetration of one star's materials by the ejecta from its companion.

2. *Data.*—The groups of facts, and inferences by their observers, to which we shall relate our calculations are as follows.

(i) Z Andr. A sequence of researches, especially by Merrill (**3**) and by Swings and Struve (**4**), on the shells ejected in 1939–40 and 1946, discusses the separated components of lines at different speeds. In their interpretation, Swings and Struve postulate a small P Cygn shell, of the order of 10^{11} cm. compared with Beals' mean $20\odot$ shells in more typical P Cygn stars: the sub-dwarf companion to R Aqar also has been associated with a small shell radius. On the other hand, these writers call for a far wider extent of the subsequent nebulosity here as in α Scor, 10^{14} cm. or even 10^{16} where the forbidden lines [*Fe* II] arise. We shall compare the Grotrian calculation for the shell with Struve's own use of the same method for recovery of the nebulosity when the shielding shell was penetrated in 1940 August.

(ii) Kuiper's (**5**) model of β Lyra traces a spiral stream from the B9 component flowing across the F component to a diminishing density discussed by Struve, and the location of the point at which the asymmetric ejection occurs is significant. The transient opacity preceding eclipse of the B component ($r = 2{\cdot}8\odot$) of ζ Auri in 1939 is ascribed by Kopal (**6**) to a giant prominence at $1{\cdot}7 \times 10^{11}$ cm. above the K component's photosphere ($r = 200\odot$). McLaughlin (**7**) finds recent evidence for some permanent asymmetry of the K component.

(iii) Baldwin's (**8**) model of γ Cass, rotating at variable speed over a pulsation cycle, enables our treatment to compare the meanings of stratification when there is a difference of 70 km. per sec. between *H* and *He*, in contrast to the behaviour of other ringed systems: many other Be stars show cyclical swing between double components of a single line, commonly *H*, more rarely Fe^+ and Ca^+.

(iv) Greenstein's (**9**) treatment of the brief changes in radial velocity and opacity of ρ Cass in 1947 November, as explainable in terms of the collapse of a shell upon lower strata, when a burst of radiation ionized the distant hydrogen, making it nearly transparent and removing its radiative support, offers ground for exhibiting McCrea's and Grotrian's theories of adjustment, in a case resembling more closely Grotrian's original model.

3. *Gas separations limited by viscous drag.*—A well-known attempt to refer spectrophotometric changes to motions in gaseous ejecta is ter Haar's (**10**) model of molecular clouds in N Herc (1934), based on suggestions by Chandrasekhar and Stratton. The single depression in ρ Cass has attracted somewhat similar ideas, which merge into the older "veil" theory of long-period variables and may also be relevant to the irregular dimming of R Cor B stars. The meeting, mixing and separating of gases postulated in all such theories, and more readily examined in the simpler stars of the present paper, would occur when stellar radiation fluctuates or even where steady radiation becomes differentially absorbed by mixed gases; the motions would certainly exemplify our first meaning (Section 1) of stratification, if initial impulses due to radiation pressure can be maintained until shells develop. Similar considerations apply along radii when the asymmetric streams we have mentioned can only provide segments of a shell.

Optical changes will accompany such altering composition of a mixture, of partial concentrations n_1, n_2, ... per unit volume, when dn_1/dR, dn_2/dR .... reverse in sign at various values of R, permitting maxima to develop in the partial pressures of constituents with differing opacities. To decide the possibility and the time for establishment of such segregations, we proceed to apply McCrea's criteria; these state where the interchange of momentum at atomic or ionic collision can permit initially differing accelerations to maintain a difference in radial velocity. The equations needed from McCrea's paper are as follows.

If g_1, g_2 are the effective values of radial acceleration from a star for two substances, or for one material in two states of excitation and therefore subject to different radiation pressure, and ρ is the density often determined mainly by one constituent, then McCrea's velocity U of separation permitted by viscous drag is given by

$$dU/dt = g_1 - g_2 - \rho\gamma U^\epsilon.$$

We shall assess below (Section 5) the range of $(g_1 - g_2)$ including both gravity and radiation pressure. McCrea distinguishes two approximations, $U \ll v$ when $\epsilon = 1$ and $\gamma = \alpha$, and $U \gg v$ when $\epsilon = 2$ and $\gamma = \beta$, where v is thermal velocity. The quantities α (temperature-dependent because of the intrusion of v) and β (independent of temperature because v is relatively smaller) can be evaluated from

$$\alpha = \tfrac{8}{3}(\sigma_1 + \sigma_2)^2 \left[\frac{2\pi\kappa T}{m_1 m_2 (m_1 + m_2)}\right]^{1/2},$$

$$\beta = \pi(\sigma_1 + \sigma_2)^2 \frac{1}{m_1 + m_2}.$$

The σ's and m's are collision diameters and masses of the two kinds of atom. McCrea justifies in considerable discussion the approximation of gas-kinetic diameters for stellar ions. In the first case a limiting velocity of separation U_0 is attained, and in the second case U_0'. A defined "time of relaxation" T_0, T_0', governs rise or decay in transition, for a given fraction or multiple of each limiting value:—

$$U_0 = g_1 - g_2/\rho\alpha, \qquad T_0 = 1/\rho\alpha,$$

$$U_0' = \sqrt{\frac{g_1 - g_2}{\rho\beta}}, \qquad T_0' = \frac{1}{\sqrt{\rho\beta(g_1 - g_2)}}.$$

For the purpose of our applications we compute α and β for a set of gases relevant to our stars, Fig. 1 indicating that the possibility of stratification by actual separation between *H* and any other material increases tenfold between *He* and *Fe*, and that the greatest sensitivity to temperature in the temperature-dependent approximation occurs in the lightest pairs. We find also that for non-hydrogenic mixtures the dominant variable is the product $m_1 m_2$, β altering by only about 10 per cent for the *He* mixtures while α falls to half of its (hydrogen) value, which means a velocity of separation rising by 100 per cent.

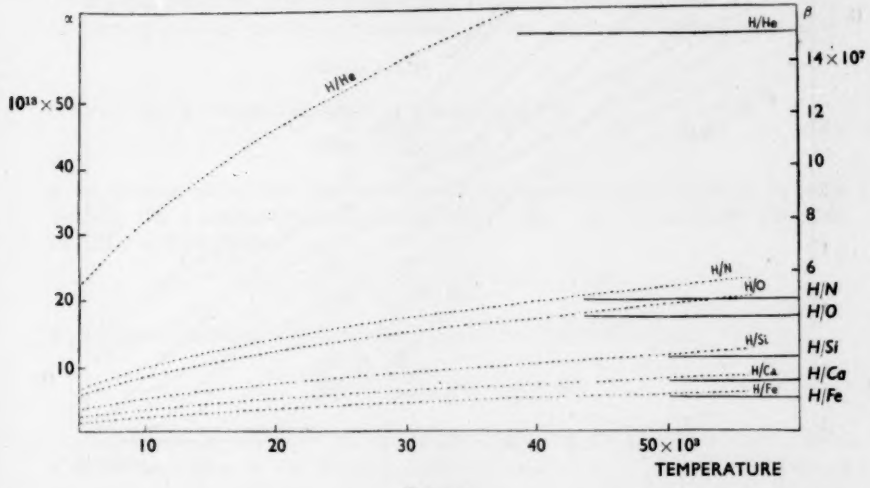

FIG. 1.

It is apparent that besides the variable ρ explored by McCrea in his applications, e.g. to solar prominences, the difference $(g_1 - g_2)$ will become decisive in the larger mass-motions of erupting stars and of Struve's non-static shells. The possible range of $(g_1 - g_2)$, treated below in Section 5, will be satisfied if we take extremes from 1/100 to 10 times the solar value of g (grav.). This will allow inclusion of velocities of separation as function of concentration for pairs of gases in both giant and dwarf atmospheric extrusions at high and low temperature, with extremes of 60,000 deg. and 6000 deg., with instances when one gas is dominated by gravity or rotation and the other gas subject to either a balancing or a reducing or a dominating radiation pressure. Accordingly, from Fig. 1 we plot Fig. 2, covering a sufficient range to read off the separation velocities for pairs of gases

with extremely differing absorptive properties. Both approximations U_0 and U_0' are plotted, as in critical cases the permission to separate may differ at different thermal velocities, which are themselves not homogeneous around an erupting star. Arrows on the plot indicate what displacement from the graph of *H/He* will cover other likely mixtures with hydrogen, and we recollect that with non-hydrogenic mixtures U is somewhat increased.

Fig. 2 shows sufficiently how velocity of separation can rise very high at nebular concentrations ($\nu<10^5$ per cm.^{3}), but at high chromospheric and prominence concentrations ($\nu>10^8$) can only become appreciable at the largest reversed values of g conferred by selective radiation pressure and leading to motions actually observed in eruption. The separations are considerably reduced by temperature. At $\nu>10^{11}$ separation from hydrogen is inappreciable for *He* even under the highest radiation pressure, and is only incipient for heavier atoms.

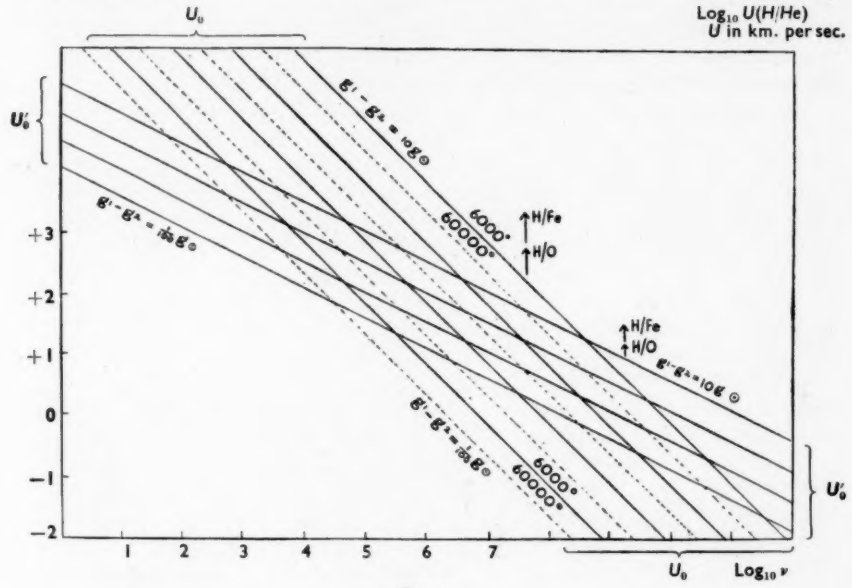

FIG. 2.

4. *Time of adjustment of shell or segment to fluctuating radiation.*—In spectrophotometric changes following gas motions, adjustment of the system depends not only upon momentum exchanged at collision as in McCrea's theory, but also upon the fact that some of the relevant values of g are due to radiation pressure: for an extensive circumstellar atmosphere will require finite time in reacting to even an instantaneous change of radiation. Merrill's lag of 1/5 period at some of the fluctuations of very large shells may well be such a finite travel of the locus of self-adjustment. It becomes relevant to apply Grotrian's problem of a hydrogen sphere at whose centre a Planck spectrum at enhanced temperature is established within an interval brief compared with that needed for the gas to come into equilibrium. It is important to note that Grotrian's

approach has not the immediate generality of McCrea's; he considers for one band of frequencies in one element, the time "τ" for ionizing absorptions and recombinations to raise to within a given large fraction of its maximum the fluorescence stimulated by a Lyman continuum as studied by Zanstra. Only to rough order of magnitude does this give information about the over-complex problem of unspecified gas mixtures exposed to fluctuations in other frequencies; but hydrogen is a striking feature of most stellar eruptions, and the equations we shall quote indicate where other ionization potentials and other temperatures both rising together enforce upon other materials a comparable behaviour. We point out some differences in Section 7. Grotrian applied his calculation to the recovery of N Herc (1934) after its minimum of 1935, and Struve and Swings have also applied it to the recovery of Z Andr after its P Cygn shell had ceased to impede radiation from the star in 1940. Adaptation to any segment of the sphere is legitimate except at the bounding edge of asymmetric distribution such as a jet, since R is the only dimension involved. But the serious limitation to which we refer in considering generalization in Section 7 is that of *total* absorption as end-point, demanding a sufficient depth of gas; for thinner atmospheres, Grotrian's τ is an upper limit only.

If α is a constant controlling the rate of recombination and N the total number of ionizing quanta from the star absorbed per sec. in the surrounding nebulosity,

$$\tau = 1/2\sqrt{\alpha N}, \qquad \alpha = \alpha'/V,$$

where V is the volume contained by the gas shell and

$$\alpha' = z/n'^2;$$

n' is the number of ions, also of free electrons in this approximation, per unit volume, and z is the number of recombinations per unit volume to the mth state in Cillié's (**11**) formula,

$$z = \frac{2^9\pi^5}{(6\pi)^{3/2}} \frac{\epsilon^{10}}{\mu^2 c^3 h^3} \left(\frac{\mu}{\kappa}\right)^{3/2} M(m, T,) n'^2.$$

In Zanstra's (**12**) discussion of fluorescence in circumstellar gases,

$$N = \frac{8\pi^2 R^2 \kappa^3}{c^2 h^3} T^3 \int_x^\infty \frac{x^2}{e^x - 1}\, dx,$$

$x = h\nu/kT$ and in this case ν is the frequency at the Lyman limit. We utilize Cillié's tabulation of the function $M(m, T,)$ for $m = 2, \ldots, 10$, and Zanstra's tabulation of the integral, and we compute τ for 15,000 deg. and 20,000 deg.

TABLE I

τ in seconds

		$r = 10^{12}$	10^{13}	10^{14}	10^{15}
$R = 10^{10}$	15,000	$2{\cdot}4 \times 10^3$	$7{\cdot}5 \times 10^4$	$2{\cdot}4 \times 10^6$	$7{\cdot}5 \times 10^7$
	20,000	$6{\cdot}3 \times 10^2$	$2{\cdot}0 \times 10^4$	$6{\cdot}3 \times 10^5$	$2{\cdot}0 \times 10^7$
10^{11}	15,000	$2{\cdot}4 \times 10^2$	$7{\cdot}5 \times 10^3$	$2{\cdot}4 \times 10^5$	$7{\cdot}5 \times 10^6$
	20,000	$6{\cdot}3 \times 10^1$	$2{\cdot}0 \times 10^3$	$6{\cdot}3 \times 10^4$	$2{\cdot}0 \times 10^6$
10^{12}	15,000	...	$7{\cdot}5 \times 10^2$	$2{\cdot}4 \times 10^4$	$7{\cdot}5 \times 10^5$
	20,000	...	$2{\cdot}0 \times 10^2$	$6{\cdot}3 \times 10^3$	$2{\cdot}0 \times 10^5$

for the cases of R (of star) 10^{10}, 10^{11}, 10^{12}, and r (of shell or nebulosity) 10^{12}, 10^{13}, 10^{14}, 10^{15}. The heavy line marks the conditions in R and r, to the right of which the time of adjustment reaches the order of a day and rises to the order of three years, a range covering the stellar distances we here consider.

5. *Differences in acceleration contributing to incipient gas separation.*—We now consider grounds on which the range in $(g_1 - g_2)$ was selected for applying McCrea's theory in Section 3, and the conditions bringing our particular applications within that range. The effective radial acceleration of a particle outside a star at distance R is

$$g(\text{eff.}) = [GM/R^2 - \omega^2 R] - g(\text{rad.}).$$

The following will be relevant sources of variation in this quantity:—(i) Since Struve's shells have radii several times the stellar radius, the latter itself greatly exceeding solar in some cases, the first term on the right-hand side can alter enormously between photosphere and outer envelope but to the same extent for all atoms; in an extreme case, Z Andr can exhibit spectra at values of R perhaps 10^4 times solar. (ii) In rotating stars the second term rises at the equator, until after expansion to large R, ω is diminished by viscous drag; Baldwin's discussion of γ Cass, where line widths fluctuate over a pulsation cycle between 260 and 480 km. per sec., compares the maximum velocities permissible under rotational stability, 300 in Jeans' liquid star, with 500 needed to make the second term exceed the first at the M and ρ of a Be star. Elvey's classical measurements trace a single line from 50 to 250 km. per sec. in a series of stars. (iii) The third term is the only one to vary from element to element at a fixed R, both by differential absorption and by monochromatic screening and backward re-radiation, and by Milne's mechanism of escape from a screened frequency through Doppler displacement. (iv) During temperature changes, e. g. in γ Cass, Z Andr and the flash of ρ Cass, the third term will also alter in integrated amount as well as among different elements. (v) During binary eclipse, e. g. of β Lyra and of ζ Auri, the third term can alter suddenly on emergence of one star from the shadow of a companion which is not radiating symmetrically over its whole surface.

The analysis of Gerasimovic (**13**), deriving the *absolute* value of g(rad.) in the particular case of absorption within the Lyman continuum, and showing it 2 or 20 times the gravitational term in a Be star even without rotation, can be adapted as follows for tracing the *variation* among other elements:—

$$g(\text{rad.}) = \frac{(1-x)\, f r \pi}{mc} \int_{\nu}^{\infty} \kappa(\nu) I(\nu)\, d\nu,$$

$(1-x)$ and f are the fractions, neutral and in a given state, appropriate to ionizing absorptions in the continuum beyond ν, r is residual intensity; corresponding quantities take their place at higher continua for second ionization, etc., in other elements than hydrogen. The rise of g(rad.) from 10 to 10^4 cm. per sec.^{2} in H between 7000 deg. and 15,000 deg. is checked, soon after exceeding gravity, by the fall in the neutral fraction and, for this case of a transparent ion, Gerasimovic finds a dependence upon electron pressure making the main expansions begin at a low level almost photospheric. The high velocities observed in P Cygn shells up to 300 km. per sec., 1000 in W stars, 2000 in novae, involve not only the drag by the hydrogen but the fact that no other materials are confined to neutral

absorption only. To obtain some insight into likely differential effects contributing to McCrea's (g_1-g_2), we plot in Fig. 3 the most variable of Gerasimovic's factors, $\log I(\nu)/m$, where m is atomic mass as multiple of that of hydrogen. The other important variations will be in "dilution" and "screening" effects upon r, and the time spent in a state capable of the particular absorption, represented here by $(1-x)$. Gerasimovic derives his rise and fall of radiation pressure on H by combining the temperature coefficients of $(1-x)$ and $I(\nu)$, but for the present purpose of comparing elements these are better exhibited by graphing the actual intensity *at* the series limit, and indicating separately where the control by $(1-x)$ makes one or another portion of the several graphs significant. Accordingly we bias our graphs by thickening the line over the range where fraction in the relevant neutral or singly ionized state has not fallen below 10 per cent: the required information we derive from an auxiliary graph of $\log n^+/n$ (**14**) according to ionization potential and temperature. The actual range over which Gerasimovic found H liable to radiative extrusion from a star is dotted on our graph, and extends to $n^+/n \rightarrow 10^3$, showing that for comparable $I(\nu)/m$ we are underestimating rather than overestimating the liability of other elements to motion under radiation pressure.

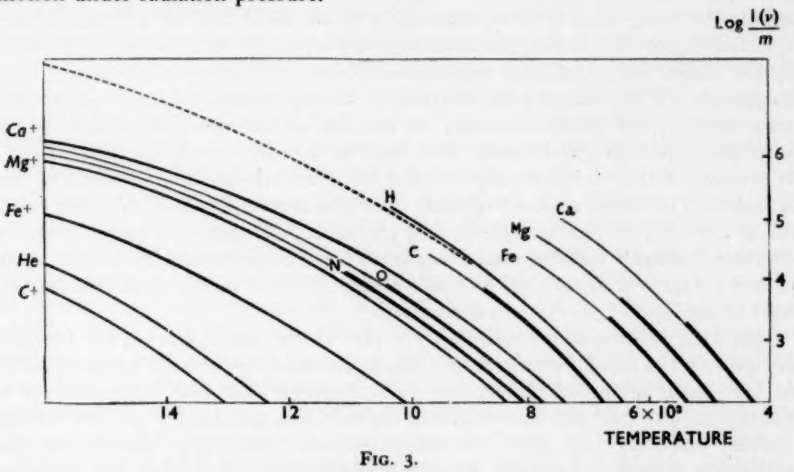

FIG. 3.

Fig. 3 indicates that in the temperature range where Be stars can extrude their hydrogen, metals in their exceedingly brief neutral states would be comparably accelerated, but in their much more prevalent ionized states would suffer accelerations 1/10 or 1/100 that of H, rivalling the latter only when it becomes transparent through ionization. Neutral gases of ionization potential comparable with H fall to below 1/10 of the latter's acceleration, but experience line absorptions pending second ionization. At Be temperatures the graph indicates factors up to 10^3 or 10^4 between the $I(\nu)/m$ of different atoms, each having considerable abundance in the same excitation stage; so that although at Wolf-Rayet temperatures all elements may be moving outward and at solar temperature only rare local prominences, B stars will be particularly rich in large values of the critical (g_1-g_2) between pairs of gases. Of any pair, both experience the same g (grav.), large near the photosphere and small in a distant shell or modified at a rotating equator;

but one of the pair may show an effective g reversed compared to the other, and a negative multiple of g(grav.) when its ionization continuum is favourably situated in the Planck spectrum of that temperature. Such cases will be covered by our selection of (g_1-g_2) between a pair of elements up to 10 times and down to 1/100 of the solar g(grav.) in Fig. 2.

6. *Applications.*—In proceeding to find where a few particular stars may exemplify the features obtained from our graphs and table of McCrea's and Grotrian's arguments, it will suffice at this stage to work to orders of magnitude only.

(I) *Shell and nebulosity of Z Andr.*—(*a*) Viscous drag conferring common shell velocity: if the estimate which we quoted from Swings and Struve for the P Cygn shell of Z Andr is correct, Fig. 2 indicates a high degree of drag. For strong lines in so small a shell, concentrations will probably exceed 10^{11} per cm.^{3}, and we see that even with (g_1-g_2) at its maximum of 10 $g_\odot$ concentrations exceeding 10^{10} per cm.^{3} will prevent separation between *He* and *H* or *H* and *O* from reaching 10 km. per sec. and only allow *H*/*Fe* slightly to exceed that separation under the most favourable conditions of temperature. Since P Cygn shells are not themselves an indication of localized jet extrusion, and we classed Z Andr among the lesser degrees of asymmetry, it would seem that the differential line velocities in the 1939 and 1946 extrusions must represent stratification of different optical stages, not of different materials separated, the alternative (*b*) in our first paragraph. These stages must interchange absorption and emission predominance within quite short distances, the dilution of radiation being due to steep local absorption gradient rather than here to any inverse-square attenuation. It is arguable that the phase lag between line velocities in those portions of the Z Andr system which appear to pulsate must also denote strata of excitation only, not of material, perhaps complicated by the lag in propagation of response which we discuss below: whether similar argument can include the multiphase pulsation of Mira stars will depend on finding whether all their visible gases can also be held to exceed 10^{10} per cm.^{3} concentrations.

(*b*) Gas separation in nebulosity: the above conclusions here become reversed. The [*Fe* II] region at 10^{15} cm. is perhaps large enough for asymmetry to have become smoothed out, but concentrations may well have fallen to a nebular 10^4 per cm.^{3} and cannot exceed the very high nebular 10^6 per cm.^{3} of the "stellar planetary" IC 4997. At that maximum density Fig. 2 indicates that separation between any gases absorbing as selectively as in Fig. 3 can readily exceed 100 km. per sec., and indeed there is nothing in the viscosity to prevent separations up to 10^4 km. per sec. being reached, exceeding Wolf-Rayet and nova ejection velocity, for *He*/*H* and *Fe*/*H* if (g_1-g_2) becomes sufficiently great. The net effect will only remain small when the radiation pressure is a mere correction to a predominant gravitation.

(*c*) Time of adjustment to radiation: Struve and Swings have already applied Grotrian's equations to estimating three or four weeks for the hypothetical "old nebulosity" to react to light restoration when the P Cygn shell became transparent in 1940 August. We add to this, from Table I, the very different situation in the shell itself; at the estimate quoted, where shell radius is five times the small stellar, the time of relaxation of a completely absorbing hydrogen shell following alteration of the Lyman radiation will be certainly much less than a day, and for many values of the quantities included in Grotrian's equations,

only a few minutes. This ensures the premiss omitted in the argument of Struve and Swings concerning the outer nebulosity, that time for the alteration of the screen must be negligible compared with time for the more distant target to adjust itself.

(*d*) Time for adjustment of gas velocities: in comparison, in the [*Fe* II] region where alone gases can separate, stabilization of the separations in McCrea's theory can be shown from our Section 3 to occupy the following times, at a concentration of 10^5 per cm.^{3}, at 10,000 deg. The times are maxima, taking the smallest (g_1-g_2), of the order of 10^2, capable of providing large separations.

$$T_0(H/He)=5 \text{ hours}, \qquad T_0(H/Fe)=84 \text{ hours},$$
$$T_0'(H/He)=5\tfrac{1}{2} \text{ hours}, \qquad T_0'(H/Fe)=19 \text{ hours}.$$

(II) *Adjustments among the ejecta from binaries.*—(*a*) Viscous drag:—(i) In RY Pers, Hiltner (**15**) has distinguished rotational velocity range of 200 km. per sec. in *He* compared with 110 km. in *H*, both rotating round the F5/B4 pair. RZ Scut and several other binaries also present slowly rotating *H* shells or rings around faster spinning *He* with velocity ranges up to 250 km. If this is a separation by McCrea's mechanism, Fig. 2 shows that concentrations must be far below 10^{11} per cm.^{3} where any large (g_1-g_2) becomes capable of enforcing a noticeable *U*. But the process leading to stratification is here susceptible of a different solution from that expressed in Section 5; it may not have developed from the differential radiative accelerations within an initially mixed gas, if Struve's suggestion is correct that such ringed binaries with sharp lines are exhibiting the debris of their original formation, not contemporary ejection. (ii) The close binary β Lyra and the more open ζ Auri are not instances of spherical shell stratification at all, and indeed Fig. 3 suggests that radiative extrusion is unlikely from the cooler components of either except at particular points where gravitational attractions from two components can compete. But consideration of those points allows McCrea's theory to become relevant in the novel question of lateral drag between adjacent streams side by side, as follows. Kuiper distinguishes an "A" type of ejection from contact binaries, emerging at a point between the two stars and wrapping round the hotter with a large apsidal rotation which causes intersection of streams. At distances not large compared with the stellar dimensions, the ejecta will therefore possess all the requirements for exchange of momentum to enforce common velocity. The binary models of AX Pers and Z Andr are assignable to this "A" form, but β Lyra belongs to Kuiper's "B" form, where ejection occurs instead at the distant edge of the smaller star. Either model allows adjacent regions of excess or defect density, and the meeting or divergence of material from the two stars; in general the mixing will occur at densities above the minima needed in Fig. 2 for functioning of McCrea's drag, but configurations of a binary system are possible in which a "pocket" of abnormally low "*g*" between the stars allows radiation pressure to become effective at unusually low temperature: separation of gases would then be locally possible. Kuiper's "B" mechanism produces a ring only, whose optical development in the second spiral convolution is a measure of the collisions exchanging momentum; the slightness of contribution from the F component in β Lyra to its B5 ring denotes the shallowness of the former's atmosphere, but such depth as the B9 stream penetrates into the F atmosphere will give a very complete drag of the one stream into the other, owing to atomic concentration at such small

distance from the target star lying well within the limiting region in Fig. 2. Struve's (**16**) observation of a retardation from 300 to 200 km. per sec. on return of the ejecta, and the observed turbulent broadening of lines, are further indications that the gas filaments could not maintain separation for long even if they had initially differing accelerations. This instance of the carrying of adjacent gas at lateral contact, instead of solely when strata overtake one another, is applicable to the spread of jets into cones in some models of novae. (iii) In Kopal's model of an obscuring prominence above the K component of ζ Auri, gas so shallow and yet opaque enough for the observed dimming must be considered to have a concentration well within the "drag" region of Fig. 2, and indeed Kopal estimated on other grounds 10^{11} per cm.^{3}. This drag would account for the obscuration being general, not monochromatic, even the extrusion of a single substance carrying the remaining gases with it—an extension of McCrea's own application of his theory to the Sun.

(*b*) Time lag in adjustment: although McCrea's time of adjustment would be very brief in β Lyra, it is important to know whether Grotrian's time for absorption of radiation is small or great compared with the time taken for a new target area to be exposed by orbital travel and rotation. Using Kuiper's, Kopal's and Struve's estimates for β Lyra, $R(\text{star}) = 3{\cdot}5 \times 10^{12}$ cm., $r(\text{interposed ejecta}) = 1{\cdot}1 \times 10^{13}$ cm. as averaged over the first convolution, so that our Table I gives time for absorption of Lyman radiation less than 10^3 sec. Since exposure of the ejected material from F5 to radiation from B9 was estimated by those writers to occupy the fourth to fifth day after ejection, the radiative adjustment occurs in a time brief compared to even the relevant fraction of the short orbital period of 12·9 days. On the other hand, in ζ Auri, our Grotrian calculation for the linear dimensions $R(\text{K}) = 200R_\odot$, $R(\text{B}) = 2{\cdot}8R_\odot$ provides times of adjustment ranging from three hours to two days compared with the period of 973 days, according to assumptions chosen as to orbital geometry and asymmetry of ejection. Since the observed veiling of B occurs in 24 hours, when the new absorption lines in the B spectrum have already appeared several days previous to eclipse, Struve and Swings' assumption of instantaneous exposure in using Grotrian's equations for Z Andr is no longer valid in these cases : in Z Andr the fastest completion was the unveiling of the source of light and the slowest the reaction of the distant absorbing target, but in β Lyra the reaction is more rapid than the unveiling, and in ζ Auri the processes are comparable in speed. McCrea's times are again briefer, for ζ Auri T_0 being less than one second and T_0' not greatly exceeding one minute.

(III) ρ *Cassiopeiae*.—In Greenstein's treatment, which we quoted, the suggestion is that the shell collapsed in 1947 November with an inward velocity reaching 31 km. per sec. after about a day. At the estimate $R(\text{star}) = 160\odot = 10^{13}$ cm. with a much larger shell, say, $r = 10^{14}$ cm., Table I gives times for adjustment $2{\cdot}4 \times 10^3$ sec. at 15,000 deg. and $1{\cdot}5 \times 10^4$ at 10,000 deg., Grotrian's model being almost exactly the process of hydrogen ionization postulated by Greenstein. Not only this response to radiation but also the adjustment of any differential gas velocity is rapid compared with the time of general collapse, since if we insert a minimum concentration 10^8 per cm.^{3} appropriate to this large shell, in our treatment of McCrea's theory

$$T_0(H/He) = 19 \text{ sec.}, \qquad T_0(H/Fe) = 5 \text{ min.},$$

$$T_0'(H/He) = 10\tfrac{1}{2} \text{ min.}, \qquad T_0'(H/Fe) = 36 \text{ min.}$$

At the density implied by the dimensions, real stratification in the sense of separation of materials is not prohibited if there were sufficient radiation pressure to cause it; but in so far as the spectrum suggests a K type this would scarcely be sufficient. In the "normal" star differences in velocity up to 7 km. per sec. were observed. When the "collapse" occurred Greenstein's change from −60 to −12 km. in a day was drawn from 70 lines, so that if his explanation of loss of hydrogen support is correct, either the *H* was dragging other elements in the lower and denser portion of its path of fall, or the radiation had failed in its support of other absorbers too and all were experiencing together the common "*g*" which Greenstein evaluates. Explanation of how all the materials had previously been extruded from the shell is not so forthcoming: radiation pressure is not the only agency, as has been proved in the Sun, but it may be relevant that before 1946 the star showed F character, and even when seemingly K or M its excited levels in *Fe*, *Mg*, *Si*, *N*, *O* exceed those expected at the *contemporary* temperature. So the envelope may be a relic, on small scale like a nebulosity surviving from an eruptive past. The evidence of Keenan (**17**) and of Thackeray (**18**) is against an erupting *companion* of the Z Andr or R Aqar type.

(IV) *γ Cassiopeiae*.—In Baldwin's account of this as a single star, he lists stratification from upper to lower atmosphere in a large number of successive emission and absorption lines, but suggests that this need not imply separation of materials if the "shell" is merely the optical effect of atoms streaming through a stationary absorbing region, visible only when each shows itself suitably excited. It is useful to check our treatment by asking whether it gives reason for such restriction to "excitation strata" instead of material separation. The case is of special importance in view of the likelihood that here the equatorial ring extrusion of Be type is accompanied by pulsation, *T* and *R* varying with a period long compared to that of rotation; this confers periodic velocity change along radii but varying with latitude, so that if radiation pressure passes a peak at phase of high temperature, differential motions are bound to be initiated. Furthermore, the range quoted by Baldwin, 8000 deg. to 13,000 deg., does cover the critical rise to radiative extrusion in the Be stars of Gerasimovic. Baldwin's stellar radius pulsates from 10 to 18 solar radii and his shell radius from 20 to 100; relative therefore to a 10^{15} cm. nebular radius of Z Andr, where concentrations may have fallen to 10^{4} or 10^{6} per cm.^{3}, the shell of γ Cass or the ring, at one-hundredth of that radius implies concentrations of 10^{10} or 10^{12} per cm.^{3}. At such densities, Baldwin's separations up to 100 km. per sec. between *H* and *He* cannot be a separation of materials, Fig. 2 indicating that this would only occur below a maximum of 10^{8} per cm.^{3} at very high radiation pressure. Hence in any use of the term "stratification", stages of excitation only must be involved as Baldwin suggested, unless future analysis of the periodic velocity in each line were able to prove that simultaneous radiation from photosphere and ring was capable of simulating a radial distribution. If the former is true, the explanation we classified as (*b*) instead of (*c*) in Section 1, the lack of correlation between Baldwin's radii and ionization potentials shows that no general "dilution" of the inverse square type familiar in nebulae is to be expected; the local gradients in line absorption and population of levels for emission must be very steep as in the inner shell of Z Andr.

7. *Conclusion*.—We have distinguished, with the aid of McCrea's equations, some of the rare cases where gases can be driven apart under differential radiation pressure, from the commoner cases where stratification can only imply a radial

spread of the loci of excitation stages. With the aid of Grotrian's equations added to those of McCrea, the time of adjustment of gas velocity or of response to changing radiation has been related to time of transient exposure in some eclipsing binaries and stellar extrusions. We have treated only a few aspects of five stars; in extension to other binaries with interpenetrating atmospheres, e. g. W binaries, and to recurrent novae and peculiar variables, the following are among the points needed to be taken into account. Whereas McCrea's theory is subject to the limitations which he himself stated, and Grotrian's treatment of hydrogen spheres is essentially adaptable to other elements and to sectors of a sphere, the whole simplification of adjustment to radiation will lose validity for light emitted beneath an insufficient depth of gas, since the equations depend upon total absorption. This makes our estimate of Grotrian's "τ" to be upper limits only. It also introduces the important difference between the times of adjustment at mere eruption of a hitherto quiescent photosphere into empty space and eruption into a nebulosity surviving from a previous outburst as in Z Andr in 1946. The spectral sequence of "repeater" novae, R Aqar, T Cor B, SS Cygn, etc., may be dominated by terms in Grotrian's "τ" which do not arise when the outburst is the first which a steady star has ever perpetrated, and it may become possible to infer quiet or unquiet previous history from analysis of present rate of development. The stratification of W binaries is a related problem, since here the ejecta incessantly impinge upon other ejecta, and will demand the greatest complexity in employment of the method whose simplification has only been possible in the few cases quoted. It is also worthy of note that in atmospheres where simultaneous application, e. g. to *He* and Ca^+ were attempted, in stars with such very discordant energy levels, the time of adjustment in fluorescent response in Grotrian's theory will be so different as itself to constitute a source of separation of the stages in excitation—an optical stratification altering with time. When to a single change in radiation one fluorescent response takes days and another takes weeks to establish, a fresh set of interpretations will be necessary to some of the fluctuations in spectrophotometry.

The University,
Birmingham :
1949 *December* 29.

References

(1) W. H. McCrea, *M.N.*, **95**, 509, 1935.
(2) W. Grotrian, *Z. Astr.*, **13**, 226, 1937.
(3) P. W. Merrill, *Ap. J.*, **99**, 15, 1944; **105**, 120, 1947; **107**, 317, 1948.
(4) P. Swings and O. Struve, *Ap. J.*, **93**, 356, 1941; **101**, 230, 1945.
(5) G. P. Kuiper, *Ap. J.*, **93**, 133, 1941.
(6) Z. Kopal, *Ap. J.*, **103**, 310, 1946.
(7) D. B. McLaughlin, *Ap. J.*, **108**, 237, 1948.
(8) R. B. Baldwin, *Ap. J.*, **92**, 82, 1940; **93**, 333, 1941.
(9) J. L. Greenstein, *Ap. J.*, **108**, 78, 1948.
(10) D. ter Haar, *M.N.*, **106**, 283, 1947.
(11) G. Cillié, *M.N.*, **92**, 820, 1932.
(12) H. Zanstra, *Ap. J.*, **65**, 50, 1927.
(13) B. P. Gerasimovic, *M.N.*, **94**, 737, 1934.
(14) S. Rosseland, *Theoretical Astrophysics*, (Oxford), 1936, p. 157.
(15) W. A. Hiltner, *Ap. J.*, **104**, 396, 1946.
(16) O. Struve, *Ap. J.*, **93**, 116, 1941.
(17) P. C. Keenan, *Ap. J.*, **106**, 295, 1947.
(18) A. D. Thackeray, *M.N.*, **108**, 276, 1948.

SPECTROPHOTOMETRIC MEASUREMENTS OF EARLY-TYPE STARS. 1. METHODS OF OBSERVATION AND RESULTS FOR Oe5 STARS*

E. A. Baker

(Communicated by the Astronomer Royal for Scotland)

Summary

This paper gives an account of a technique of measurement and reduction of line intensities which has been developed at Edinburgh. The photographed spectra are measured with a non-recording microphotometer at over a thousand fixed wave-lengths between λ 4100 and λ 6800, and the measures are combined for five or more negatives of each star, thereby reducing grain and other accidental errors without smoothing out real detail. The results so obtained for five of the Oe5 stars, selected as having narrow Balmer lines, have been further combined; and a mean continuum derived from these is used as a basis for the reduction of the results for individual stars. It is found possible by this procedure to free the results from the effects of continuum curvature due to the sensitivity curve of the emulsion.

Results are given for seventeen lines in each of seven stars of Draper type Oe5. They are in good agreement with those obtained by E. G. Williams at Mount Wilson and are systematically lower than those found by Petrie at Victoria. In addition the broad "interstellar" absorption centred near λ 4430 has been studied and found to cover a wider wave-length range than previously supposed. For this limited sample of seven stars it is noticed that the central absorption of λ 4430 shows a remarkably high correlation with colour or gradient excess, whereas the correlation of any of these with the intensity of the interstellar D lines is much weaker. Discussion of these results is postponed until further material is reduced and a larger sample of stars thereby rendered available.

* The full text of this paper appears in *Publications of the Royal Observatory, Edinburgh*, 1, No. 2, 1949.

THE VARIABLES IN THE SELECTED AREAS AT 75° AND 60° NORTH DECLINATION. 2. WORKING METHODS AND RESULTS FOR AREAS 5–7*

E. A. Baker and R. W. Wrigley

(Communicated by the Astronomer Royal for Scotland)

Summary

In continuation of a previous publication, this paper describes the methods used in a search for variables in these Areas, and gives results for Areas 5 to 7. Since results for Areas 2 to 4 have already been published† this completes the search of the Areas centred at declination +75°. The published results include only such stars as lie within three degrees of the centres of the Areas, become brighter than magnitude 14 at maximum, and show changes of at least 0·5 magnitude on more than one occasion.

From plates taken with a ten-inch triplet eight pairs of each Area are "blinked" and a list of suspected variables drawn up, each with its own comparison stars. The photographic magnitudes of the comparison stars, accurate to about 0·1 magnitude, are obtained from various sources, that preferred being the *Bergedorfer Spektral-Durchmusterung*, extended in range by a short and long exposure method and in area by examining the field corrections on de-centred plates. If after a preliminary test the suspected variable promises to fulfil the above criteria, it and its comparison stars are compared on all plates by the step method and the results combined to give in the first place more self-consistent comparison star magnitudes and finally the magnitudes of the variable for the date of each plate.

Maps with photographic magnitudes of comparison stars, positions correct to about one second of arc, and from twenty to thirty observations are given for each variable. In Areas 5 to 7 these particulars are given for two known and seven new variables.

* The full text of this paper appears in *Publications of the Royal Observatory, Edinburgh*, **1**, No. 3, 1949.

† *M. N.*, **97**, 541, 1937; **98**, 65, 1937.

CONTENTS

Printed in London by Taylor & Francis, Ltd., 1950 July.